Identification and Characterization of TPRKB Dependency in TP53 Deficient Cancers.

by

Kelly Kennaley

A dissertation submitted in partial fulfillment
of the requirements for the degree of
Doctor of Philosophy
(Molecular and Cellular Pathology)
in the University of Michigan
2019

Doctoral Committee:

Associate Professor Zaneta Nikolovska-Coleska, Co-Chair
Adjunct Associate Professor Scott A. Tomlins, Co-Chair
Associate Professor Eric R. Fearon
Associate Professor Alexey I. Nesvizhskii

Kelly R. Kennaley

vandenbk@umich.edu

ORCID iD: 0000-0003-2439-9020

Acknowledgements

I have immeasurable gratitude for the unwavering support and guidance I received throughout my dissertation. First and foremost, I would like to thank my thesis advisor and mentor Dr. Scott Tomlins for entrusting me with a challenging, interesting, and impactful project. He taught me how to drive a project forward through set-backs, ask the important questions, and always consider the impact of my work. I'm truly appreciative for his commitment to ensuring that I would get the most from my graduate education. I am also grateful to the many members of the Tomlins lab that made it the supportive, collaborative, and educational environment that it was. I would like to give special thanks to those I've worked closely with on this project, particularly Dr. Moloy Goswami for his mentorship, Lei Lucy Wang, Dr. Sumin Han, and undergraduate students Bhavneet Singh, Travis Weiss, and Myles Barlow.

I am also grateful for the support of my thesis committee, Dr. Eric Fearon, Dr. Alexey Nesvizhskii, and my co-mentor Dr. Zaneta Nikolovska-Coleska, who have offered guidance and critical evaluation since project inception. Many thanks to those in the MCP program for providing an exceptional learning environment and support for interests both inside and outside the lab, including my Translational Pathology Pilot Training Program award. I'd also like to recognize the graduate student community at the University of Michigan. I've made many lifelong friends here, and I'm excited by what the future holds for us all.

Finally, I'd like to give a most heartfelt thanks to my family. My husband, parents, grandparents, aunts, uncles, cousins, and in-laws have all provided immeasurable love and

encouragement throughout graduate school. I would like to give special thanks to my parents John and Cheryl VanDenBerg for instilling in me a love of learning and desire for personal growth. I would not have been able to do this without their everlasting support. I'm especially grateful for my husband Dylan Kennaley for keeping me grounded throughout graduate school with his enouraging words, limitless understanding, and steadfast support.

A final thank you to everyone who helped make this a reality.

Table of Contents

List of Tables

List of Figures

Abstract

Tumor protein 53 (*TP53*) is a transcription factor involved in regulating various facets of cellular functionality from its canonical functions in DNA damage response, cell cycle arrest, and apoptosis, to newer roles in metabolism, protein translation, and more. *TP53* is also the most frequently altered gene in human cancer, and identification of vulnerabilities imposed by *TP53* alterations may enable development of effective therapeutic approaches. Through analyzing shRNA-screening data, we identified TP53RK binding protein (TPRKB) as the most significant vulnerability in *TP53*-mutated cancer cell lines. To date, TPRKB's only known role is as a poorly characterized member of the transfer RNA (tRNA)-modifying Endopeptidase-like and Kinase associated to transcribed Chromatin/Kinase, Endopeptidase and Other Proteins of small Size (EKC/KEOPS) complex, responsible for depositing the t6A37 modification on all ANN decoding tRNAs. *In vitro* and *in vivo*, across multiple benign-immortalized and cancer cell lines, we confirmed that *TPRKB* knockdown in *TP53*-null, *TP53*-mutated, and Mouse double minute 2 homolog (*MDM2*; an E3-ubiquitin ligase for TP53)-amplified cells significantly inhibited proliferation, with minimal effect in *TP53* wild-type cells. Furthermore, we used isogenic cell lines to demonstrate *TP53* reintroduction into *TP53*-null cells resulted in loss of TPRKB sensitivity, while deletion of *TP53* in wild-type cells enhanced sensitivity, confirming specificity for *TP53* status. Sensitivity was accompanied by cell cycle arrest and reduced expression of anti-apoptotic proteins – B-cell lymphoma 2 (BCL2) and BCL2 like 1 (BCL2L1). Depletion of other

EKC/KEOPS complex members exhibited *TP53*-independent effects, supporting novel, complex-independent functions of TPRKB.

To explore mechanisms surrounding this sensitivity, we characterized several protein-protein interactions in this context. We demonstrate dynamic regulation of TPRKB, whereby TP53 indirectly mediates TPRKB degradation through the proteasome, while TP53 Regulating Kinase (TP53RK or PRPK), an interacting member of the EKC/KEOPS complex, directly stabilizes TPRKB. Furthermore, through co-immunoprecipitation followed by mass spectrometry (IP:MS) analysis we identify and validate that TPRKB interacts with another tRNA-modifying complex, tRNA methyltransferase 6/tRNA methyltransferase 61A (TRMT6/TRMT61A), responsible for the m1A58 tRNA modification. However, knockdown of TRMT6/TRMT61A in our characterized cell lines showed no proliferative differences and m1A levels in TPRKB depleted cells were unaltered, leaving the functional consequence of the interaction unknown. Nonetheless, TPRKB depletion was accompanied by a TP53-dependent reduction in protein translation and general reductions in other tRNA modifications (t6A, ms2t6A, m3C, and m3U), Polymerase RNA III DNA directed polypeptide G 32kD-like (*POLR3GL;* involved in transcription of tRNA) expression, and altered sensitivity to tRNA and ribosomal RNA (rRNA) polymerase inhibitors. Together, these results identify a unique and specific requirement of TPRKB in a variety of TP53-deficient cancers, and implicate TPRKB in several aspects of protein translation. Future studies aimed at elucidating the mechanism for TPRKB sensitivity are critical to explore the potential for therapeutic targeting in TP53-deficient cancer.

Chapter 1 Introduction

1.1 Introduction to Tumor Protein 53 (TP53 or p53)

Tumor protein 53 (TP53 or p53) was first discovered and described by multiple independent groups in 1979[1-6]. At this time, cancer research was focused on studying cancer-causing viruses, such as simian virus 40 (SV40), and viral tumor antigens, particularly viral oncogenes. It was through studying the SV40 large T antigen that these groups discovered an interacting partner of 53kDa that would later be known as TP53. Due to the nature of its discovery and early experiments inadvertently studying mutant forms of the protein, TP53 was initially thought to be an oncogene. It wasn't until 1989 that TP53 would be reclassified as a tumor suppressor[7].

1.1.1 Role of wild-type TP53

TP53 is an 11-exon gene that encodes a 53kDa transcription factor. The TP53 protein has 3 domains with 7 regions that are critical for proper localization and functioning: 1) the N-terminal domain contains both a transactivation domain and a proline-rich domain with an apoptosis-related region within it; 2) the core domain contains the DNA-binding domain; and 3) the C-terminal domain contains a nuclear localization signal, a tetramerization domain, a nuclear export signal, and a basic domain. Mutations in any of these domains may lead to aberrant TP53 functionality.

TP53 is largely regulated at the protein level through proteasomal degradation during normal conditions or stabilization by post-translational modifications during times of stress[8]. The most influential negative regulators of TP53 are members of the MDM family, MDM2 (murine double minute 2, also known as HDM2) and its homolog MDM4 (murine double minute X, also known as MDMX, HDMX, or HDM4). MDM2 is an E3 ubiquitin ligase that associates with TP53 and marks it for proteasomal degradation. Concurrently, MDM4 inhibits TP53 independently from proteasomal degradation by binding to the N-terminus of TP53 and facilitating heterodimerization with MDM2. Conversely, during stressed conditions, post-transcriptional modifications stabilize TP53, often through interfering with its interaction with MDM2 and MDM4. While the MDM family of proteins is one of the most heavily studied, TP53 can also be regulated by other post-translational modification enzymes and molecular chaperones[9].

Upon activation by DNA damage or other genotoxic stressors, wild-type TP53 forms a tetramer, binds genomic DNA, and acts as a transcription factor to mediate the expression of genes involved in regulating the cell cycle, senescence, and apoptosis[10]. As a result, TP53 has been dubbed the "Guardian of the Genome." Beyond these canonical functions, TP53 has also been implicated in cellular metabolism, autophagy, angiogenesis, migration, and more[11]. As illustrated in **Figure 1.1,** TP53 has the potential to regulate nearly every aspect of cellular functionality, and studies continue to uncover novel regulators and mediators of TP53 activity. Thus, comprehensive elucidation and modulation of TP53 functionality within specific contexts is often challenging.

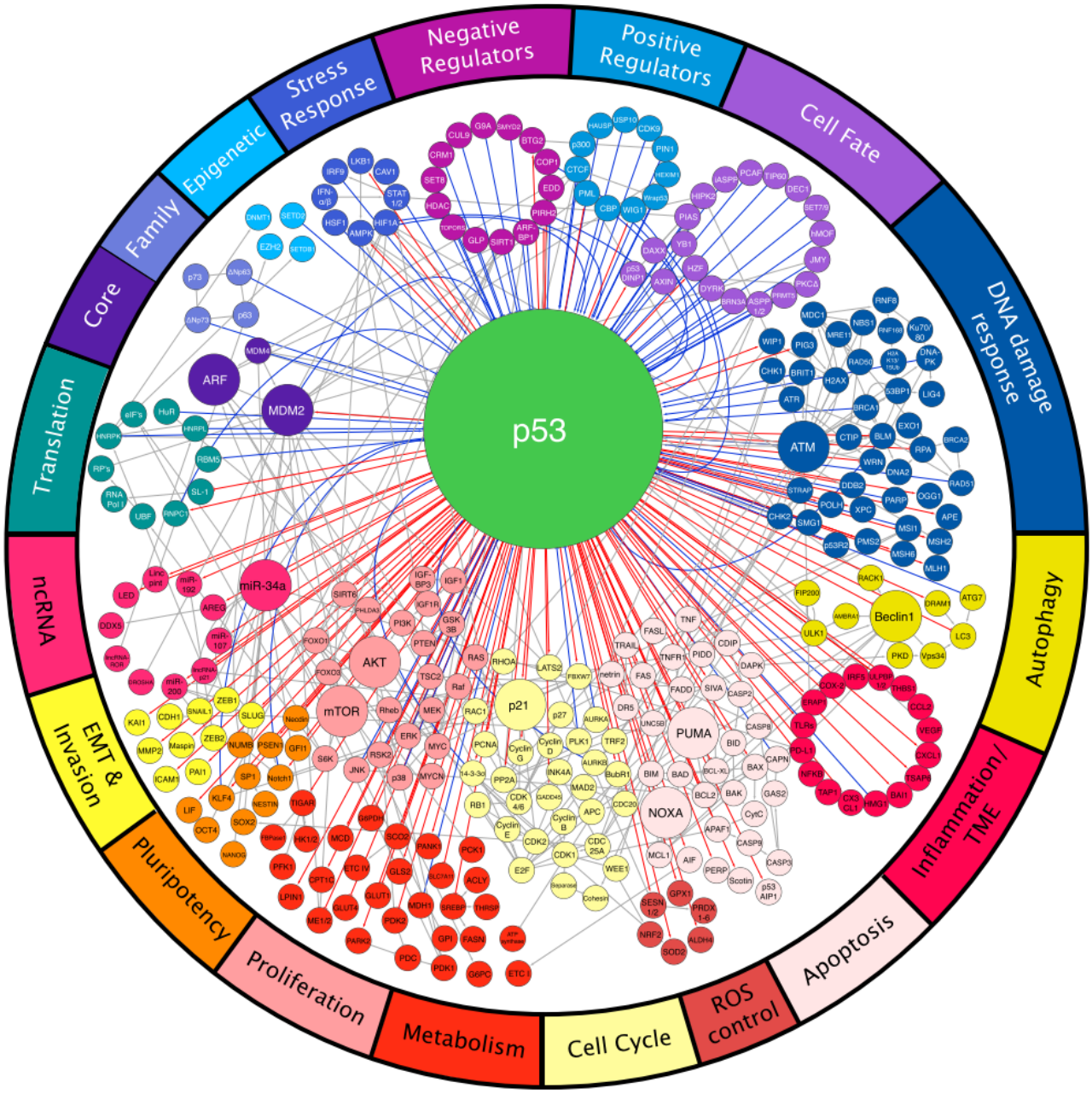

Figure 1.1: Intricate networks mediate diverse cellular function of TP53

TP53 has many regulators (top portion, indicated by blue lines) and effectors (bottom portion, indicated by red lines) that impact various cellular processes. Image from Kastenhuber and Lowe 2017[12].

1.1.2 Malfunctioning of TP53 in cancer

Cancer cells are inherently deregulated entities that must often develop ways to evade cell cycle arrest and apoptotic signaling mechanisms fundamentally maintained to protect the organism from such malfunctioning. Inhibition of TP53 through deletion, mutation, or deregulation often results in release from these protections. This is highlighted by the observation that that over 50% of all cancers harbor *TP53* mutations and that germline *TP53* mutations occur in approximately 70% of individuals with Li-Fraumeni Syndrome, an autosomal dominant disorder that pre-disposes individuals to early onset cancer[13-15].

While *TP53* mutations have been reported to occur throughout the length of the protein, resulting in missense, frameshift, and nonsense mutations, the vast majority of mutations are missense mutations occurring in the DNA-binding domain. These mutations can produce proteins that are classified as either structural mutants, with some of the most frequent being R175H, G245S, R249S, and R282H, or DNA-contact mutants, with some the most frequent being R273H, R248Q, and R248W (**Figure 1.2**).

Although mutant TP53 is naturally unstable, once it stabilizes it is typically substantially overexpressed and can contribute to overall tumorigenesis and progression[15, 16]. Importantly, these mutations may not only impede proper TP53 functioning, but they may also gain dominant-negative functions to repress the activity of any remaining wild-type TP53 within the cell or they may exhibit oncogenic gain-of-functions[17, 18]. Notably, numerous studies have found that certain TP53 mutants are able to regulate transcription of new sets of genes that mediate enhanced proliferation, metastasis, and survival, among others.

In addition to alterations of TP53 itself, other proteins also exhibit pathological regulation of TP53. One of the most prominent examples of this is in the case of MDM2-amplified or

overexpressing cancers. Amplification of MDM2 has been documented in approximately 3-7% of all cancers, and is particularly enriched in sarcomas[19, 20]. Overexpression of MDM2 results in TP53 dysregulation and cancer cell evasion of cell cycle arrest and apoptosis, among other oncogenic capabilities[21].

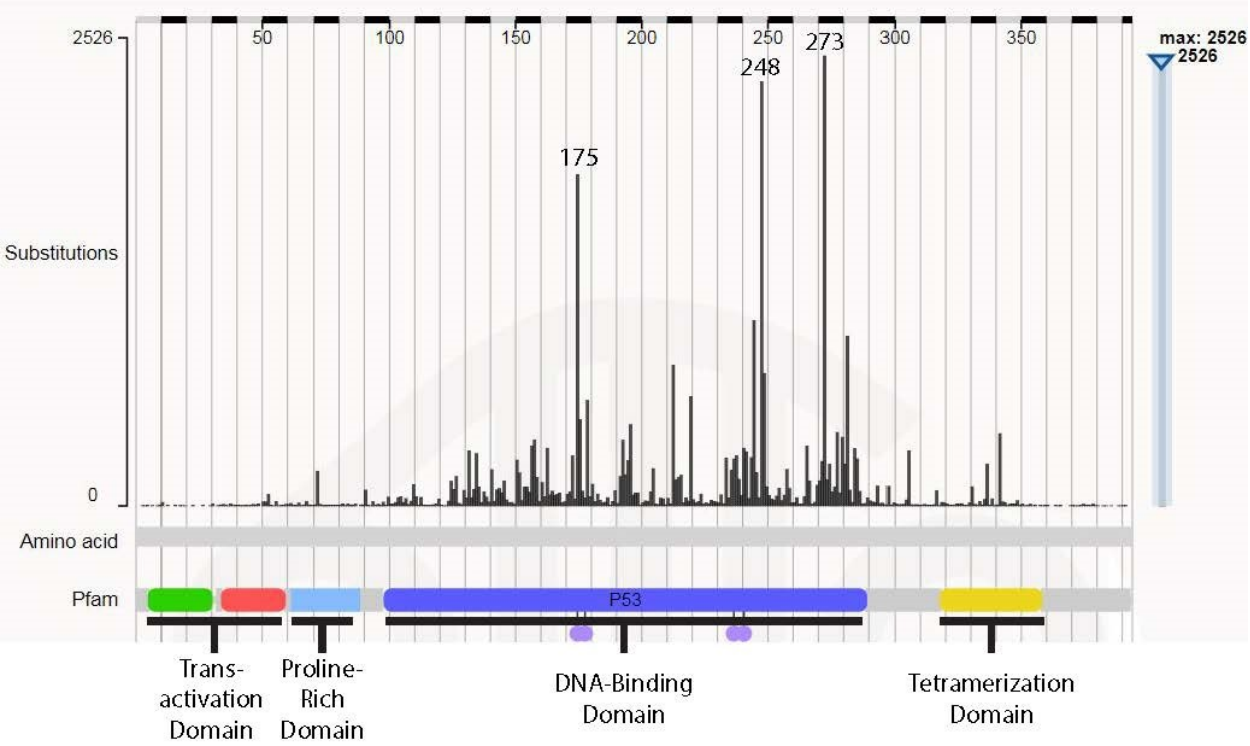

Figure 1.2: Most *TP53* mutations occur as missense mutations in the DNA-binding domain

The top horizontal bar indicates amino acid position along the TP53 protein. Quantification of witnessed substitution mutations at each location is indicated by vertical bars with the maximum count being 2,536 at position 273. The bottom of the figure contains an annotation of the major domains in which these mutations are seen. Image captured and amended from the Catalogue of Somatic Mutations in Cancer (COSMIC) database, GRCh38, COSMIC v87[22].

1.2 Strategies for targeting TP53-deficient cancers

Targeting TP53-deficient cancers has been complicated for two key reasons. First, developing therapies that target tumor suppressors is challenging due the difficulty of developing therapeutic approaches that restore wild-type functionality. Second, the majority of TP53 alterations in cancer are not merely loss of wild-type function, but can also encompass novel oncogenic gain-of-function that varies from mutant to mutant. However, there are several approaches under development to treat TP53-deficient cancers that can fall under three broader categories: restoration or enhancement of wild-type TP53 function, inhibition of mutant TP53, or exploitation of unique vulnerabilities imposed by TP53 dysfunction, such as synthetic or collateral lethality (**Figure 1.3)**[23-26].

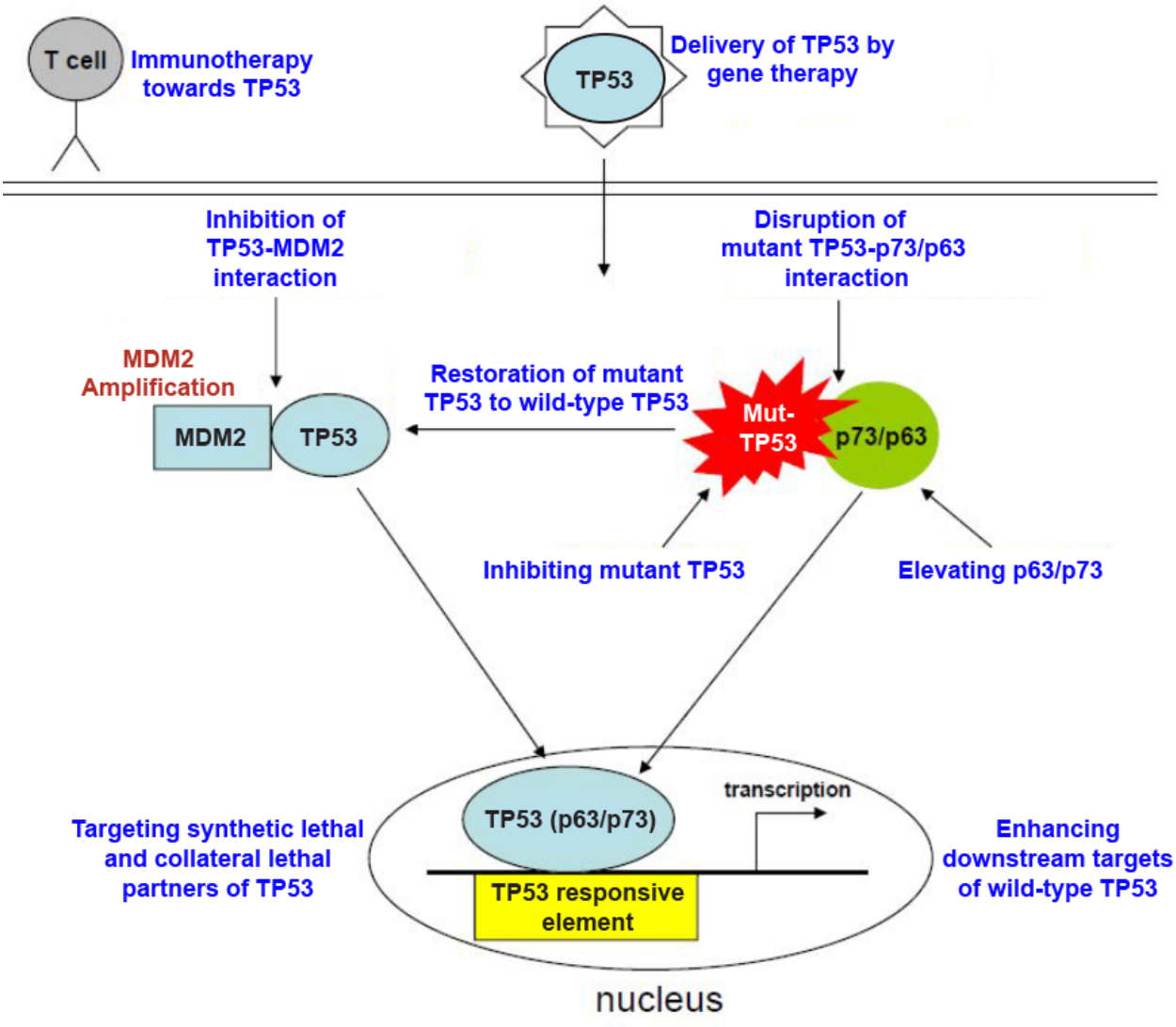

Figure 1.3: Strategies for targeting TP53-deficient cancers

Due to the difficulty of targeting TP53 in cancer, numerous strategies are under development to effectively target these cancers. As TP53 can be deregulated by MDM2-mediated inhibition, *TP53* loss or mutation, or inhibition of downstream functionality, strategies occur at each of these levels. Blue labels indicate targeting strategy. Figure adapted and amended from Hong et al. 2014[24].

1.2.1 Restoration of wild-type TP53 function

In order to restore wild-type TP53 function through gene therapy, studies have attempted to use replication-deficient adenovirus to reintroduce wild-type *TP53* or its other tumor suppressive family members *p63* and *p73* [27, 28]. Multiple studies have demonstrated efficacy of this technique in various cancer models and clinical trials. However, there are two major limitations of this approach. The first is the inability to deliver and infect all cancer cells within a patient, requiring additional treatment strategies, and the second is complications from host antibodies against the virus that further reduces infectivity.

One of the most advanced strategies for restoring wild-type TP53 function is the chemical disruption of the MDM2-TP53 interaction in TP53 wild-type cancers. Cancers with MDM2-amplification are known to exhibit enhanced growth in part through inhibition of TP53[21]. Thus, various drugs have been created to disrupt the MDM2-TP53 interaction in these cells. Doing so leads to stabilization and activation of TP53 with subsequent cell cycle arrest and death[29]. A few of these compounds have shown great promise in pre-clinical studies and are now under clinical investigation[30-32]. However, recently Jung et al. observed that patients can develop resistance to MDM2 inhibitors[33]. Through the use of circulating cell-free DNA, they found that patients who become resistant acquire *TP53* mutations. Consequently, effectively targeting these cancers will likely require combination therapy to address both the MDM2-TP53 interaction and additional treatments targeting TP53-mutated cells, such as those discussed below.

Various groups have created molecules or peptides that can restore certain aspects of wild-type TP53 functionality to mutant TP53, reviewed extensively elsewhere[26, 34]. These include molecules that bind directly to particular mutant TP53 and induce a conformational

change to a more wild-type conformation, such as PRIMA-1/PRIMA-1MET[35-37], MIRA-1/2/3[38], and STIMA-1[39] among others[24, 25]. There are also molecules that can restore TP53 sequence-specific DNA binding and transcriptional activity to certain mutants such as p53R3[40], SCH529074[41], and RITA[42, 43]. Importantly, these compounds have only been tested in a few TP53-mutant backgrounds (generally 1 to 5 mutants), and the matter of whether any can reactivate all mutants is still unclear. Without further evidence supporting their broad-spectrum efficacy, these compounds may only provide value in certain circumstances. If that is the case, to implement these strategies clinically, knowledge of a patient's specific TP53 status will be necessary to determine which drug to use. Further complications emerge if patients harbor more than one kind of TP53 mutation or develop novel TP53 mutations during cancer progression. Therefore, at this time, these therapies may have limited clinical utility, given the spectrum of TP53 deficiencies seen in patients and current limitations in mainstream diagnostics.

Thus, while preclinical studies looking at the therapeutic efficacy of strategies to restore wild-type TP53 function to TP53-deficient tumors look promising, evidence for broad-spectrum efficacy of these therapies is uncertain.

1.2.2 Inhibition of mutant TP53 function

As demonstrated above, many strategies used to enhance some aspect of wild-type TP53, also act by inhibiting mutant TP53, usually through release of dominant-negative effects. In addition to those strategies covered in the previous section, approaches for destabilization and degradation of mutant TP53 are also under investigation. Since mutant TP53 is inherently unstable, these approaches aim to target stabilizers of the protein[16]. For example, the molecular chaperone, heat shock protein 90 (HSP90) is able to bind to and stabilize mutant

TP53[44, 45]. Consequently, inhibition of HSP90 by over a dozen inhibitors has shown promise in preclinical studies, and one such compound, ganetespib, is currently in clinical trials[46, 47].

A relatively new approach for targeting TP53 mutant cancers is through an anti-aggregation approach. Studies have demonstrated that both wild-type TP53 and certain TP53 mutants can form aggregates in cancer, contributing to wild-type TP53 inactivation and mutant TP53 gain-of-functions [48-53]. Importantly, mutant TP53 appears to increase aggregation propensity and is believed to be at least partially responsible for the dominant-negative phenotype of mutant TP53[52, 54]. Thus it has been proposed that targeting these protein aggregates may yield therapeutic benefit[54]. To date, only three studies have attempted to disrupt TP53-mutant aggregates using either small stress molecules or designer peptides. This includes treatment of cells with arginine and its analogues to inhibit R248Q and R175H mutant peptides [55], treatment with acetylcholine chloride to inhibit R248W peptide aggregation *in vitro*[56], and treatment with a peptide created by Soragni et al. called ReACp53 in multiple ovarian cancer models[57]. The studies looking at arginine and ReACp53 also looked at proliferation and found that in addition to inhibiting peptide aggregation, there was a concurrent reduction in cell growth. However, these studies are still in their infancy, and additional systemic effects of such treatment are currently unknown.

1.2.3 Exploiting novel vulnerabilities imposed by TP53 dysfunction

Synthetic lethality refers to the phenomenon whereby obstruction of two or more genes within a cell is sufficient to induce cell death whereas loss of only one or another of these genes allows cells to remain viable. This concept was first described in *Drosophila* in 1922, but the term “synthetic lethality” would not be coined until 1946[58-60]. It would take even longer

before the first studies of this concept were done in human cells. The first chemically-based synthetic lethality screen was performed in 2001, while the first genetically-based synthetic lethality screens would emerge in 2003 and 2004[61-63]. Since these initial screenings, many more have been adapted and undertaken in an attempt to identify novel partners that display a synthetic lethal relationship, particularly in cancer. This approach is especially attractive in cancers that are intractable or where emergence of resistance is a recurrent issue, such as the case with KRAS, Myc, and TP53 altered cancers.

The most advanced example of exploiting synthetic lethal relationships in cancer is seen in the use of PARP inhibitors in *BRCA1/2* mutated cancers[64, 65]. Both BRCA1/2 and PARP1 play key roles in DNA damage repair, and when both pathways are simultaneously defective cells are unable to maintain sufficient DNA integrity and undergo mitotic catastrophe. Cancer cells harboring *BRCA1/2* mutations are thus sensitive to PARP inhibitors, while similarly treated normal cells that maintain BRCA1/2 repair mechanisms remain largely viable. In 2014, olaparib was the first PARP inhibitor approved by the FDA for use in treating BRCA mutated ovarian cancer[66]. Since then, several other PARP inhibitors have been approved for treatment of cancers harboring BRCA mutations, highlighting the clinical utility of exploiting these relationships[67].

Within the last two decades, a number of potential synthetic lethal partners for TP53 have been proposed[23, 68]. The function of these partners generally falls into one of two categories: cell cycle regulators and metabolic regulators.

Since TP53 plays a major role in halting the cell cycle at the G1/S phase to repair DNA damage, cells that lack functional TP53 rely heavily on the G2/M checkpoint to repair DNA damage and maintain genomic stability. In TP53-null cancers, it has been shown repeatedly that

blocking key players in G2/M - including ATR, Chk1, ATM, Chk2, and Wee1 - and treating cells with DNA-damaging agents leads to selective death through mitotic catastrophe[23, 69-73]. The most advanced of these targets is Wee1, a kinase responsible for arresting the cell cycle at the G2-M checkpoint[74]. Phase I and II clinical trials with the Wee1 inhibitor AZD1775 have shown efficacy in treating advanced tumors and enhancing efficacy of carboplatin in patients with mutant TP53[75, 76]. Additionally, Wang and Simon conducted a computational study of 5 gene expression databases and proposed numerous mitotic kinases as potential synthetic lethal partners for TP53-null cells[77]. These included various members of the CDK family, PLK1, PLK4, AURKA, NEK2, BUB1, and TTK. Of those kinases identified, few have been validated and consistent in TP53-dependent contexts. For example, several studies have shown that TP53-deficient cells are more sensitive to PLK1 inhibitors[78, 79], while others have shown little to no TP53-dependent difference[80-82]. There have also been challenges in creating optimal drug combination studies (as many of these inhibitors are tested alongside DNA-damaging agents) and in developing inhibitors that are both safe and effective enough to make it through clinical trials.

Deregulation of TP53 is also linked to enhancing the Warburg effect, a metabolic shift observed in cancer cells that favors glycolysis over mitochondrial respiration for energy production[83]. When glycolysis is suppressed in cancer, cells are unable to appropriately upregulate mitochondrial respiration and ultimately undergo cell death[84]. Indeed, several studies have identified metabolic vulnerabilities in TP53-deficient cancers. Both, Phosphatidylinositol-5-Phosphate 4-Kinase Type 2 components (PI5P4Kα/β)[85] and serine starvation[86] selectively impair TP53-null cells through disruption of glucose metabolism and impaired reactive oxygen species homeostasis. Furthermore, Kumar at al. found that TP53 null

and mutated cells accumulate arachidonic acid and undergo apoptosis in response to treatment with the mitochondrial uncoupler niclosamide[87]. Normally, TP53 can upregulate lipid oxygenation genes that allow the breakdown of arachidonic acid; however, TP53-null and mutated cells appear unable to mediate this response. Thus as arachidonic acid builds, inducing mitochondrial stress, cyctochrome c is released, caspases are activated, and apoptosis is triggered. Although metabolic synthetic lethal partners for TP53 are relatively limited compared to those in the cell cycle pathway, these studies demonstrate that various metabolic components could represent opportunities for identification of novel vulnerabilities.

In addition to the concept of synthetic lethality, a newly proposed concept of collateral lethality has emerged. This concept utilizes the knowledge that upon genomic deletion of tumor suppressers in cancer, neighboring genes on the chromosome may often also be deleted. Consequently, loss of these neighboring genes may provide novel opportunities to exploit synthetic lethal relationships in cases of tumor suppressor co-deletion. Over the past few years, two such collateral lethal relationships have been identified within *TP53*-deleted cancers. The first was found in 2015, when Liu et al. observed that there were frequently hemizygous deletions of *POLR2A*, located 200 kb downstream of the *TP53* gene, concurrent with hemizygous *TP53* deletion in colorectal cancer[88]. The authors further confirmed that inhibition of POLR2A in this context specifically reduced cell growth. The second study, by Fan et al., identified homozygous deletion of *FXR2*, located 100kb downstream of *TP53*, concomitant with homozygous *TP53* deletion across various cancer types[89]. Through inhibition of the *FXR2* family member, *FXR1*, the authors were able to selectively inhibit cell proliferation of cells with *FXR1/TP53* co-deletion. While collateral lethality studies appear promising in the context of *TP53*-deleted cancers, the general applicability is limited due to the vast majority of *TP53*

alterations being missense mutations. As such, other synthetic lethal approaches that cover a range of *TP53* deficiencies will likely reveal greater clinical promise.

Lastly, normal cells maintain low levels of wild-type TP53 while mutant TP53 is often vastly overexpressed in cancer, creating an opportunity to use TP53 as an antigen for vaccination. Various TP53-based cancer vaccines have gained traction in Phase I and II clinical trials using synthetic peptides, such as TP53 synthetic long peptide (p53-SLP) vaccine[90, 91], genetically engineered MVA-virus transduced with wild-type TP53[92], and adenoviral transduction of TP53 into dendritic cells (DC-ad-p53)[93, 94]. However, clinical response to these vaccines alone are generally lacking. More recent efforts have focused on combination immunotherapy and chemotherapy for more effective treatment[95-97].

1.3 Introduction to the EKC/KEOPS complex

The Endopeptidase-like Kinase Chromatin-associated protein complex (EKC)/Kinase putative Endopeptidase and Other Proteins of Small size protein complex (KEOPS) is an evolutionarily conserved complex that has been primarily studied in non-human organisms. This complex is comprised of five known members in human cells: O-sialoglycoprotein endopeptidase (OSGEP), L antigen family member 3 (LAGE3), C14ORF142 or Gon7, the atypical serine/threonine kinase TP53 Regulating Kinase (TP53RK or PRPK), and TP53RK binding protein (TPRKB)[98-102].

1.3.1 Role of the EKC/KEOPS complex across organisms

Since the EKC/KEOPS complex has not been heavily studied in humans, much of what we know about it is derived from its role in other organisms. Canonically, the EKC/KEOPS

complex is recognized for its role in forming the N6-threonylcarbamoyladenosine (t6A) modification at position 37 of all ANN-codon recognizing tRNAs. It has also been implicated in telomere length regulation and gene transcription in yeast[99, 100, 102-104].

Although the human EKC/KEOPS complex structure has not been solved, the yeast complex has. Through the use of homology modeling and statistical analysis of published co-fractionation/mass spectrometry data, a human model was created that matches the functions and interactions reported in the literature (**Figure 1.4**)[105]. This model illustrates the direct binding between TPRKB and PRPK, PRPK and OSGEP, and OSGEP with LAGE3 and C14ORF142.

While the exact role of each member of the EKC/KEOPS complex has not been fully solved, in Archaea the minimal functional complex involves Bud32 (PRPK ortholog), Kae1 (OSGEP ortholog), and Pcc1 (LAGE3 ortholog)[103]. In this context, Kae1 was identified as the catalytic subunit that condenses an active threonylcarbamoyl-adenylate with tRNA. Bud32 acts as an ATPase and Pcc1 has dimerization capabilities not inherently related to t6A formation. The purpose of these and functions of the remaining members is unclear[103, 106, 107]. It has been proposed that the other components act as supporting units for Kae1's biosynthetic functions. This is supported by the observation that neither Bud32 nor CGI-121 (TPRKB ortholog) participates directly in t6A biosynthesis; however, the binding of CGI-121 to Bud32 is believed to affect overall conformation and ultimate efficiency of t6A production[103].

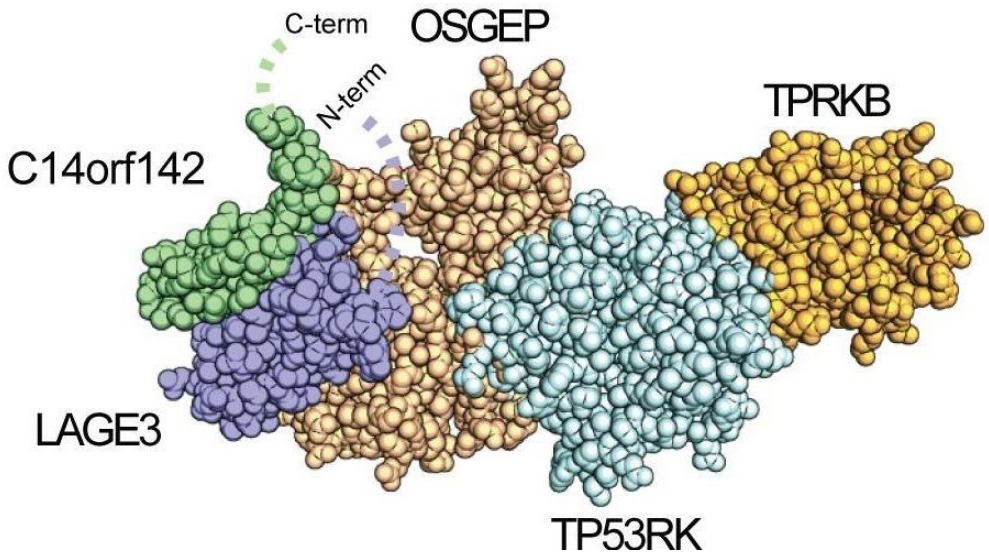

Figure 1.4: EKC/KEOPS Complex Modeled

The human EKC/KEOPS complex is comprised of 5 subunits: TPRKB, TP53RK (or PRPK), OSGEP, LAGE3, and C14ORF142. Drew el al. utilized what is known about the yeast complex and a statistical analysis of previously published co-fractionation/mass spectrometry experiments to model the human complex. Figure from Drew et al. PLoS Comput Biol. 2017[105].

1.3.2 Role of the EKC/KEOPS complex in human disease

Despite the relatively few publications covering the role of the EKC/KEOPS complex and its constituents in humans, there are several studies emerging that have implicated them in the development or progression of two diseased states – Galloway-Mowat Syndrome (GAMOS) and some cancers.

A recent study by Braun et al. demonstrated that dysfunction within various members of the complex contributed to the development of GAMOS, a rare autosomal-recessive condition characterized by early-onset nephrotic syndrome, microcephaly, and developmental delays[108]. Through whole-exome sequencing of patients with GAMOS, the authors report that 37/907 patients carried a mutation in one of four EKC/KEOPS complex members: OSGEP, PRPK, TPRKB, and LAGE3. They further showed that depletion of individual members of this complex

in human podocytes led to reduced cell proliferation, slightly impaired protein translation, and activation of the Unfolded Protein Response and the DNA Damage Response. Additional studies have since confirmed the occurrence of OSGEP and PRPK mutations in individuals with GAMOS and GAMOS-like phenotpyes[109-112].

In 2012 a study connected the EKC/KEOPS complex to the oncoprotein Preferentially Expressed Antigen in Melanoma (PRAME), a transcriptional repressor of the retinoic acid pathway that is overexpressed in numerous malignancies[113, 114]. This study claimed that PRAME interacts with the EKC/KEOPS complex to recruit Cullin2 ubiquitin ligases and that the complex is present at PRAME-bound promoters[113]. The authors suggest that these interactions support a functional link in their pathways. However, a limitation of these claims is that the data presented only demonstrates interactions between OSGEP and LAGE3 with PRAME and the Cullin2 ligases, leaving the possibility that OSGEP and LAGE3 may form a separate complex that associates with these factors independently from the rest of the EKC/KEOPS complex. This possibility is further substantiated by a recent study which performed AP:MS on the members of this complex individually and found differing yet overlapping interactomes between members of the complex that suggest the potential for sub-complex formation[101].

Aside from the complex, overexpression of PRPK has been implicated in several cancer types. First, PRPK was linked to poor prognosis in patients with multiple myeloma and either genetic or pharmacological inhibition of PRPK triggered apoptosis in multiple myeloma cell lines[115]. PRPK is also phosphorylated and activated by the serine-threonine kinase T-LAK-cell-originated protein kinase (TOPK) in colorectal cancer leading to enhanced metastasis[116]. Finally, PRPK has been shown to interact directly with the tumor suppressor TP53 and phosphorylate it on Ser-15[117].

While the EKC/KEOPS complex and its components are implicated in GAMOS and cancer, there are limited and lacking mechanisms proposed for these pathologies.

1.4 tRNAs and protein translation in cancer

Cancer is a complex set of diseases that can harbor alterations in nearly every aspect of the cell from genetic mutations to protein deregulation and shifts in microenvironment dynamics. As such, massive –omics-scale datasets have emerged to identify and characterize changes that promote tumorigenesis and metastasis. In particular, genomics and transcriptomics have exploded in an effort to identify gene mutations, chromosomal changes, and gene expression patterns in particular cancers. While this data has provided insight as to how cells are able to develop the classic hallmarks of cancers[118], several reports have demonstrated that these changes do not always correlate with functional proteomic alterations[119, 120].

Furthermore, a growing body of evidence implicates protein translation defects as major contributors to cancer promotion and progression. Interest in studying translational alterations have shifted over the past decade from early studies on translation initiation to those focusing on translational elongation, mRNA structure, and tRNA pools. Given the essentiality of the EKC/KEOPS complex in performing the t6A modification of tRNAs, we are particularly interested in how tRNA modifications may contribute to cancer phenotypes and the role that TP53 may have in this context.

1.4.1 Overview of protein translation

Ribosomes are an intricate complex formed by four types of ribosomal RNA (rRNA) and over eighty different ribosomal proteins that facilitate protein synthesis within the cell[121]. In

mammalian cells, RNA Polymerase I (Pol I) is required for transcription of rRNAs that, after processing, make up the 18S, 5.8S, and 28S rRNA species. The fourth rRNA found in ribosomes, 5S, is transcribed by RNA Polymerase III (Pol III). Together these four rRNAs associate with ribosomal proteins to form the 40S and 60S mature ribosomal subunits that are needed for protein translation.

As mentioned previously, initiation of protein translation is seen as one of the major regulators of protein synthesis as it is the most complicated phase[122]. During canonical protein translation initiation, the initiator-methionyl transfer RNA (tRNAi-Met) associates with various eukaryotic initiation factors (eIFs) and is recruited to the 40S small ribosomal subunit to form 43S-preinitiation complex (PIC). The eIF4F complex, responsible for recognizing and binding mRNA that has acquired a m^7GpppN cap at its 5'-end, is then recruited along with its associated mRNA to 43S-PIC to form 48S-PIC. At this point, the complex scans the 5' untranslated region (UTR) of the mRNA until tRNAi-Met recognizes the AUG start codon. After a GTP:GDP hydrolysis reaction of eIF2, the remaining eIFs are released, and the 60S ribosome binds the 40S ribosome to form the 80S ribosome commencing protein translation.

The above process is termed "cap-dependent" protein translation, but a growing body of evidence has emerged for "cap-independent" protein translation. Cap-independent translation does not require the 5'-m^7GpppN cap on mRNA, but instead relies on a particular region of the mRNA, such as an internal ribosome entry segment (IRES) or a cap-independent translational enhancer, for recruitment to the 40S ribosome[123]. This alternative method of translation is important as shifts to greater utilization of cap-independent protein translation have been witnessed in states of cellular stress and cancer[124, 125].

After the complex process of translation initiation has occurred, the relatively simpler process of translational elongation commences[126]. The elongation factor EF-1, GTP, and an aminoacetylated tRNA enter the A site of the ribosome. Once the mRNA codon and tRNA anticodon are matched, GTP is hydrolyzed, EF-1 departs, and the ribosome undergoes a conformational change to move the new aminoacetylated tRNA to the P position where it merges with the growing polypeptide chain. A second elongation factor EF-2 then enters the A site, hydrolyzes GTP and resets the ribosome to its original conformation, prepped for aminoacetylated tRNA acceptance. This process continues until the mRNA has been fully decoded and the new protein product has formed.

Thus, there are many opportunities for translational regulation of proteins. Beyond regulation of rRNAs, eIFs, and ribosomal proteins during translation initiation or regulation of tRNAs and elongation factors in translational elongation, there are numerous other factors that can contribute to regulation at the protein biosynthesis level, such as RNA structures, modifications, and so on. Those factors relevant for the current study will be further highlighted below.

1.4.2 Overview of tRNA biology

tRNAs are small nucleotide sequences of approximately 70-90 nucleotides in length that are required for translating codons within mRNA species to their amino acid counterpart. As one of the most abundant RNA species in a cell, tRNAs account for approximately 10% of a cell's total RNA by weight. Due to codon "wobble" capabilities of tRNA isoceptors, only 49 isoceptors are required in humans, but these are encoded by 513 nuclear tRNA genes and 22 mitochondrial

tRNA genes[127]. As such, isoceptors for the same anti-codon may have variable expression and regulation depending on cell type and environment[128].

Early analyses of tRNAs focused primarily on structure and biology which have now been heavily studied. The tRNA secondary structure resembles a cloverleaf comprised of 5 key regions: 1) the acceptor stem containing the 5' terminus and the 3'-terminus, including the CCA sequence required for aminoacetylation, 2) the D-arm, 3) the anti-codon arm, 4) the variable loop, and 5) the T-arm[129, 130] (**Figure 1.5**). Together, the D- and T-arms facilitate folding into an L-shaped tertiary structure[131].

tRNAs are some of the most widely modified RNAs within a cell. There are over 170 known modifications that can occur on RNA molecules, and each tRNA has an average of 13 modifications that contribute to the proper structure, stability, and functionality of the tRNA[132-135]. Modifications within the D- or T- arms contribute to proper structure and stability[130]. Meanwhile those occurring at or in the anticodon loop, particularly at positions 34 (also known as the "wobble" position) and 37, are critical for proper codon:anti-codon pairing and thus overall translational efficiency and fidelity[130, 136]. Each modification is deposited by specific tRNA-modifying enzymes that, in turn, determine the overall functionality of the tRNA.

For the most part, tRNAs were believed to have "housekeeping" functions and the pool of available tRNAs was rarely a limiting factor or influencer for protein translation. However, within the last decade, a body of evidence has emerged challenging this view. Disproportionate expression of specific tRNA isoceptors controls translational speed as use of low-abundance tRNAs produce ribosome pausing, slowed translation rate, and co-translational protein folding[137]. Furthermore, the heterogeneity of tRNA pools is tissue-specific and reflects the needs of a cell at a particular time[138]. For example, proliferative cells have a unique tRNA

pool from that of a differentiated cell, whereby tRNAs expressed in proliferating cells are repressed in differentiated cells[139]. Thus, there exist multiple levels of tRNA regulation from expression, modification, and adaptation to cellular demands.

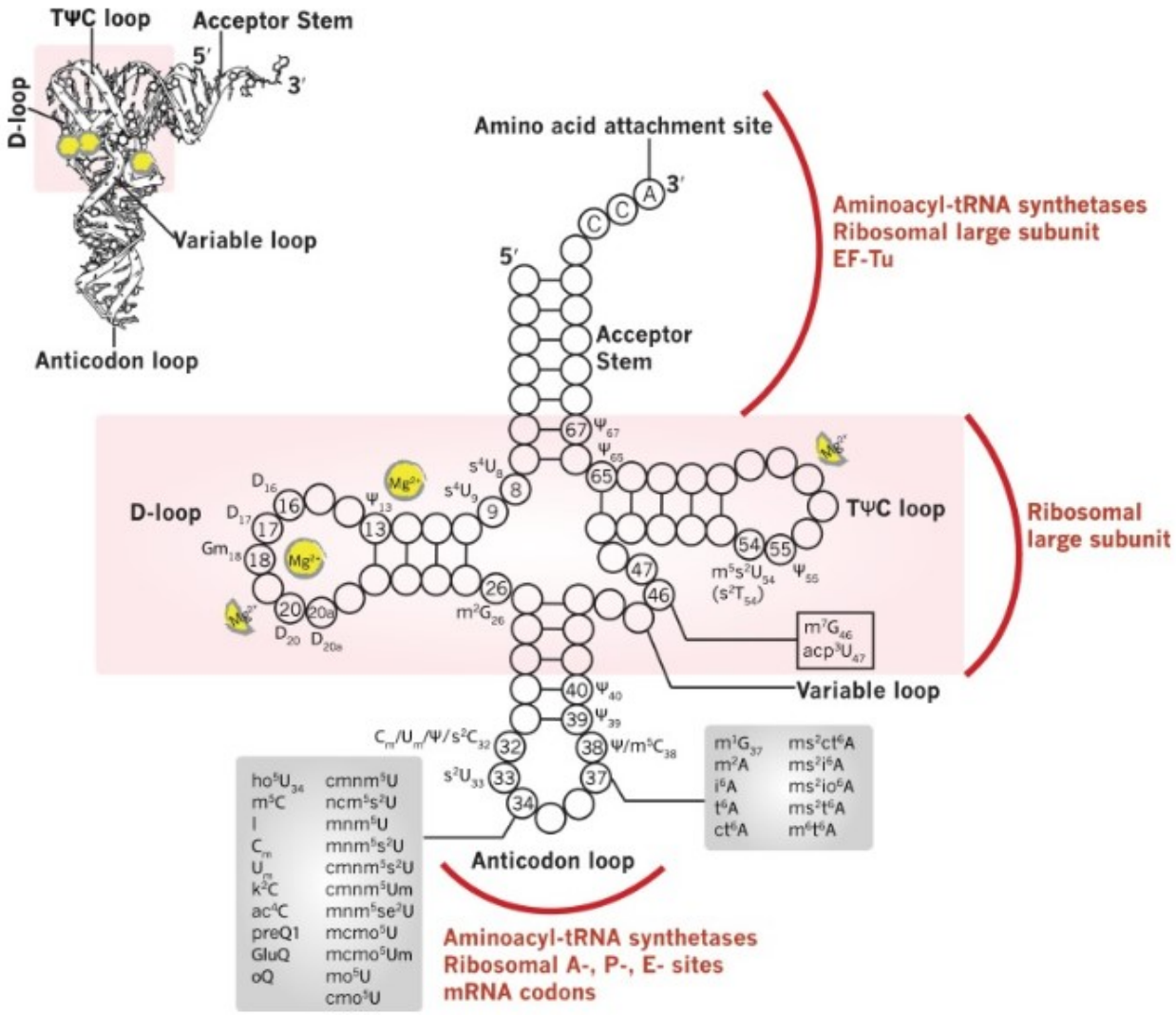

Figure 1.5: tRNA structure, modifications, and interaction sites

tRNA secondary structure resembles a cloverleaf whose structural domains are noted in black and interaction sites are indicated in red. As tRNA molecules are heavily modified, frequently occurring (prokaryotic) nucleoside modifications are denoted alongside their position of placement. The corresponding tertiary structure can be found in the upper left portion of the figure. Figure from Koh and Sarin, 2018[140].

1.4.3 tRNA and translation defects in human disease

It has been logically proposed that cancer cells require enhanced protein synthesis to maintain demands of their highly proliferative states[141]. Barna et al. demonstrated that the enhanced protein synthesis observed in Myc-transformed cells could be attenuated by the heterozygous deletion of ribosomal protein L24[142]. Concurrently, mice that had been transformed with Myc and had partial deletion of L24 had significantly delayed onset of lymphomas compared to Myc-transformed L24-wild-type mice, demonstrating the importance of protein synthesis in tumorigenesis. Indeed, it has been shown that major oncogenic signaling pathways including Myc, PI3K/AKT, and Ras, are able to reprogram translational machinery to facilitate their oncogenic capabilities[143].

Beyond direct ribosomal control, emerging evidence links alterations in the overall pool of tRNAs, including relative tRNA abundances and modifications found on these tRNAs, to larger cellular processes and various human diseases. An overview of some alterations found across diseases can be seen in **Figure 1.6,** but for the purposes of this dissertation, an overview of tRNA alterations in cancer will be the main focus**.**

In the case of cancer, overall tRNA levels tend to be elevated[144, 145]. Beyond this observation, several studies have characterized certain tRNA alterations that occur in cancers. Overexpression of the tRNA modifying enzyme TRMT12 was identified in 87% (n=30) of breast tumors[146], and overexpression of tRNA-Leu was seen in ErbB2-positive breast cancer and is linked to enhanced cell proliferation under amino acid starvation conditions[147]. More recently, Goodarzi et al. demonstrated that tRNA-GluUUC and tRNA-ArgCCG are upregulated in breast cancer cell lines, acting to promote breast cancer metastasis[148]. Meanwhile, downregulation of the tRNA methyltransferase TRM9L was linked to enhanced tumor survival in several carcinoma

models and poor prognosis in lung cancer[149, 150]. While these correlative studies provide initial understandings that tRNAs may contribute to cancer progression, causal studies are only now emerging. In 2019 Chen et al. demonstrated that the m1A and m3C tRNA demethylase ALKBH3 promotes cancer proliferation, migration, and invasion through induction of tRNA derived small RNAs[151]. These small RNAs were able to regulate ribosome assembly, modulating translational capabilities, and prevent apoptosis through binding to cytochrome c. Thus, tRNA dysregulation may promote cancer and have crucial roles in disease etiology.

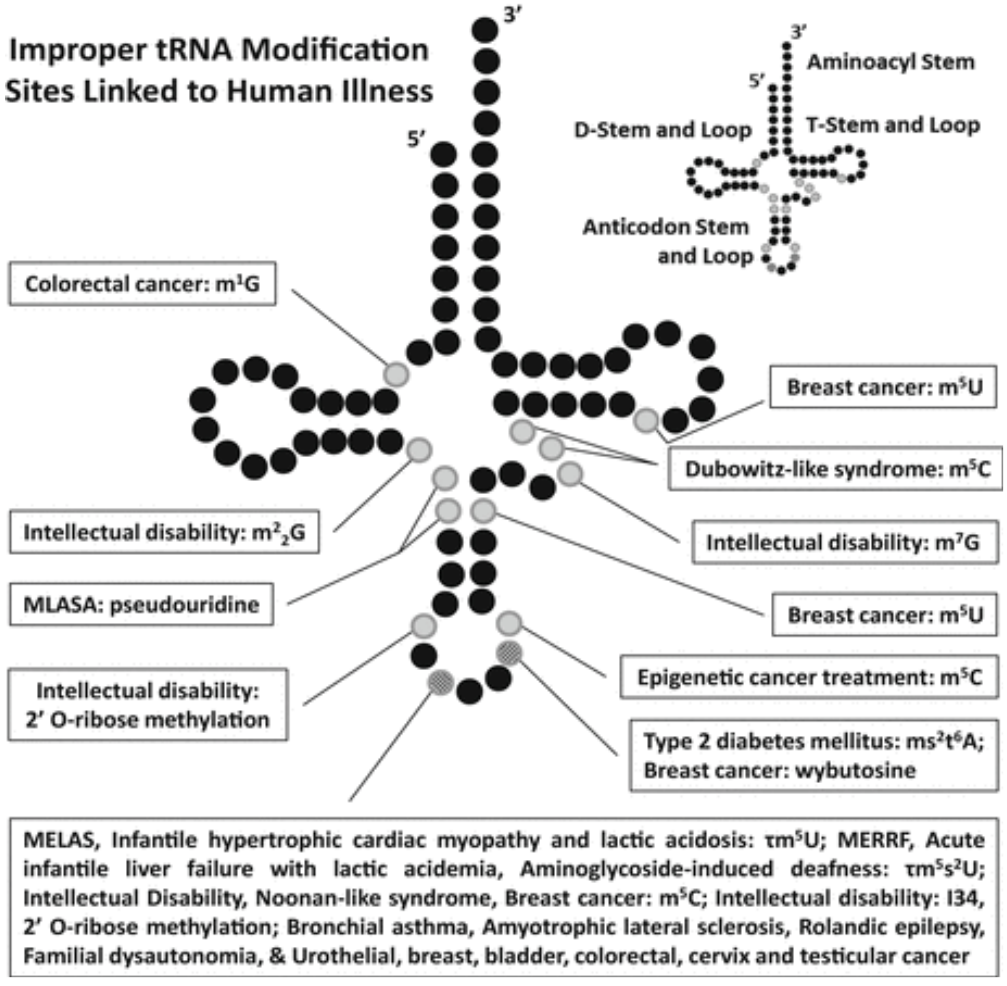

Figure 1.6: tRNA modifications are altered in human disease

Studies have linked various alterations in tRNA modifications with several diseased states. The above figure represents documented tRNA modifications associated with specific diseases. Figure from Frohlich et al. 2016[152].

1.4.4 Role of the t6A modification

The EKC/KEOPS complex is responsible for the second step in the t6A modification at position 37 of ANN-coding tRNAs. After Sua5 converts threonine, adenosine triphosphate, and bicarbonate into threonylcarbamoyl-adenylate, the EKC/KEOPS complex then deposits this modification on the appropriate tRNA[103, 106]. The t6A37 modification is one of the few tRNA modifications universally conserved across organisms and is important for normal cell growth and accurate protein translation in a range of bacterial, archaeal, and eukaryotic species[102, 153-157]. It has been found that this modification stabilizes the codon:anticodon interaction contributing to overall translational accuracy and efficiency[102, 155, 158]. Furthermore, in yeast t6A deficiency allows for upstream non-AUG codon translation initiation and increased frame-shift events in specific genes[159, 160].

In addition to the cytoplasmic EKC/KEOPS complex discussed above, in humans there is also a mitochondrial complex comprised of YRDC and OSGEPL1 that are involved in t6A37 formation in mitochondrial tRNAs[161, 162]. This complex has been implicated in normal mitochondrial functioning and mitochondrial genome maintenance further highlighting the important of t6A within the cell[157, 163].

1.4.5 Translation regulation by TP53

TP53 can regulate translational processes at both the transcriptional and translational level. Using RNA-seq and Ribo-Seq, Loayza-Puch et al. found that compared to proliferative cells, TP53-induced quiescent and senescent cells repressed ribosomal proteins exclusively during translation while genes encoding rRNA processing and ribosomal assembly proteins were largely downregulated transcriptionally[164]. The authors propose that tumor suppressive effects

of TP53 not only include cell-cycle arrest through transcriptional regulation, but also repression of translation to inhibit cell growth.

Furthermore, overall ribosome biogenesis and TP53 expression are interrelated. Certain ribosomal proteins can interact with and inhibit MDM2 when they are not complexed with rRNAs, allowing for stabilization of TP53 protein levels[165-171]. Under normal conditions, there is a balance in rRNA transcription and ribosomal protein synthesis that allows for some ribosomal protein association with MDM2, keeping TP53 levels relatively low. In the case of cancer, when rRNA synthesis is upregulated to accommodate enhanced proliferation, more ribosomal proteins are involved in ribosome formation than MDM2-binding, allowing MDM2 to mediate enhanced degradation of TP53[165]. Conversely, stabilized TP53 has been shown to inhibit both Pol I and Pol III transcription leading to overall reductions in rRNAs and tRNAs, thus negatively impacting protein translation[172-174].

Compared to the wealth of knowledge surrounding its DNA-binding capabilities, relatively little is known about TP53 RNA-binding. However, a series of biochemical approaches have suggested TP53 may modulate translation directly through RNA-binding[122, 175]. This concept was first proposed in the literature in 1991 with the discovery that 5.8S rRNA could attach to the C-terminal domain of TP53 at position S389[176]. Further, Oberosler et al. showed that not only does TP53 interact with RNA, but it has a stronger affinity for RNA than DNA[177]. The same study shows that TP53 facilitates DNA:DNA and, more efficiently, RNA:RNA hybrids. Since these discoveries, the nature of these interactions has been largely debated, particularly with regard to specificity and functionality. Some evidence implicates TP53 in the regulation of specific genes, such as FGF2[178], CDK4[179], MDMX[180], and its own[181] translation through 5'-UTR binding. However, these authors and others also

acknowledge non-specific RNA interactions occurring, proposing instead that structural motifs or post-translational modifications may impact interactions [175, 178, 180, 182]. Although these studies are largely in their infancy, a recent report made an interesting observation that mutant TP53 p.R273H has altered activity toward *MDMX* mRNA compared to wild-type TP53[180]. These investigations raise some exciting questions surrounding TP53 translational regulation through direct RNA binding, and more studies are needed to determine the extent of TP53 influence on not only mRNA, but also other RNA species, such as rRNAs and tRNAs.

1.5 Summary and Goals

Herein, we explore the role of TPRKB in human cells, particularly as it relates to cancer. We identified TPRKB as a vulnerability specifically in TP53-deficient cancers, with minimal effect in TP53 wild-type cells. We show that this reliance is largely independent of other EKC/KEOPS complex members, defining a novel function of TPRKB in human cancer. Further characterization of this phenotype reveals dynamic regulation of TPRKB by TP53 and PRPK. Attempting to parse out additional EKC/KEOPS-independent functions for TPRKB, we conducted co-immunoprecipitation experiments followed by mass spectrometry analysis to identify novel protein interactors for TPRKB. We discovered potential interactions with several proteins involved in protein translation and validate that TRMT6, a member of another tRNA modifying complex (TRMT6/TRMT61A), interacts with TPRKB, suggesting a potential role for TPRKB in several facets of protein translation. With this and TPRKB's role in t6A formation on tRNA, enhancing translational fidelity, and emerging roles of TP53 in translation regulation, we were interested in exploring whether this overlap could explain TPRKB sensitivity in TP53-deficient cells. We demonstrate that TPRKB depletion in TP53-null cells results in reduced

protein translation, several alterations in tRNA modifications, and downregulation of the RNA Polymerase III component, *POLR3GL*. Thus, we characterized TPRKB dependency across a range of human cell lines to determine its potential as a therapeutic target in TP53-deficient cancers.

Chapter 2 Identification and initial characterization of a specific TPRKB dependency in TP53-deficient cancers

Abstract

TP53 is a tumor suppressor that is activated by various stressors to mediate diverse cellular responses. As the most frequently mutated gene in cancer, therapeutically targeting the full spectrum of TP53-deficient cancers offers great clinical promise. However, developing these targeted strategies has been challenging. Through utilizing the Broad Institute's Project Achilles database, comprised of shRNA screening data across genomically characterized cell lines, we identified *TPRKB* as a novel vulnerability in *TP53*-mutated cancers. Using a panel of cell lines, we confirmed cells that were *TP53*-null, *TP53*-mutated, and those that harbored amplification of the TP53 negative regulator *MDM2* were more sensitive to TPRKB depletion than *TP53* wild-type cells, which showed little to no change in proliferation. We further confirmed with several isogenic cell lines that *TP53* and *MDM2* statuses are key factors for determining this vulnerability, as expression of wild-type *TP53* rescued negative phenotypes while over-expressing *MDM2* sensitized normally resistant cells. TPRKB is a member of an evolutionarily conserved tRNA-modifying complex known as the EKC/KEOPS complex; however, depletion of other members of this complex PRPK, OSGEP, and LAGE3 did not produce the same TP53-dependent phenotype as TPRKB depletion did, suggesting novel roles for TPRKB in human cells. Furthermore, this TPRKB dependency was accompanied by cell cycle arrest and reductions in anti-apoptotic proteins BCL2 and BCL2L1. Through the use of DNA-damaging agents in

conjunction with TPRKB depletion, we observed TPRKB-dependency was likely not mediated through overwhelming the DNA-damage response and cell cycle regulation pathways, as is the case with most other synthetic lethal partners identified for *TP53*-null cancers. Thus, our results identified a unique and specific requirement of TPRKB in a variety of TP53-deficient cancers and suggest novel roles for TPRKB in human cells that require further investigation.

Introduction

Tumor protein 53 (*TP53* or p53) is a transcription factor that mediates the expression of genes involved in a myriad of cellular processes. In response to DNA damage or other genotoxic stressors, TP53 acts to regulate cell cycle, senescence, and apoptosis[10]. Beyond these canonical functions, TP53 has also been implicated in cellular metabolism, autophagy, angiogenesis and migration[11]. The importance of TP53 as a tumor suppressor is highlighted by the observation that approximately half of all cancers harbor inactivating *TP53* mutations and these mutations are a driving force in cancer development and progression[14, 15]. Importantly, the majority of *TP53* mutations involve the production of mutant TP53 that loses wild-type function while potentially gaining oncogenic capabilities, in addition to deleterious mutations or homozygous deletion.

Development of effective therapies for tumor suppressors, such as TP53, have been challenging in part due to the difficulty of developing therapeutic approaches that restore function. Several potential approaches for targeting *TP53*-deficient cancers have been described[23-26], including those exploiting non-oncogenic addiction to induce anti-tumorigenic cellular events, such as synthetic lethality[183]. In this concept, genetic alterations render cancer cells dependent on genes that are not inherently oncogenic. The most advanced example of this is

the use of PARP inhibitors in *BRCA1/2* mutated cancers[64, 65]. Both BRCA1/2 and PARP1 play key roles in DNA damage repair, and when both pathways are simultaneously defective cells are unable to maintain sufficient DNA integrity and undergo mitotic catastrophe. Cancer cells harboring *BRCA1/2* mutations are thus sensitive to PARP inhibitors, while similarly treated normal cells that maintain BRCA1/2 repair mechanisms remain largely viable.

Herein, we analyzed shRNA-screening data from the Project Achilles cancer cell line compendium to identify *TP53RK Binding Protein* (*TPRKB*) as a specific vulnerability in *TP53*-altered cancers[184]. TPRKB is a member of the evolutionarily conserved Endopeptidase-like Kinase Chromatin-associated protein complex/Kinase putative Endopeptidase and Other Proteins of Small size protein complex (EKC/KEOPS), along with TP53RK (PRPK), OSGEP, LAGE3, and C14ORF142[98-102]. EKC/KEOPS is responsible for the essential N6-threonylcarbamoyladenosine (t6A) modification of all ANN-codon recognizing tRNAs, and it is important for telomere length regulation in yeast[99, 102-104]. Interestingly, previous studies of the EKC/KEOPS complex have demonstrated that PRPK interacts with, phosphorylates, and activates TP53[98, 117, 185]. Recently, germline mutations in EKC/KEOPS complex members have been linked to Galloway-Mowat syndrome, a rare condition characterized by early-onset nephrotic syndrome and microcephaly[108].

Herein, we identify TPRKB as a vulnerability specifically in TP53-deficient cancers, with minimal effect in TP53 wild-type cells. Furthermore, we show that this reliance is independent of other EKC/KEOPS complex members, defining a novel function of TPRKB in human cancer.

Results

Identification and validation of TPRKB dependency in TP53-mutant cell lines from Project Achilles

To identify potential vulnerabilities in cancers with specific genomic alterations, we mined data from the Broad Institute's Project Achilles[184]. Project Achilles contains information from genome-scale knockdown screens linked to observed cell survival in genomically-characterized cancer cell lines. We analyzed the original shRNA data set[184], using the raw microarray $\log_2$ fold change in shRNA abundances for each cell line at the conclusion of the screening relative to the initial plasmid DNA reference pool fold change. Cell lines were annotated based on the presence or absence of hotspot (in oncogenes) or hotspot/deleterious (in tumor suppressors) mutation status, and significant over-expression of mutations in highly growth inhibited cell lines was identified by a Fisher's exact test. We confirmed several expected oncogenic vulnerabilities, such as *BRAF* in *BRAF* mutated cancer and *ARID1B* in *ARID1A* mutated cancers (**Figure 2.1A**)[186].

Hence, we were intrigued as only a single gene *TPRKB*—a poorly characterized member of the EKC/KEOPS complex—was identified as a significant vulnerability in *TP53*-mutated (both hotspot and deleterious mutation) cancer cells (**Figure 2.1B**). Importantly, analysis of the COSMIC (https://cancer.sanger.ac.uk/cosmic)[187] and MiPanda (http://mipanda.org)[188] databases demonstrated that *TPRKB* is both ubiquitously expressed across normal and cancer tissues/cells and infrequently genomically altered in cancer**.** To confirm the Project Achilles data, we used siRNA in select Project Achilles' cancer cells lines, and confirmed marked decrease in proliferation in *TP53*-mutant vs. *TP53* wild-type cells (**Figure 2.1C**). Similar results were obtained with stable *TPRKB* knockdown using two independent shRNAs (**Figure 2.1D**),

validating the Project Achilles data identifying TPRKB-dependence in *TP53*-deficient cancers. Like *ARID1A* altered cell lines insensitive to *ARID1B* deficiency[186], we confirmed that some *TP53* altered cell lines were insensitive to *TPRKB* depletion, such as the *TP53*-mutant HT-29 cell line, which was predicted to be non-responsive in the Project Achilles screen and confirmed *in vitro* (**Figure 2.1E**), highlighting the need for further characterization of determinants of *TPRKB* sensitivity.

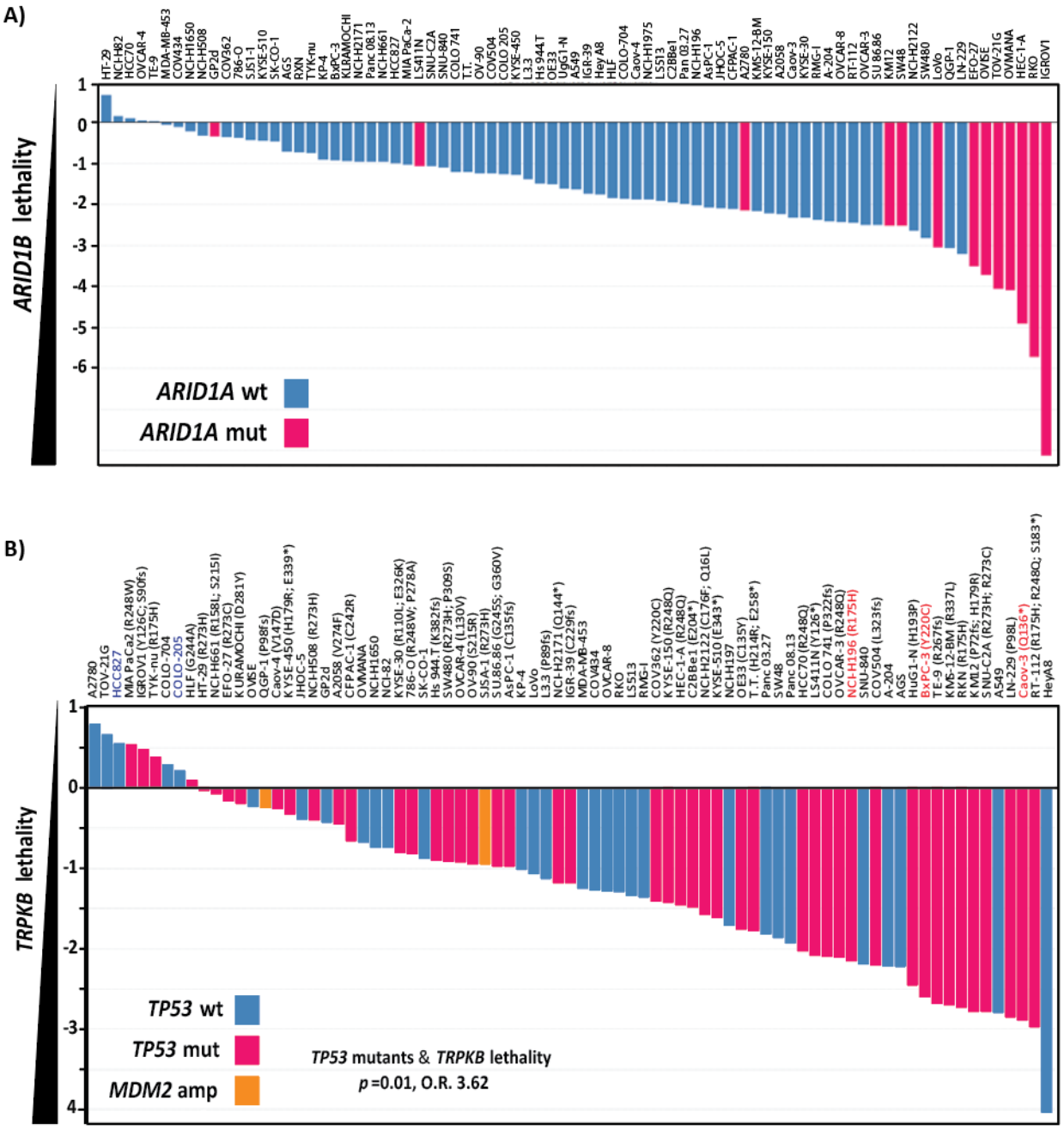
A)
ARID1B lethality
ARID1A wt
ARID1A mut
B)
TRPKB lethality
TP53 wt
TP53 mut
MDM2 amp
TP53 mutants & TRPKB lethality
p =0.01, O.R. 3.62

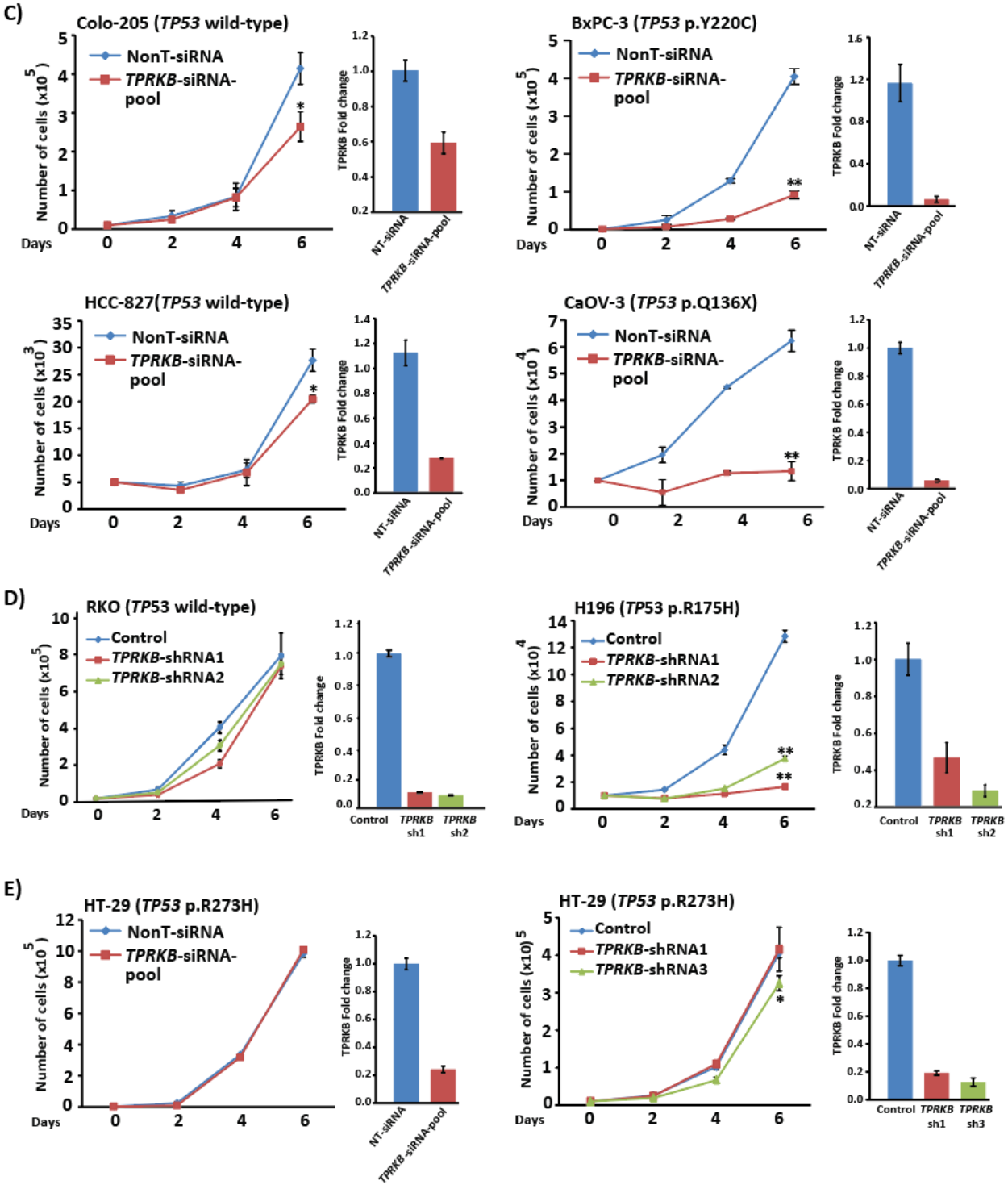
C)
Colo-205 (TP53 wild-type)
NonT-siRNA
TPRKB-siRNA-pool
Number of cells (x10 5)
Days
TPRKB Fold change
NT-siRNA
TPRKB-siRNA-pool
BxPC-3 (TP53 p.Y220C)
HCC-827(TP53 wild-type)
Number of cells (x10 3)
CaOV-3 (TP53 p.Q136X)
Number of cells (x10 4)
D)
RKO (TP53 wild-type)
Control
TPRKB-shRNA1
TPRKB-shRNA2
Number of cells (x10 5)
TPRKB sh1
TPRKB sh2
H196 (TP53 p.R175H)
Number of cells (x10 4)
E)
HT-29 (TP53 p.R273H)
NonT-siRNA
TPRKB-siRNA-pool
Number of cells (x10 5)
HT-29 (TP53 p.R273H)
Control
TPRKB-shRNA1
TPRKB-shRNA3
Number of cells (x10) 5
TPRKB sh3

Figure 2.1: Identification of TPRKB dependency in TP53-deficient cancers

A) We found cell dependence on *ARID1B* was significantly enriched in *ARID1A* mutated cancers. *ARID1B* dependency (fold-change in shRNA abundance versus control transfected cells) for cancer cell lines from Project Achilles is plotted, with cell lines ordered by increasing *ARID1B* dependency. The color of the bars indicates *ARID1A* status: red and blue bars indicate cell lines with mutant or wild-type *ARID1A*, respectively. **B)** *TPRKB* was the only gene identified in the Project Achilles genome-wide shRNA database as showing significant enrichment for dependency in *TP53* altered cell lines (two-sided Fisher's exact test odds ratio (O.R.) and p-value are shown for original (2015) *TP53* annotation status; O.R. = 2.6 and *p*=0.06 for *TP53* status and *TPRKB* dependency [> or < 1.4] for 2019 comprehensive cell line encyclopaedia [CCLE] *TP53* annotation status). *TPRKB* dependency (fold-change in shRNA abundance versus control transfected cells) for cancer cell lines from Project Achilles is plotted, with cell lines ordered by increasing *TPRKB* dependency. The color of the bars indicates mutational status from 2019 CCLE annotation: blue bars indicate *TP53* wild-type cells, red bars indicate *TP53* hotspot/deleterious mutants, and orange bars indicate *MDM2* amplifications. Blue and red arrows indicate cell lines with wild-type and mutant *TP*53, respectively, that were chosen for validation experiments. **C**) Differential effects of pooled siRNA against *TPRKB* (or scrambled control) on cell proliferation were confirmed in TP53 wild-type (Colo-205 and HCC-827) and *TP53* mutant cell lines (BxPC-3 and CaOV-3). **D**) As in **C**, but using independent shRNAs against *TPRKB* (or scrambled control) in RKO (*TP53* wild-type) and H196 (*TP53* mutant). **E)** *TP53* mutant HT-29 cells with TPRKB knockdown through siRNA pools or stable shRNA act as a counterexample of this phenomenon and do not respond to TPRKB depletion. Confirmation of *TPRKB* knockdown was completed by accompanying qPCR analysis. All experiments utilized triplicate samples, with the average and standard error plotted. * indicate p-values < 0.05 and ** indicate p-values <0.01.

Multiple types of TP53 alterations confer TPRKB sensitivity

TP53 is genomically altered through multiple mechanisms, including hotspot mutations, deleterious mutations, and through activation of pathways that modulate TP53 protein, such as amplification of the E3-ubiquitin ligase *MDM2*. Hence, to determine if *TPRKB* dependency was conferred by a spectrum of *TP53* perturbations, we tested for TPRKB sensitivity in additional, non-Project Achilles *TP53*-deficient cell lines MDA-MB-231 (*TP*53 p.R280K), MDA-MB-468 (*TP53* p.R273H), Hu-09 (*TP53* loss through fusion), SAOS-2 (*TP53* null), SJSA-1 (*MDM2*-amplified) and 93T449 (*MDM2*-amplified). As shown in **Figure 2.2A**, all of these cell lines showed a striking decrease in cell proliferation upon *TPRKB* knockdown. We confirmed these *in vitro* observations *in vivo* through SJSA xenografts in mice, which demonstrated a profound reduction of tumor size and burden in SJSA-1 cells with *TPRKB* knockdown (**Figure 2.2B**).

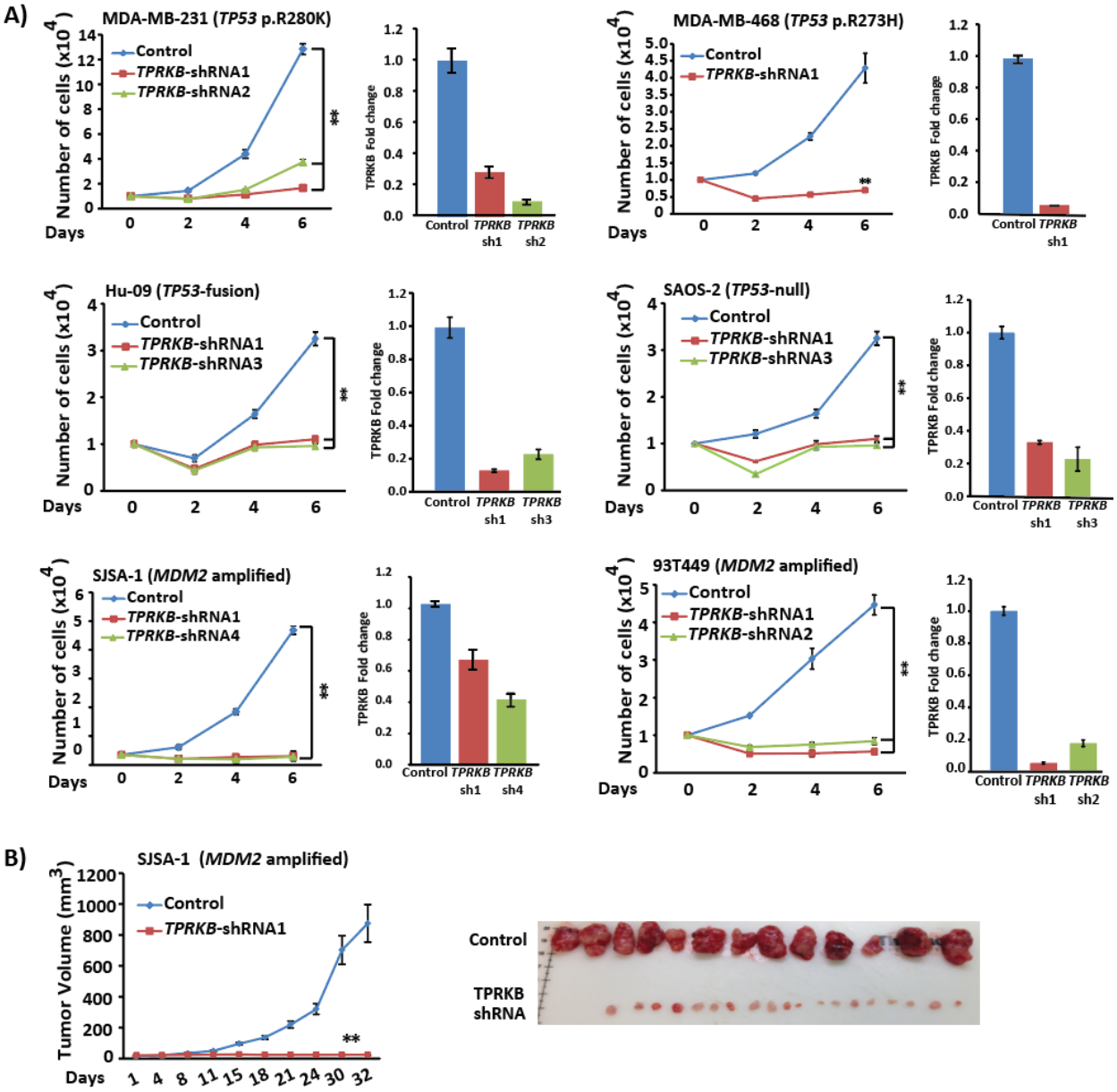

Figure 2.2: Various classes of TP53 perturbation result in marked TPRKB-dependent proliferation

A) Cancer cell lines with hotspot *TP53* perturbations or *MDM2*-amplification were assessed for TPRKB dependent proliferation using shRNA. **B)** *In vivo* mouse xenografts of SJSA-1 (*MDM2*-amplified) with TPRKB knockdown results are shown with tumor volume plotted and tumors at sacrifice shown. *TPRKB* knockdown was confirmed through qPCR analysis using *HMBS* as a normalization control. All experiments utilized triplicate samples, with the average and standard error plotted. * indicate p-values < 0.05 and ** indicate p-values <0.01.

Confirmation of TPRKB sensitivity in TP53 altered cancer cells through CRIPSR knockout

To unambiguously confirm *TPRKB* sensitivity in *TP53* altered cancer cell lines, we used CRISPR-Cas9 to knockout either *TPRKB* or a reported interacting member of the EKC/KEOPS complex, *PRPK*, in various cell lines: HEK293T (*TP53* wild-type), MDA-MB-231 (*TP53* p.R280K) and H358 (*TP53*-null)[98]. Sanger sequencing and Western analysis confirmed knockout of the genes and proteins, respectively (**Figure 2.3)**. Consistent with the siRNA and shRNA results described above, MDA-MB-231 and H358 *TPRKB*-knockout cells showed severely reduced cell proliferation, while HEK293T *TPRKB*-knockout cells exhibited slightly increased proliferation (**Figure 2.3**). Interestingly, knockout of another member of the EKC/KEOPS complex *PRPK* in MDA-MB-231 cells only resulted in a marginal reduction in proliferation, while *PRPK* knockout in HEK293T cells resulted in increased proliferation, underscoring the greater dependence on *TPRKB* in *TP53*-perturbed cells (**Figure 2.3B**). As PRPK stabilizes TPRKB (demonstrated in Chapter 3), we consider the modest proliferation defect observed upon *PRPK*-knockout as an indirect effect due to TPRKB reduction. Importantly, these results confirm those seen by siRNA and shRNA described above and demonstrate an essential role for *TPRKB* in a wide range of cancer cells with altered TP53 function.

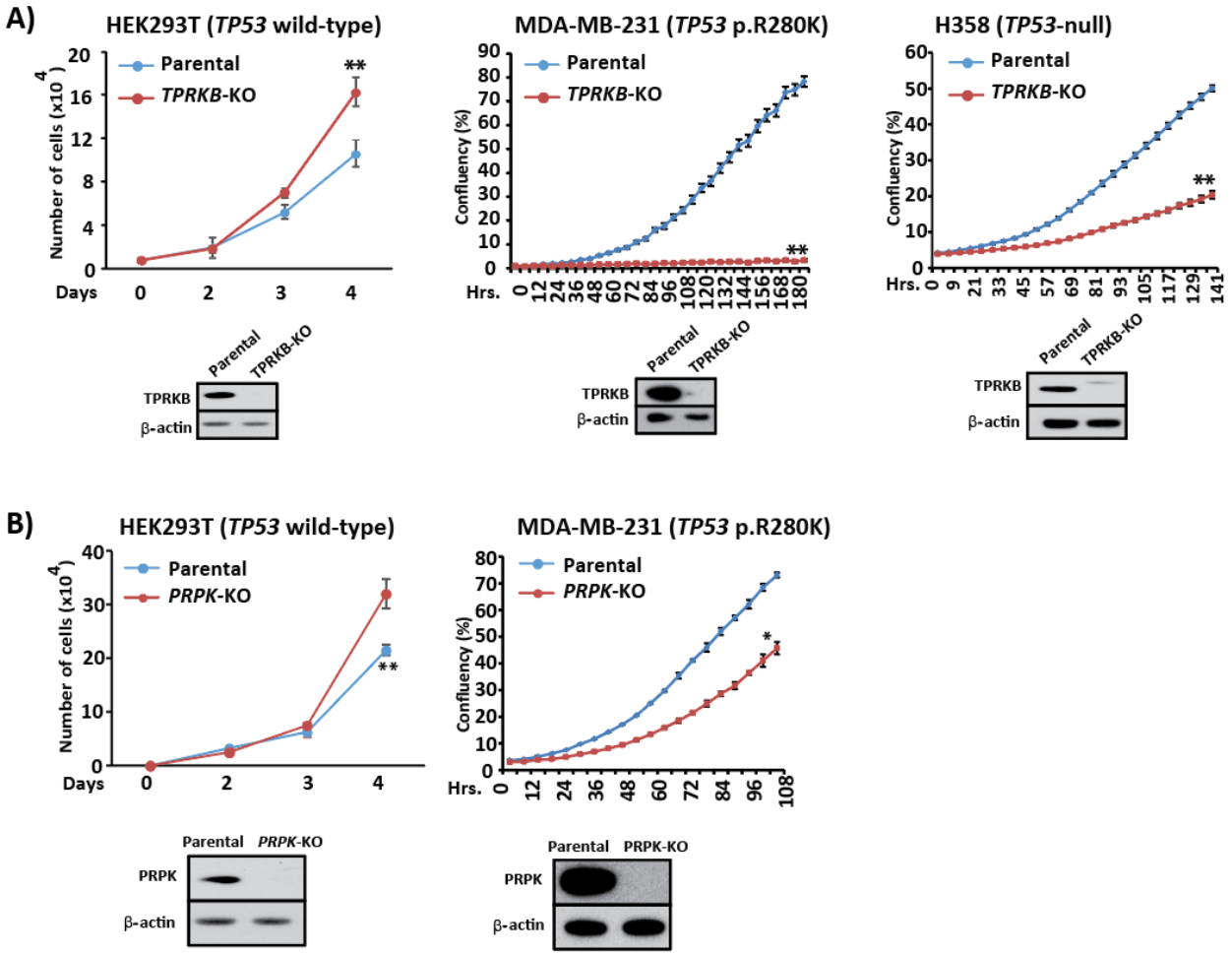

Figure 2.3: CRISPR knockout of TPRKB mimics knockdown data, and knockout of another EKC/KEOPS complex member PRPK does not produce the same magnitude of response

CRISPR-Cas9 mediated **A)** TPRKB knockout or **B)** PRPK knockout in *TP53* wild-type (HEK293T), *TP53*-mutant (MDA-MB-231), and *TP53* deep deletion (H358) cells confirmed results from siRNA/shRNA. Knockout was confirmed by Western blotting, and % confluency or cell number was plotted at the indicated time points. All experiments utilized triplicate samples, with the average and standard error plotted. * indicate p-values < 0.05 and ** indicate p-values <0.01.

TP53 reintroduction rescues proliferation upon TPRKB knockdown in TP53-null cells

To confirm that the above effects of *TPRKB* knockdown/knockout in *TP53*-mutated cancer cells was directly *TP53*-dependent, we first utilized the isogenic colorectal cancer cell line HCT116, HCT116 $TP53^{-/-}$, and HCT116 $TP53^{wt/R248W}$. Notably, HCT116 is a *TP*53 wild-type cell line, and HCT116 $TP53^{wt/R248W}$ express dominant-negative *TP53* p.R248W and wild-type *TP53*. As shown in **Figure 2.4**, parental HCT116 cells with stable *TPRKB* shRNA knockdown did not show significant proliferative defects *in vitro* or in a mouse xenograft model compared to scrambled shRNA control cells. In contrast, stable *TPRKB* knockdown in HCT116 $TP53^{-/-}$ and HCT116 $TP53^{wt/R248W}$ resulted in modest, but significantly decreased proliferation *in vitro* and *in vivo* compared to scrambled shRNA control cells (**Figure 2.4**).

As the above HCT116 isogenic system represents an exogenous *TP53*-deficient model, we sought to evaluate *TPRKB* dependency in an endogenous *TP53*-deficient model where *TP53* could be reintroduced. Hence we created isogenic cell lines from *TP53*-null H358 lung cancer cells (H358 $TP53^{-/-}$). We generated H358 cells through lentiviral infection that stably expressed wild-type *TP53* (H358 $TP53^{wt}$), recurrent *TP53* mutants (H358 $TP53^{R175H}$, H358 $TP53^{R249S}$, H358 $TP53^{R273H}$ and H358 $TP53^{R280K}$) or *LacZ* (H358 $TP53^{-/-}$ *LacZ*) as a control. As shown in **Figure 2.5A**, stable *TPRKB* knockdown reduced cell proliferation to a much greater extent in H358 $TP53^{-/-}$ *LacZ* compared to H358 $TP53^{wt}$. In contrast, stable expression of the above *TP53* mutants in H358 cells did not rescue the proliferation defect upon stable *TPRKB* knockdown (**Figure 2.5B**). Taken together, these results confirm the *TP53*-dependent response to *TPRKB* depletion specifically in *TP53*-mutant or null cells.

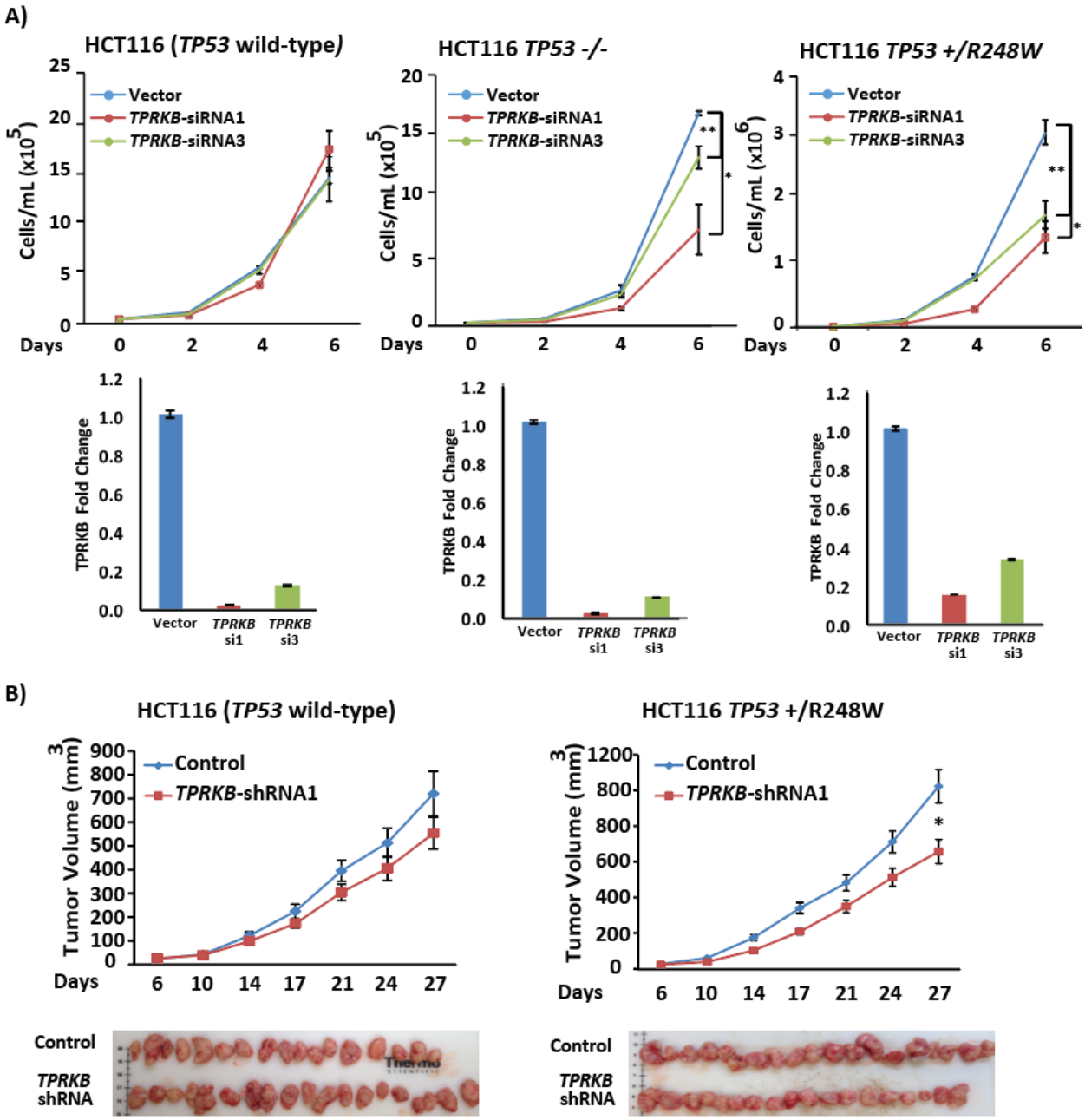

Figure 2.4: *TP53* deletion or dominant-negative mutation in *TP53*^{WT} HCT116 cells sensitizes cells to proliferative defects imposed by TPRKB loss

TPRKB was stably knocked down with two distinct shRNAs in isogenic HCT116 (*TP53* wild-type), HCT116 *TP53*$^{-/-}$, and HCT116 *TP53*$^{WT/R248W}$ cells. **A)** The knockdown was confirmed by qPCR and the cells were assay for cell proliferation and **B)** tumor formation in nude mice. * indicate p-values < 0.05 and ** indicate p-values <0.01.

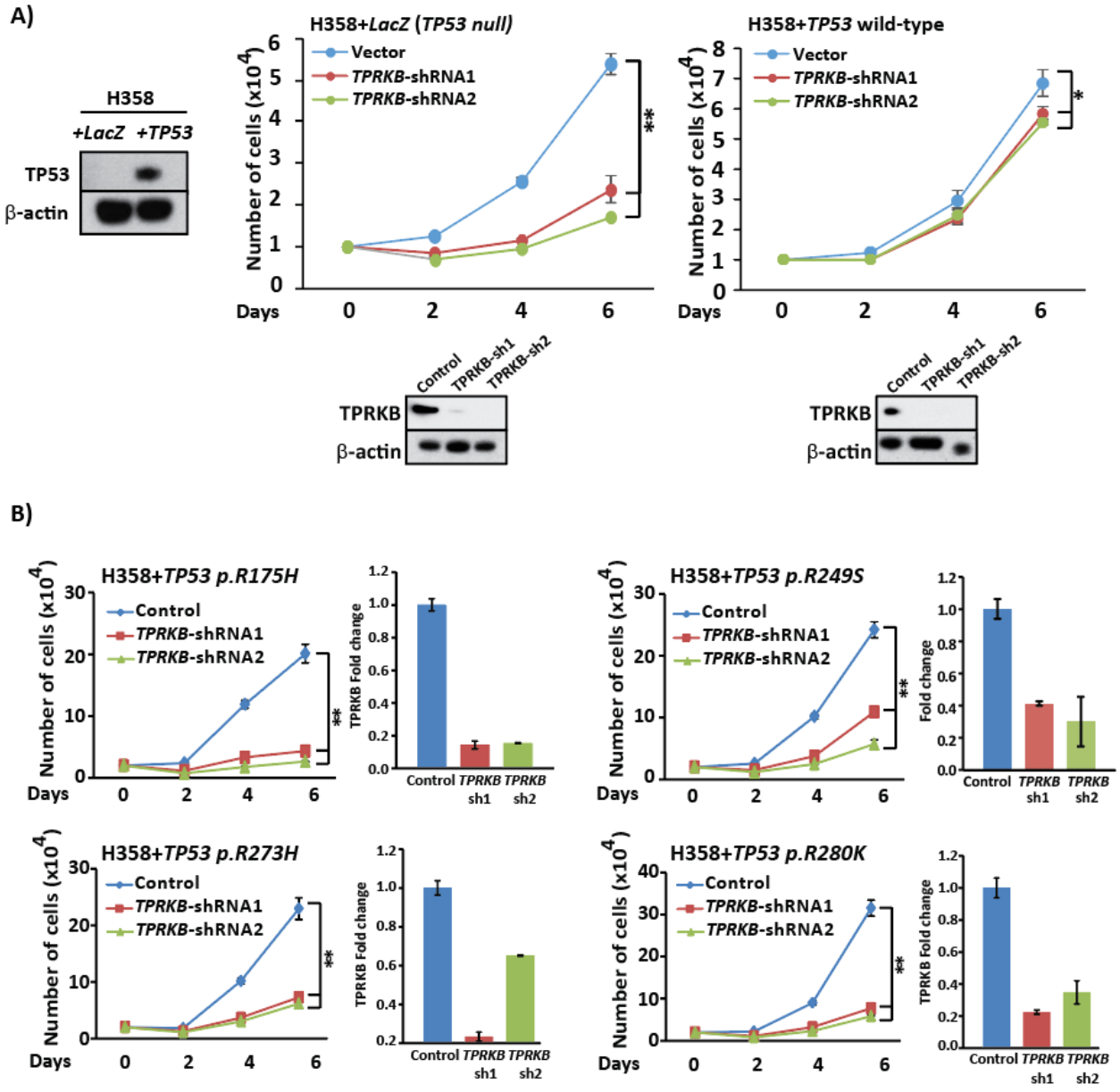

Figure 2.5: Wild-type *TP53* reintroduction, but not mutant *TP53*, rescues proliferation defects from TPRKB knockdown in *TP53*$^{-/-}$ H358 cells

TPRKB knockdown by shRNA was performed in **A)** H358 cells stably expressing *LacZ* control or *TP53,* and **B)** H358 cells stably expressing *LacZ, TP53* p.R175H, *TP53* p.R249S, *TP53* p.R273H, or *TP53* p.R280K, and proliferation was monitored. Inset Western blot or qPCR panels confirm TP53 over-expression from lentiviral transduction and TPRKB knockdown. All experiments utilized triplicate samples, with the average and standard error plotted. * indicate p-values < 0.05 and ** indicate p-values <0.01.

Overexpression of MDM2 is sufficient to confer sensitivity to TPRKB

As we witness response to TPRKB depletion in *MDM2*-amplified cells (**Figure 2.2)**, we sought to determine if overexpression of MDM2 was sufficient for TPRKB sensitivity. To address this, we created U2OS isogenic cell lines that stably overexpress *LacZ* control or *MDM2* and performed TPRKB knockdown in these cells. *TP53* wild-type U2OS cells do not respond to TPRKB knockdown. However, once *MDM2* is overexpressed the cells show massive reductions in cell proliferation, demonstrating that in addition to loss of wild-type *TP53,* overexpression of *MDM2* is sufficient to induce *TPRKB* sensitivity.

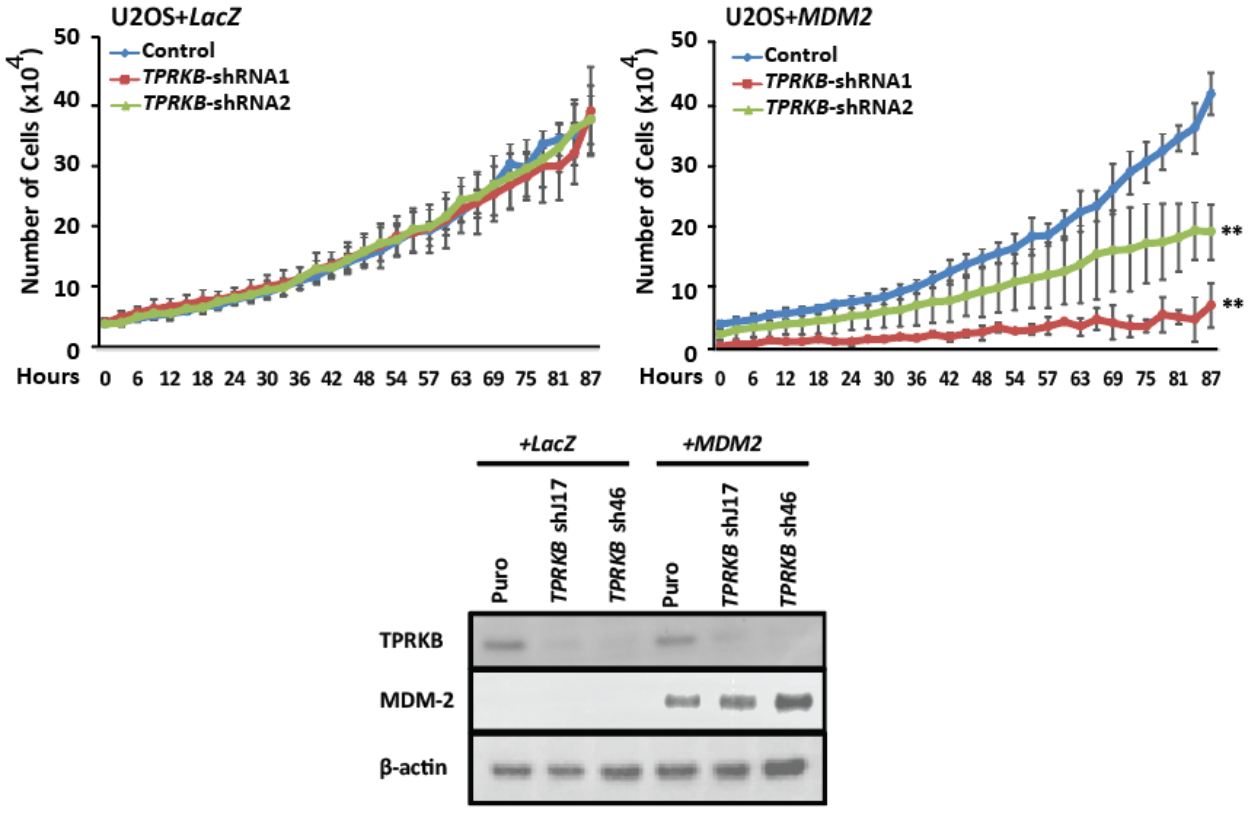

Figure 2.6: Expression of *MDM2* in *TP53* wild-type U2OS cells induces vulnerability to *TPRKB* depletion

TPRKB knockdown by shRNA was performed in U2OS cells stably expressing *LacZ* control or *MDM2,* and proliferation was monitored. Western blot panel confirms MDM2 over-expression from lentiviral transduction and TPRKB knockdown. All experiments utilized triplicate samples, with the average and standard error plotted. * indicate p-values < 0.05 and ** indicate p-values <0.01.

TPRKB dependency in TP53 mutant cells is unique amongst EKC/KEOPS complex members

As described above, TPRKB is a member of EKC/KEOPS complex, which plays a major role in tRNA modification. We first addressed the question of how benign-immortalized *TP53* wild-type MCF10A cells respond to stable knockdown of the other individual canonical complex members – *PRPK*, *OSGEP* and *LAGE3* – to determine the role of these members and the complex in relatively normal cells. *TPRKB* or *PRPK* knockdown in MCF10A had minimal impact on proliferation, while *OSGEP* and *LAGE3* knockdown significantly affected cell proliferation (**Figure 2.7A**). We then addressed the effect of individual EKC/KEOPS member knockdown in H358 *TP53*$^{-/-}$ *LacZ* and H358 *TP53*^{wt} cells (**Figure 2.7B**). *PRPK* knockdown in H358 *TP53*$^{-/-}$ showed modestly reduced proliferation that was rescued by *TP53* expression in H358 *TP53*^{wt} cells. In contrast, knockdown of *OSGEP* or *LAGE3* significantly reduced cell proliferation independent of *TP53* status in H358 cells. These experiments have been expanded to other cell lines, such as *TP53* wild-type A-204 sarcoma cells, which did not exhibit reduced proliferation upon knockdown of any members of the EKC/KEOPS complex. Thus, we have found that *OSGEP* and *LAGE3* phenotypes do not clearly stratify by *TP53* status. Our observations support general insensitivity to *TPRKB* or *PRPK* depletion in *TP53* proficient cells, in contrast to non-*TP53* related sensitivity to depletion of other EKC/KEOPS complex members.

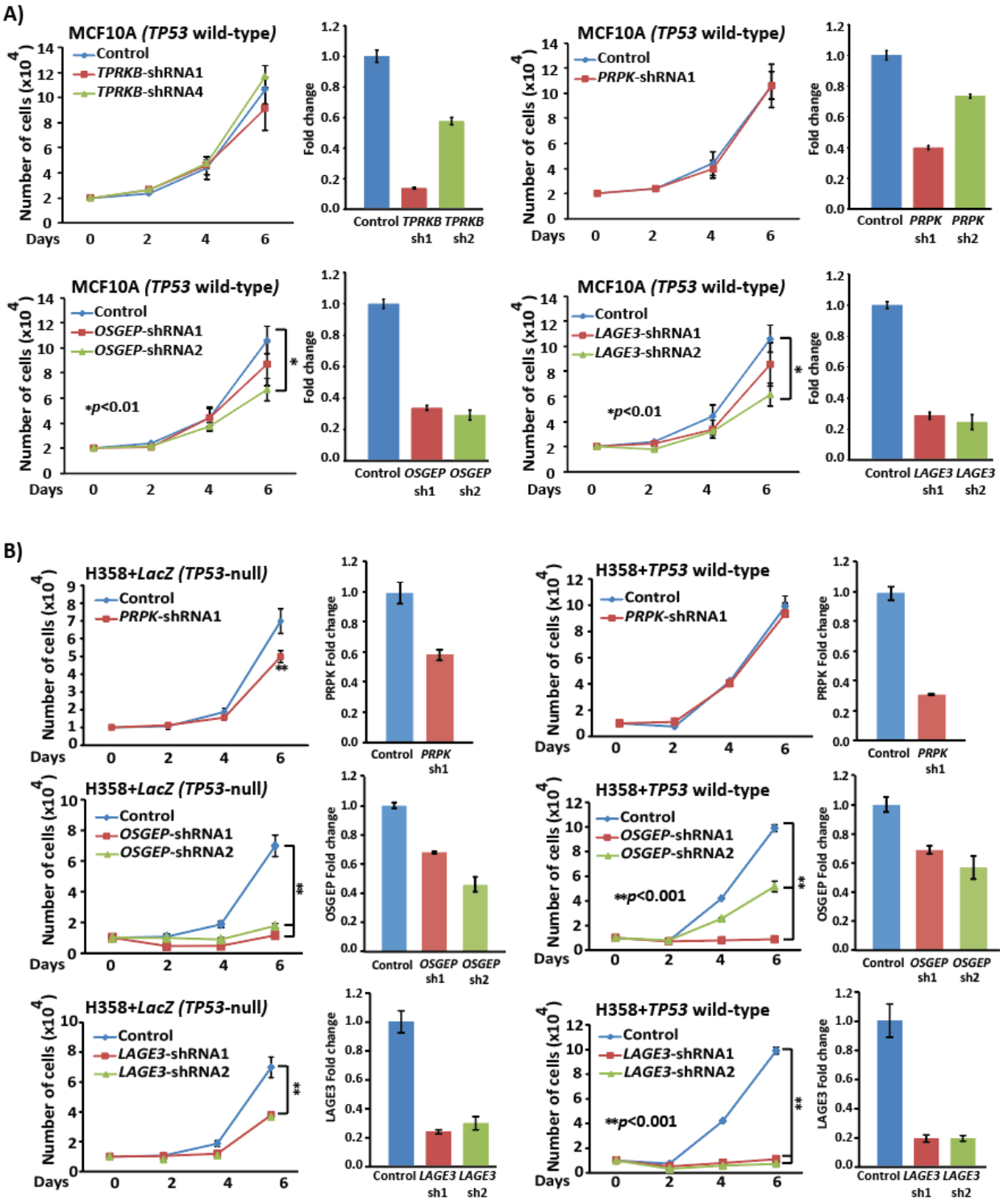

Figure 2.7: Knockdown of other EKC/KEOPS complex members does not produce the same TP53-dependent effects as TPRKB loss

Other members of the EKC/KEOPS complex, *PRPK*, *OSGEP* and *LAGE3* were knocked down using shRNA in A) benign breast MCF10A (*TP53* wild-type) cells, and B) H358 *TP53*$^{-/-}$ *LacZ* and H358 *TP53*^{WT} cells. Knockdown was confirmed by qPCR. All experiments utilized triplicate samples, with the average and standard error plotted. * indicate p-values < 0.05 and ** indicate p-values <0.01.

Loss of TPRKB leads to cell cycle arrest and a reduction in the expression of anti-apoptotic proteins in TP53-deficient cells

To investigate the mechanism of *TPRKB* dependency in *TP53* altered cells, we first assessed the impact of *TPRKB* depletion on cell cycle progression in H358 *TPRKB* knockout cells and SJSA-1 *TPRKB* knockdown cells. Compared to H358 parental cells, H358-*TPRKB* knockout cells showed marked arrest in S and G2/M phase, while SJSA-1 *TPRKB* knockdown cells arrested in G1 and G2/M. (**Figure 2.8A**). As cell cycle arrest has been closely linked with modulation of the anti-apoptotic proteins B-cell lymphoma extra-large (Bcl-xL or BCL2L1) and B-cell lymphoma 2 (Bcl-2 or BCL2)[189], we assessed BCL2L1 and BCL2 in a panel of cell lines, including H358 parental, H358 *TP53*$^{-/-}$ *LacZ,* H358 *TP53*^{wt}, HEK293T, MCF10A, and SJSA-1 in the context of *TPRKB* depletion. Of note, compared to their respective parental lines, *TP53*-deficient H358, H358 *TP53*$^{-/-}$ *LacZ,* and SJSA-1 cells with *TPRKB* knockout or knockdown showed reduced BCL2L1 expression, while expression was largely unaltered in *TP53* wild-type HEK293T, MCF10A, and H358 *TP53*^{wt} cells with *TPRKB* loss (**Figure 2.8B&C**). Similarly, BCL2 expression was downregulated in SJSA-1 cells with TPRKB knockdown, while HEK293T and MCF10A showed increased and unchanged expression, respectively (**Figure 2.8B&C**). BCL2 was undetectable in H358 cells (**Figure 2.8B**). Taken together, these results suggest that the expression of anti-apoptotic factors may mediate *TPRKB* dependence in *TP53*-null cells.

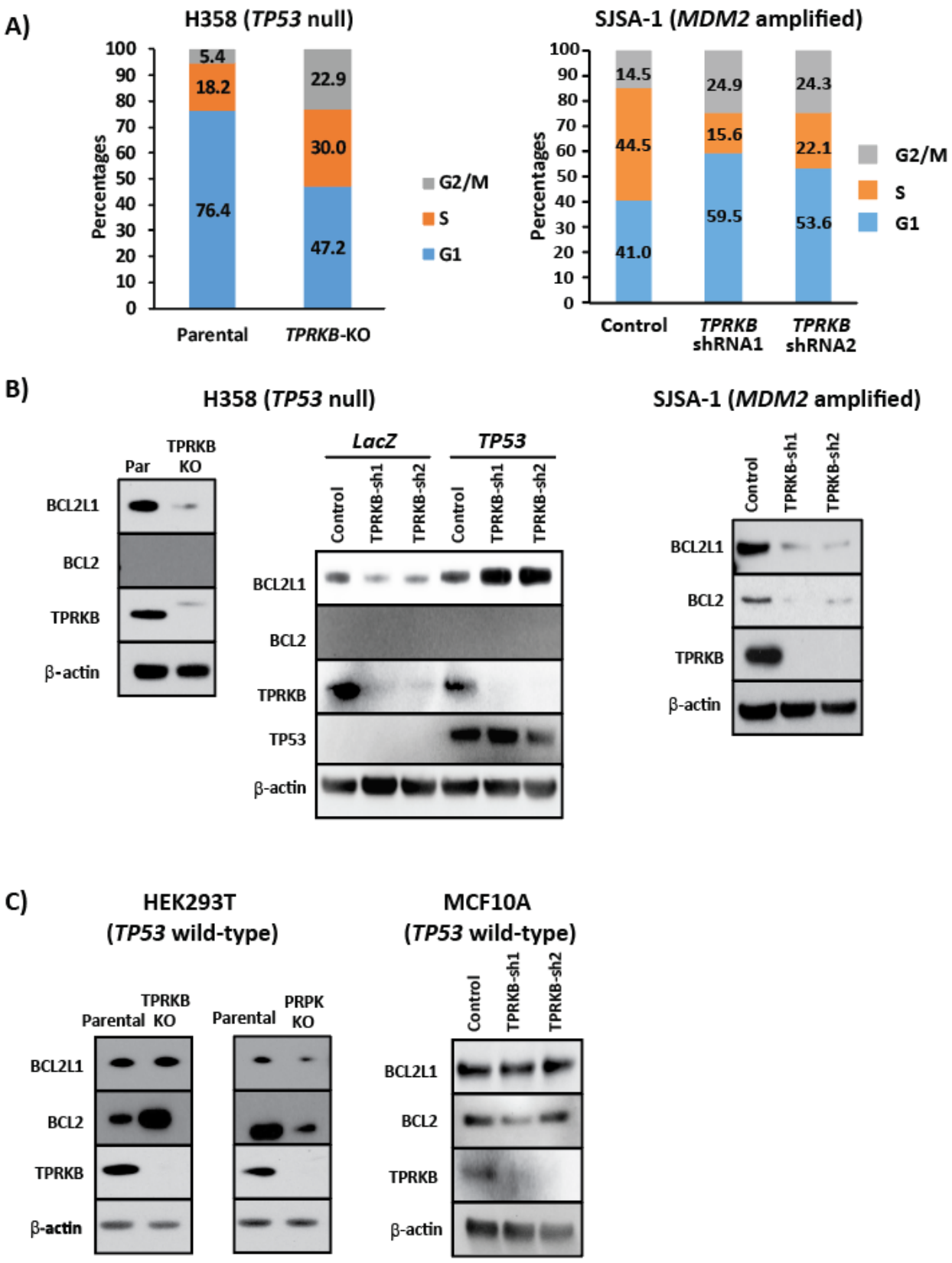
A)
H358 (TP53 null)
Percentages
100
90
80
70
60
50
40
30
20
10
0
5.4
18.2
76.4
22.9
30.0
47.2
Parental
TPRKB-KO
G2/M
S
G1
SJSA-1 (MDM2 amplified)
14.5
44.5
41.0
24.9
15.6
59.5
24.3
22.1
53.6
Control
TPRKB shRNA1
TPRKB shRNA2
B)
H358 (TP53 null)
Par
TPRKB KO
BCL2L1
BCL2
TPRKB
β-actin
LacZ
TP53
Control
TPRKB-sh1
TPRKB-sh2
TP53
SJSA-1 (MDM2 amplified)
C)
HEK293T
(TP53 wild-type)
Parental
TPRKB KO
PRPK KO
MCF10A
(TP53 wild-type)

Figure 2.8: TPRKB depletion leads to cell cycle arrest and reductions in anti-apoptotic proteins in TP53 deficient cells

A) Serum stimulated synchronized H358 (parental) or CRISPR-Cas9 generated H358-TPRKB knockout (KO) cells and SJSA-1 control or TPRKB knockdown cells were assessed for cell cycle analysis by flow cytometry. The proportion of cells in G1, S, and G2/M is plotted. **B)** Anti-apoptotic protein (BCL2L1 and BCL2) expression was determined by Western blotting in H358 control, H358 TPRKB-KO, H358 TP53-/- LacZ, and H358 TP53WT and SJSA-1 control and TPRKB shRNA knockdown cells. **C)** Additional TP53 wild-type cell lines were assayed for BCL2 and BCL2L1 expression: HEK293T cells with *TPRKB*-KO or *PRPK*-KO and MCF10A control or *TPRKB* knockdown cells.

Common TP53 activators do not reveal mechanism for TP53-dependent TPRKB sensitivity

In an attempt to elucidate a potential mechanistic pathway for TPRKB sensitivity in cells lacking wild-type *TP53,* we utilized a series of compounds that are known to activate TP53 through various pathways. Etoposide and cisplatin were used to induce DNA damage, RITA was used to activate TP53 through direct binding activities, and CoCl2 was used as a hypoxia mimetic in HEK293T and H358 parental and TPRKB-KO cells, as well as parental HCT116 cells with *TPRKB* knockdown through shRNA (**Figure 2.9**). In general, *TP53* wild-type cells show diminished sensitivity to TP53 activators upon TPRKB loss, while *TP53* null cells show enhanced sensitivity. However, while these results are consistently statistically significant, the magnitude of the changes suggest they are likely not physiologically relevant for the TPRKB-dependent phenotype we see.

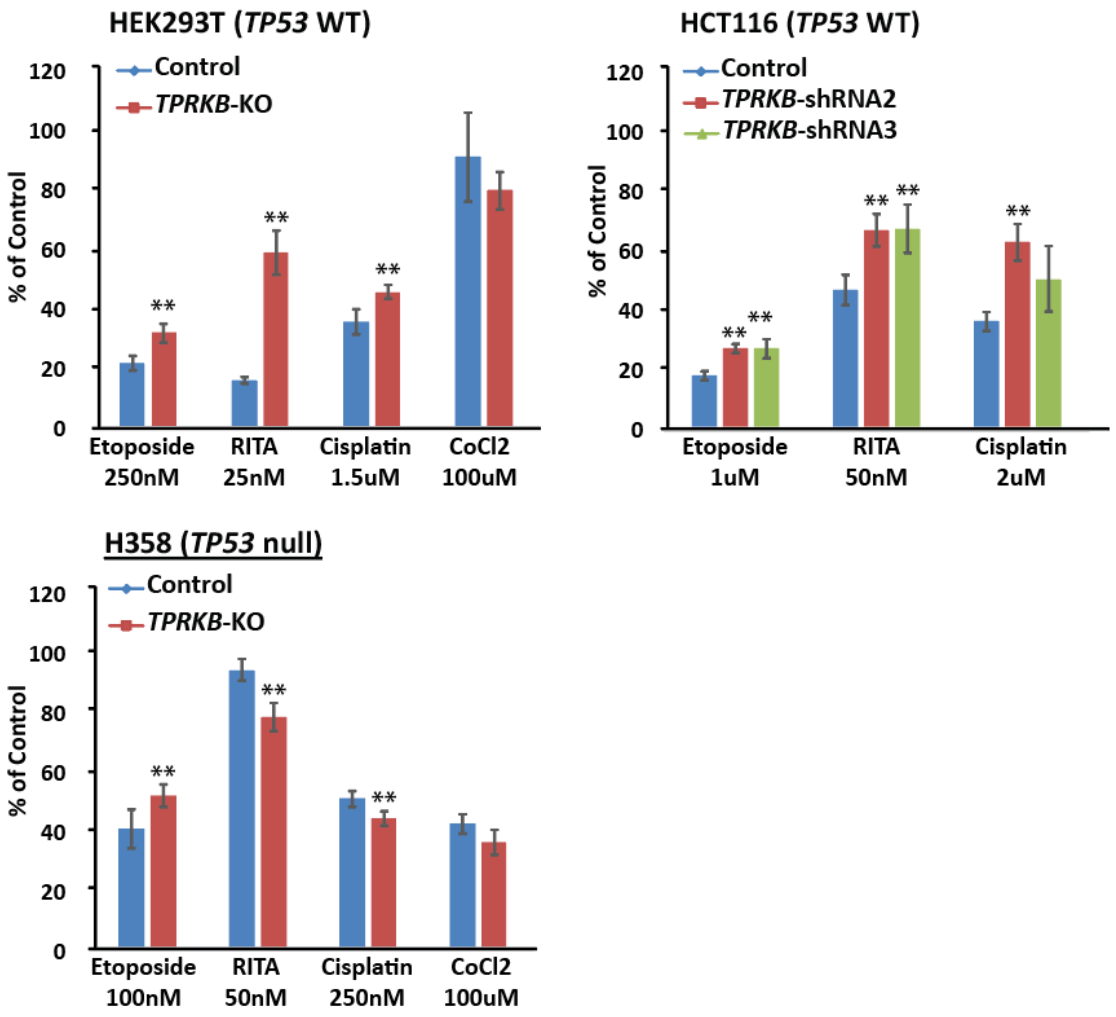

Figure 2.9: TPRKB depletion does not lead to dramatic changes in response to TP53 activators regardless of TP53 status

HEK293T (*TP53* wild-type), HCT116 (*TP53* wild-type), and H358 (*TP53* null) cells with *TPRKB* loss through either CRISPR knockout or stable shRNA knockdown were treated with various TP53 activators- etoposide, RITA, Cisplatin, or CoCl2 at indicated concentrations. Data is represented as the % of control cells (DMSO for etoposide and RITA; DMF for cisplatin; untreated for CoCl2) as measured on the final day of experimentation (4 days after treatment for etoposide, RITA, and cisplatin and 3 days after treatment for CoCl2). All experiments utilized triplicate samples, with the average percent and percent-adjusted standard error plotted. * indicate p-values < 0.05 and ** indicate p-values <0.01.

Discussion

Through *in silico* analysis coupled with *in vitro* and *in vivo* experimentation, we demonstrate that TPRKB, a member of the tRNA modifying EKC/KEOPS complex, is essential in cancer cells with TP53-alterations. We utilized multiple independent isogenic cell lines with inherently different TP53 backgrounds to demonstrate this. *TP53*-wild-type HCT116 colorectal carcinoma cells show little to no reduction in proliferation upon *TPRKB* depletion, while concurrent deletion of *TP53* or overexpression of dominant-negative mutant $TP53^{wt/R248W}$ sensitizes these cells to varying degrees. Conversely, in *TP53*-null H358 lung carcinoma cells, we demonstrate that co-expression of wild-type, but not mutant forms of, *TP53* is sufficient to rescue cell proliferation defects in response to TPRKB loss. Interestingly, these results also demonstrate increased sensitivity to TPRKB depletion when TP53 loss is a driving factor in cancer development (as seen in H358) as opposed to post factum deletion (as seen in HCT116). We further demonstrate through the use of isogenic U2OS osteosarcoma cell lines that overexpression of *MDM2*, a known E3-ubiquitin ligase responsible for degradation of TP53, is sufficient to induce *TPRKB* dependency in *TP53* wild-type cells. Thus, we show that expression of TP53 and MDM2 determine cellular responses to TPRKB depletion.

TP53 can be deregulated in human cancers through multiple classes of genomic alterations, including missense, nonsense, and frameshift mutations, copy number loss, and degradation. Previous approaches towards identifying synthetic lethal relationships in *TP53* altered cancers have largely used single alteration classes, including *TP*53-null[190], specific hotspot *TP53* mutation backgrounds[85, 191, 192] and *TP53* deletion[88]. Importantly, we found that *TPRKB* knockdown resulted in marked proliferative defects in *TP53*-null cancer cell lines (such as H358), cell lines harboring *TP53* hotspot missense mutations (such as H196 (*TP53*

p.R175H), MB-MDA 231, (*TP53* p.R280K) and MBA-MB-468 (*TP53* p.R273H)), and multiple cell lines harboring amplification of *MDM2* (such as SJSA-1 or 93T449). Interestingly, we observed that TPRKB sensitive cell lines displayed variable response to TPRKB depletion, whereby some cells underwent massive cell death (such as SJSA-1) while others showed sustained reductions in overall proliferation (such as H358). Conversely, *TPRKB* knockdown/knockout had minimal effect on proliferation in multiple benign immortalized or *TP53* wild-type cancer cells. Overall, we tested this hypothesis in 41 cell lines (including isogenic), and a summary of the general effects of TPRKB depletion in these can be seen in **Figure 3.8.** Hence, our results suggest that TRPKB may represent a dependency across a larger spectrum of TP53 altered cancers than previous efforts.

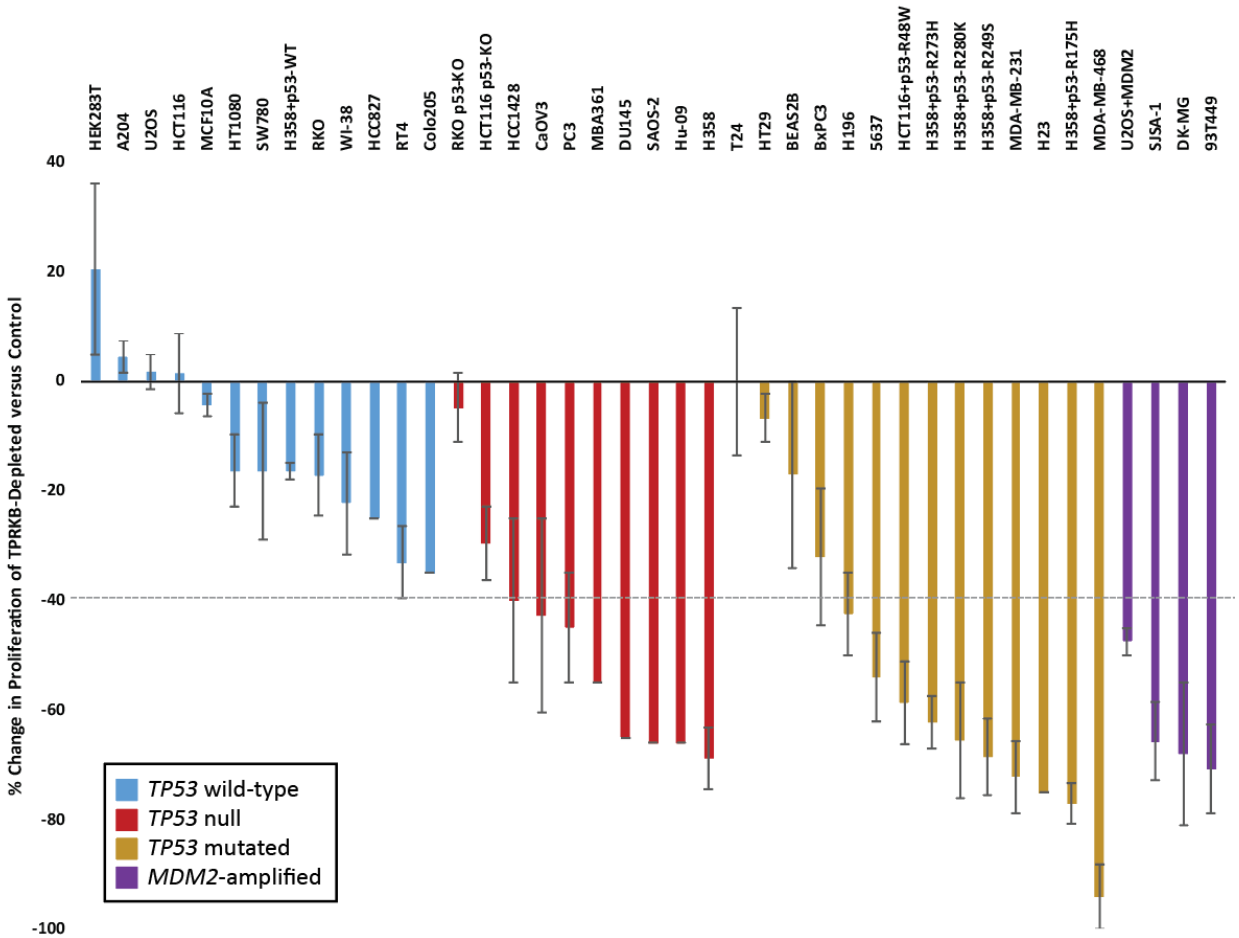

Figure 2.8: Summary of cell line response to TPRKB depletion

The above graph shows a representation of cell line response to TPRKB depletion. Each bar represents a specific cell line's average percent change in proliferation of TPRKB-depleted cells (either through siRNA, shRNA, or CRISPR knockout of TPRKB) compared to control cells (either non-targeting siRNA/shRNA or parental cells for CRISPR knockouts) on the final day of experimentation (either Day 4 or 6 depending on confluency). Each bar represents the mean of 1-8 independent proliferation experiments, and error bars represent standard error of the mean. Blue bars indicate *TP53* wild-type cells, red bars indicate *TP53*-null cells, gold bars indicate *TP53*-mutated cells, and purple bars indicate *MDM2*-amplified/overexpressing cells.

Members of the EKC/KEOPS complex – TPRKB, PRPK, OSGEP, LAGE3, and recently identified C14ORF142 – are highly conserved from yeast to mammals. In yeast this complex has been shown to regulate telomere length maintenance, tRNA modification, and transcriptional processes[99, 100, 102-104]. Further, the yeast ortholog of TPRKB, CGI-121, is non-essential for the tRNA modifying functions and instead acts as an allosteric regulator of the complex in this context[103]. Importantly, yeast lack *TP53*, and there are relatively few studies examining the role of the EKC/KEOPS complex and its constituents in humans. Consistent with our data, a recent study in multiple myeloma demonstrated that knockdown of PRPK, an atypical kinase that can also interact with and phosphorylate TP53, inhibits cellular growth independent of TP53-status[115]. PRPK expression has also been associated with invasion and metastasis potential of colorectal cancer[116]. Little is known about the other EKC/KEOPS complex members in cancer; however, a recent study found that mutations in EKC/KEOPS complex members drive Galloway-Mowat syndrome, a rare condition characterized by early-onset nephrotic syndrome and microcephaly[108]. Braun et al. found that mutation or knockdown of *OSGEP*, *PRPK*, or *TPRKB* led to reduced cellular proliferation in human podocytes, and knockout was embryonic lethal in zebra fish and mice. These results, coupled with our differing effects in multiple *TP53* wild-type cell lines, suggests that general dependency on the EKC/KEOPS complex may be

related to *TP53* status, cellular identity, and development, which must be considered in any effort to therapeutically target TPRKB.

Our results further support that TPRKB depletion in *TP53*-null H358 and *MDM2*-amplified SJSA-1 cells halt the cell cycle and alter expression of anti-apoptotic proteins—including BCL2 and BCL2L1. These may act as potential mediators of TPRKB dependency in these cells, consistent with the known convergence of TP53 and BCL proteins in cancer apoptosis[189]. While we have yet to determine the exact mechanism of this dependency, it does not appear to be explicitly through the DNA damage pathway, as agents like cisplatin and etoposide had minimal differential effects between TPRKB wild-type and lacking cells. Ongoing studies are further exploring the mechanism driving TPRKB dependency across TP53 altered cancers.

In summary, we identified and validated TPRKB dependency across cancer cell lines harboring a range of *TP53* alterations, including *TP53* missense mutations, *MDM2* amplifications, and *TP53* loss, with minimal effect in benign or cancer cell lines with wild-type *TP53*. Hence, TPRKB may represent a therapeutic vulnerability that can be exploited for therapeutic targeting of *TP53*, the most frequently altered gene in human cancer.

Materials and Methods

Cell Culture, Reagents, and Proliferation

Detailed cell line information regarding media, seeding density for proliferation, and acquisition information can be found in **Table 2.1**. Upon receipt, cells were tested for *Mycoplasma* contamination using a commercially available kit and protocol (Sigma, LookOut

Mycoplama PCR Detection Kit, MP0035). Negative cell lines were propagated and frozen until needed. Cell lines were typically used for experiments within 2-3 months post-thawing.

Table 2.1: Cell line information

Cell Line	Media (10%FBS unless noted)	Typical Cells/Well (24-well unless noted)	Acquired From
p53-WT			
HEK283T	DMEM	$0.75x10^4$	ATCC
A204	McCoy's 5a Medium Modified	$0.25x10^4$ (96-well)	Felix Fang's lab (gift)
U2OS	McCoy's 5a Medium Modified	$2.0x10^3$ (96-well)	Elizabeth R. Lawlor's lab (gift)
HCT116	RPMI	$1.0x10^4$	Horizon-HD
MCF10A	MEBM+MEGM Kit	$0.5x10^4$	ATCC
HT1080	EMEM	$2.0x10^3$ (96-well)	ATCC
SW780	Leibovitz's L-15 (No CO2)	$1.0x10^4$	ATCC
H358+p53-WT	RPMI	$1.0x10^4$	Made in Lab from H358
RKO	EMEM	$0.5x10^4$	Horizon-HD
WI-38	EMEM	$1.0x10^4$	ATCC
HCC827	RPMI	$1.0x10^4$	David Beer's lab (gift)
RT4	McCoy's 5a Medium Modified	$0.5x10^4$	ATCC
Colo205	RPMI	$1.0x10^4$	ATCC
p53-null			
RKO p53-KO	EMEM	$0.5x10^4$	Horizon-HD
HCT116 p53-KO	RPMI	$1.0x10^4$	Felix Fang's lab (gift)
HCC1428	RPMI	0.5x104	Arul Chinnaiyan's lab (gift)
CaOV3	DMEM	$1.0x10^4$	ATCC
PC3	RPMI	$1.0x10^4$	ATCC
MDA-MB-361	Leibovitz's L-15 (No CO2, FBS 20%)	$1.5x10^4$	ATCC
DU145	RPMI	$1.0x10^4$	ATCC
SAOS-2	DMEM	$0.5x10^4$	Arul Chinnaiyan's lab (gift)
Hu-09	DMEM	$0.5x10^4$	Arul Chinnaiyan's lab (gift)
H358	RPMI	$1.0x10^4$	ATCC
p53-mutant			
HT29	McCoy's 5a Medium Modified	$1.0x10^4$	ATCC
T24	McCoy's 5a Medium Modified	$0.5x10^4$	ATCC
BEAS2B	BEBM and BEGM kit	$1.0x10^4$	ATCC
BxPC3	RPMI	$1.0x10^4$	ATCC
H196	RPMI	$0.5x10^4$	ATCC
5637	RPMI	$0.5x10^4$	ATCC
HCT116+p53-R48W	RPMI	$1.0x10^4$	Horizon-HD
H358+p53-R273H	RPMI	$1.0x10^4$	Made in Lab from H358
H358+p53-R280K	RPMI	$1.0x10^4$	Made in Lab from H358
H358+p53-R249S	RPMI	$1.0x10^4$	Made in Lab from H358
MDA-MB-231	DMEM (plus NEA+Glutamax)	$1.0x10^4$	ATCC
H23	RPMI	$1.0x10^4$	ATCC
H358+p53-R175H	RPMI	$1.0x10^4$	Made in Lab from H358
MDA-MB-468	DMEM (plus NEA+Glutamax)	$1.0x10^4$	ATCC
MDM2-amplified			
U2OS+MDM2	McCoy's 5a Medium Modified	$2.0x10^3$ (96-well)	Made in Lab from U2OS
SJSA-1	DMEM	$0.5x10^4$	ATCC
DK-MG	RPMI	$1.5x10^4$	Arul Chinnaiyan's lab (gift)
93T449	DMEM	$0.5x10^4$	ATCC

Common TP53 activators were obtained from commercial vendors and reconstituted in DMF for Cisplatin (Tocris Bioscience, 2251), or DMSO for Etoposide (Sigma-Aldrich, E1383) and RITA (Selleck, S2781), or supplied in solution for CoCl2 (Sigma-Aldrich, 15862). After plating cells for 24 hours, these reagents were added and cell growth was monitored as described below. Count days for these experiments are reflective of days after treatment, as opposed to days after plating.

Cell growth was monitored through either cell counting with Beckman Coulter's Z-series Cell Counter or through Essen Biosciences' Incucyte Live Cell Analysis. Depending on the growth rate of each individual cell line, on either days 2, 4 and 6 after plating or days 2, 3, and 4 after plating cells were trypsinized for Coulter Counting analysis. All experiments utilized triplicate samples, with the average and standard error plotted. Two-sided t-test p-values <0.05 (*) and <0.001(**) for the last day of growth are indicated in each figure. For Incucyte experiments readings were taken every 4 hours and were terminated once a cell line reached confluency. All results were representative of at least two independent experiments.

RNA extraction and qPCR analyses

Cells were pelleted, lysed, and RNA was extracted as per manufacturer's instructions (Purelink RNA Mini Kit, Life Technologies). Total RNA was quantified by NanoDrop 2000 spectrophotometer (Thermo Fisher). cDNA was prepared using High Capacity cDNA Reverse Transcription Kit, per manufacturer's instruction (Applied Biosciences). SYBR green-based qPCR was performed in triplicate using various primers, as listed in **Table 2.2**. HMBS was used as a normalization control for all experiments unless otherwise specified.

Table 2.2: Primer and gRNA sequences

Gene	Strand	Sequence	Application
TPRKB	Forward	AATGCGGGAGACTTGAGAAG	qPCR
TPRKB	Reverse	GCTGCCACAAGTATCTGAAATG	qPCR
PRPK	Forward	GACAATTGGGCAGGTTTTGG	qPCR
PRPK	Reverse	TTTCAGGAGCATGTTGGAGG	qPCR
LAGE3	Forward	GTTGGGAAGGATCTCACAGTG	qPCR
LAGE3	Reverse	GGAAAGCTGGTCAAGAAAGTTG	qPCR
OSGEP	Forward	AGTGGGTAATTGTCTGGATCG	qPCR
OSGEP	Reverse	CGTCCATCCCCTTTACAGTG	qPCR
HMBS	Forward	ATACAAGAGACCATGCAGGC	qPCR
HMBS	Reverse	AGTGATGCCTACCAACTGTG	qPCR
PRPK for knockout		GAAGCGGCTGCTCCGCTCCCGG	CRISPR gRNA
TPRKB for knockout		GGACCTATTTCCCGAATGCAGGG	CRISPR gRNA
TPRKB	Forward	AATCTTTTGGTCTTTTCATTTTGTGTG CAGTAGAATCgTGCT TATCTGTGAA ATG GAC TAC AAA GAC GAT GAC GAC AAG CAGTTAACACATCAGCTcGACCTAT TTCCCGAATGCAGGGTAACCCTTCT	CRISPR gRNA
TPRKB	Reverse	AGAAGGGTTACCCTGCATTCGGGAA ATAGGTCgAGCTGATGTGTTAACTG CTTGTCGTCATCGTCTTTGTAGTCCA TTTCACAGATAAGCAcGATTCTACT GCACACAAAATGAAAAGACCAAAA GATT	CRISPR gRNA

DNA constructs, lentivirus production, and cell transfection

Mammalian expression plasmids were generated or obtained from Addgene. shRNA constructs were created using System Biosciences or purchased from Open Biosystems (**Table 2.3**). Lentiviral DNA vectors for *TP53*-V5 (22945), *TP53* p.R175H-V5 (22936), *TP53* p.R249S-V5 (22935), *TP53* p.R273H-V5 (22934), and *TP53* p.R280K-V5 (22933) were obtained from Bernard Futscher's lab via Addgene. The pLenti6 DNA vector for *LacZ* (V368–20) was obtained

from Life Technologies. The *MDM2* vector was created by the University of Michigan Vector Core.

For transient siRNA transfections, cells were plated in 6-well plates at 60-70% confluency. The day after plating, cells were transfected with 9ul of 20uM siRNA at a 1:1 ratio with Lipofectamine RNAiMAX, per manufacturer's protocol (Invitrogen, 13778) in Opti-MEM Media. Cells were collected for qPCR analysis and plated for proliferation studies 48-72 hours post-transfection, depending on confluency.

To generate lentivirus, we started by using the aforementioned vectors to transform STBL3 competent cells. Colonies were selected, DNA was isolated with the use of PureLink Quick Plasmid Miniprep Kit per the manufacturer's instructions (Invitrogen), and DNA was submitted for Sanger sequencing DNA Sequencing Core (University of Michigan Medical School) to verify the end products. DNA was then used for lentiviral production by either the UMICH Vector Core (University of Michigan) or System Biosciences. Active lentiviruses were infected to 50-60% confluent cells in either 6-well plate or 100-mm dish using polybrene (Millipore). 24 hours after infection, selection media was added. For exogenous expression plasmids, 5ug/ml blasticidin containing medium was used (Invivogen). For knockdown clones, 1ug/ml puromycin containing medium was used. For clones that had over-expression of protein and knockdown of gene; media containing both 2.5ug blasticidin and 0.5ug puromycin were used. Subsequent to selection, cells were tested for over-expression and/or knockdown either by qPCR and/or Western analysis.

Table 2.3: siRNA and shRNA sequences

Gene	shRNA sequences	Source	ID	Vector
TPRKB-sh1	GCGGGAGACUUGAGAAGAA	Custom made-System Biosciences		pLL-EF1a-GFP-T2A-Puro
TPRKB-sh2	TAAATAACAGAAGGGTTAC	Dharmacon	V2LHS_97346	pGIPZ
TPRKB-sh3	TTCAGTAGATAGAGTTCTT	Dharmacon	V3LHS_328180	pGIPZ
TPRKB-sh4	UUUCCCGAAUGCAGGGUAA	Custom made-System Biosciences		pLL-EF1a-GFP-T2A-Puro
PRPK-sh1	TGAATGAGGTCTTCATCGT	Dharmacon	V3LHS_316018	pGIPZ
Lage3-sh1	TCTGTAGTAACAAACATTT	Dharmacon	V3LHS_401667	pGIPZ
Lage3-sh2	TTTTCTGTAGTAACAAACA	Dharmacon	V3LHS_401670	pGIPZ
OSGEP-sh1	ATCCTGGGAGGTTAATCCA	Dharmacon	V3LHS_351890	pGIPZ
OSGEP-sh2	ATAGCTTTGCTAGGACTCC	Dharmacon	V2LHS_173897	pGIPZ
Gene	**siRNA sequence**	**Source**	**ID**	
TPRKB	pooled	Dharmacon	L-031944-02-0010	

Tumor Xenograft Model

All procedures for mice experiments were approved by The University of Michigan University Committee on Use and Care of Animals (UCUCA). HCT116, HCT116 *TP53*$^{wt/R248W}$, and SJSA cells were infected with either control (scrambled sequence) or *TPRKB* shRNA (**Table 2.3**), and infected cells were selected for in medium containing 1ug/ml puromycin (Invivogen) for period of at least 10 days. 1x10^6 cells/side were injected subcutaneously in the flanks of athymic nude mice (Jackson labs). Each group consisted of 10 mice. The tumor was measured biweekly, and tumor volumes were calculated using following formula: $pi/6$(LxWxW), where L is length of the tumor and W is width of the tumor [193]. Tumors were allowed to grow for 35-40 days at which point mice were sacrificed; tumors were collected and photographed.

Genomic editing using CRISPR-Cas9

The CRISPR plasmid for knockout of *TPRKB* and *PRPK* was purchased from Sigma with gRNA sequences shown in **Figure 2.2**. The gRNA sequence was cloned into CRISPR-

Cas9 and gRNA expression vector plentiCRIPSV2 (Gift from Feng Zhang, Addgene plasmid #52961). The cells were transfected using 500ng of Cas9+sgRNA vector in lipofectamine 3000 (Invitrogen) following manufacturer's protocol, and then were seeded into single cells following puromycin selection for 48 hours. Genomic DNA was extracted from the clonal lines using QuickExtract™ DNA Extraction Solution (Epicenter QE09050). Loci targeted by gRNAs were amplified using the primers listed in **Table 2.2**, and then sequenced by the DNA Sequencing Core (University of Michigan Medical School) using the forward primers.

Western Blot Analysis

Cell lysates were collected in NuPAGE LDS Sample Buffer and Reducing Agent (Life Technologies) at a 1x final concentration, sonicated, and denatured at 95ºC for 5-15 minutes. NuPAGE 4-12% Bis-Tris gels (Life Technologies) were run in 1x NuPAGE MES SDS running buffer at 120V for 1.5-2 hours, followed by semi-dry transfer in 1x NuPAGE transfer buffer containing 20% methanol at 25V for 1 hour onto Immobilon-P PVDF membranes (Millipore). Membranes were blocked in either 5% Milk or 5% Bovine Serum Albumin (based on primary antibody manufacturer's instructions) for 1 hour before probing with primary antibodies. A list of all antibodies used in this study can be found in **Table 2.4**. Washes were completed with 1x TBS + 0.1% Tween-20. Signals were detected using Immobilon Western Chemiluminescent HRP Substrate (Millipore). B-actin was used as a loading control unless otherwise specified.

Table 2.4: Antibody information

Name	Company	Catalogue #	Medium	Dilution (1:x)	Host
TPRKB	Origene	TA800166	BSA	250	Mouse
PRPK	Origene	TA808226	Milk	1000	Mouse
p53 (DO-1): sc-126	Santa Cruz	sc-126	Milk	1000	Mouse
BCL2	Cell Signaling	15071	BSA	1000	Mouse
BCL2L1	Cell Signaling	2762	BSA	1000	Rabbit
MDM2-HRP conjugate	Santa Cruz	sc-965	Milk	1000	
β-actin (13E5)-HRP conjugate	Cell Signaling	5125	Milk	5000	
Mouse secondary-HRP conjugate	Cell Signaling	7076	Milk/BSA	5000	
Rabbit secondary-HRP conjugate	Cell Signaling	7074	Milk/BSA	5000	

Cell cycle analyses

H358 cells stably infected with vector control or *TPRKB* shRNA lentiviruses were plated in 6-well plates. Following 40 hours serum starvation to synchronize the cell cycle, 10% serum containing RPMI was added to cells. Based on H358 doubling time of approximately 38 hours (ATCC), cells were collected 40 hours after serum reintroduction. Cells were then trypsinized, washed in Dulbecco's Phosphate Buffered Saline (DPBS), and spun down. Pelleted cells were then resuspended in 0.5ml of 100% ethanol and stored at 4^0C until further use. SJSA-1 cells that had been stably infected with vector control or TPRKB shRNAs were similarly processed, with the exception of collection occurring 24 hours post-serum-reintroduction with their respective media. Prior to staining, cells were re-pelleted, ethanol was decanted, and cells were resuspended in DPBS containing 50ug/ml propidium iodide and 100ug/ml RNAse A. Cells were incubated in the dark for 20 minutes before subjecting to flow-cytometry analyses. Data collected was further

processed through ModFit software (Verity Software House). Data shown is a representative bar graph of two independent experiments.

Notes

Portions of this work have been adapted from the following manuscript:

> Moloy T. Goswami*, Kelly R VanDenBerg*, Sumin Han, Lei Lucy Wang, Bhavneet Singh, Travis Weiss, Myles Barlow, Steven Kamberov, Kari Wilder-Romans, Daniel R. Rhodes, Felix Y. Feng, Scott A. Tomlins. *Identification of TP53RK Binding Protein (TPRKB) dependency in TP53-deficient cancers.* Mol Cancer Res, 2019. In Press.
>
> * Co-first authors

Contributors to data in this chapter: Kelly R VanDenBerg (Kennaley), Moloy T. Goswami, Sumin Han, Lei Lucy Wang, Bhavneet Singh, Travis Weiss, Myles Barlow, Steven Kamberov, Kari Wilder-Romans, Daniel R. Rhodes, Felix Y. Feng, Scott A. Tomlins

DRR conducted analysis of the Broad Institute's Project Achilles database to identify synthetic lethal pairs. MTG, KRV, and SAT conceived and designed these studies. MTG, KRV, and LLW conducted the proliferation studies with assistance from BS, TW, MB, and SK for completing qPCR validation of knockdown and expression. KRV and SH created CRISPR-knockout cell lines. MTG, KRV, and LLW performed Western blots. MTG performed cell cycle analysis. MTG, KWR, and FYF designed and conducted the *in vitro* mouse studies.

Chapter 3 Characterization of TPRKB protein-level interactions and translation regulation

Abstract

In Chapter 2 we identified TPRKB, a poorly characterized member of the tRNA-modifying EKC/KEOPS complex, as a unique vulnerability in a range of TP53-deficient cancers. However, the exact role of TPRKB in humans and the mechanism surrounding this sensitivity remain largely unknown. Using a series of endogenous and exogenous systems, we demonstrate that TP53 indirectly mediates TPRKB degradation, in part through the proteasome, while an interacting member of the EKC/KEOPS complex, PRPK, directly stabilizes TPRKB despite TP53 presence. Together, this reveals novel, dynamic regulation of TPRKB in human cells. As TPRKB dependency in TP53-deficient cancers appears to be largely independent from its role within the EKC/KEOPS complex, we sought to identify novel TPRKB interactors that may determine sensitivity. Using an IP:MS based approach we identified and validated that TPRKB interacts with another tRNA-modifying complex TRMT6/TRMT61A, responsible for the m1A58 modification of tRNA. However, *TRMT6/TRMT61A* knockdown did not show TP53-dependent phenotypes as TPRKB depletion does and levels of the m1A modification were unaltered in TPRKB-depleted cells, leaving the functional consequences of the interaction undetermined. Nevertheless, we found that TPRKB-depleted cells harbored additional translation-level alterations, including changes in other tRNA modifications, reduced expression of RNA polymerase III gene *POLR3GL* (responsible for transcribing tRNA), and changes in overall protein translation that correlate with proliferative response. Thus, we find that TPRKB is

implicated in various facets of protein translation, and future studies should aim to further characterize TPRKB's role in this capacity and elucidate mechanisms of TPRKB-dependency in TP53-deficient cancers.

Introduction

In Chapter 2 we characterized TPRKB dependency across a range of cell lines and discovered that generally *TP53* wild-type (cancer and benign) cells lack sensitivity to TPRKB depletion while *TP53*-null, *TP53*-mutant, and *MDM2*-amplified cancers respond strongly. This observation represents a novel strategy for targeting TP53-deficient cancers. Yet, the crucial question of how TPRKB is able to mediate this response remains.

TPRKB's only known role is as a member of the EKC/KEOPS complex [98-100, 102]. This complex is responsible for depositing the universally conserved t6A37 modification on all ANN decoding tRNAs[102]. Without this modification, translational fidelity is reduced as codon:anticodon interactions involving these tRNAs become less stable[154, 157]. With this fundamental link to protein translation, we postulated that TPRKB depletion in humans may lead to larger translational defects and that novel aspects of TPRKB function may be evident at the translational level.

Of note, TPRKB-dependent phenotypes witnessed in Chapter 2 appear largely EKC/KEOPS complex-independent. This raised numerous questions surrounding what other functions TPRKB itself may have within mammalian cells and how it mediates these functions. Through a proteomics-based approach, Wan et al. found that TPRKB and its only direct interacting partner in the EKC/KEOPS complex, PRPK, have overlapping interactomes independent from other members of the complex, suggesting that TPRKB and PRPK may form

sub-complexes within human cells[101, 105]. In our isogenic cells, PRPK depletion provided similar, yet far weaker TP53-dependent phenotypes. Consequently, we could not rule out that TPRKB-PRPK sub-complexes (as opposed to TPRKB alone) could be responsible for determining sensitivity. Alternatively, weaker phenotype with the atypical protein kinase, PRPK, may also reflect the presence of similar kinases with functional redundancies.

Thus, in order to elucidate potential EKC/KEOPS-independent TPRKB functions we sought to characterize protein-protein interactions between our key proteins of interest – TP53, TPRKB, and PRPK – and identify novel protein interactions that may be involved in generating the phenotypes we witness.

Results

Confirmation that TP53 and TPRKB do not directly interact in human cells

While PRPK has been shown to interact with, phosphorylate, and activate TP53, exogenously over-expressed TPRKB and TP53 do not interact[98, 117, 185]. However, TP53 and TPRKB interaction has not been assessed with endogenous proteins. Using CRISPR-Cas9, we endogenously tagged *TPRKB* with a Flag-epitope in HEK293T cells. By IP-Western blotting, we observed the known interaction of PRPK and TPRKB, but TPRKB and TP53 did not interact (**Figure 3.1A**). Lastly, we confirmed that exogenously expressed TPRKB and TP53 did not interact (**Figure 3.1B**). Our data is consistent with previous observations and supports an indirect relationship between TPRKB and TP53.

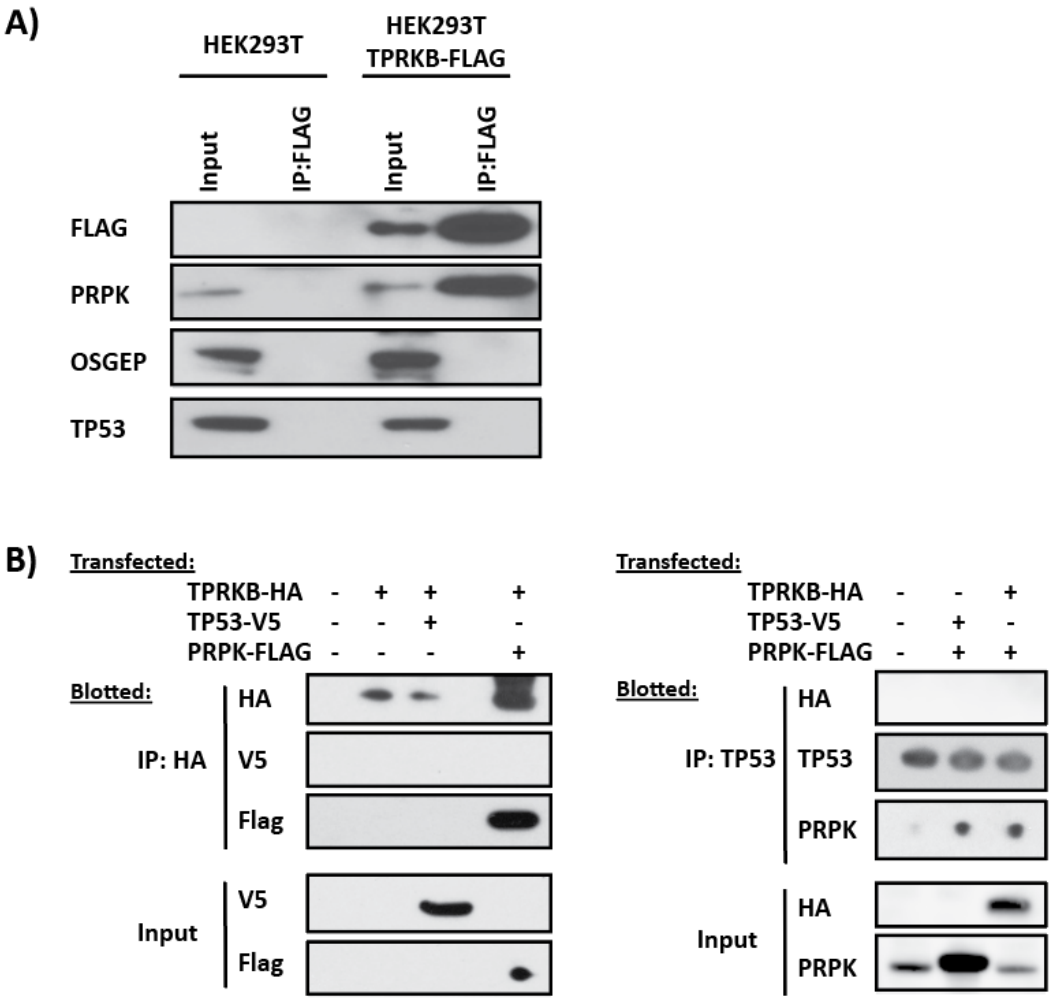

Figure 3.1: TP53 and TPRKB do not directly interact

A) Parental HEK293T and HEK293T with CRISPR introduced FLAG epitope into the endogenous TPRKB locus (HEK293T-TPRKB-Flag) were used for co-immunoprecipitation. After Flag pulldown, samples were tested for endogenous TPRKB-Flag interaction with PRPK or TP53. **B)** IP-western analyses were carried out with HEK293T cells transiently over-expressing TPRKB-HA, TP53-V5 and/or PRPK-Flag. TPRKB or TP53 were independently immunoprecipitated and western blots were performed to determine interactors.

TP53 mediates TPRKB degradation, which can be partially rescued by either PRPK or inhibition of proteasomal machinery

Given the interaction of PRPK with both TPRKB and TP53, we sought to determine whether TP53 could influence TPRKB stability through PRPK. Using exogenously expressed tagged proteins in HEK293T cells, we found that increasing amounts of TP53 led to a concentration-dependent reduction in TPRKB protein levels (**Figure 3.2**). This observation was consistent in H358 cells, where stable exogenous expression of TP53 reduced TPRKB levels (**Figure 3.2A**). Likewise, even in HEK293T cells (insensitive to *TPRKB* knockdown), siRNA-mediated *TP53* knockdown resulted in increased TPRKB levels (**Fig 3.2A**). We thus investigated the mechanism whereby TP53 mediates TPRKB by treating HEK293T cells co-expressing TPRKB and TP53 with the proteasome inhibitor bortezomib. As shown in **Figure 3.2A**, this led to a marked increase in TPRKB levels, even though a TP53-dependent reduction in TPRKB protein was still observable.

In addition to interacting with, phosphorylating, and activating TP53, PRPK is the only component of the EKC/KEOPS complex that directly interacts with TPRKB[98, 117, 185]. As we observed that PRPK was the only other member of the EKC/KEOPS complex that showed even modest differential response by *TP53* status, we hypothesized that interaction with PRPK may mediate the TPRKB dependency of TP53-deficient cells. Through exogenous expression of tagged proteins, we found that PRPK is able to significantly stabilize TPRKB protein levels in both the absence and presence of exogenous TP53 expression (**Figure 3.2B & C**). Importantly, however, co-expression of PRPK with other unrelated proteins did not prevent their TP53-mediated degradation, highlighting the specificity of PRPK-mediated TPRKB stabilization (**Figure 3.2D**). Additionally, stable *PRPK* knockout in HEK293T cells (**Figure 3.2B**)

substantially reduced TPRKB levels. The markedly reduced TPRKB levels upon PRPK depletion suggests that the mild phenotypes observed with *PRPK* knockdown/knockout, as described in Chapter 2, are likely due to reduction in TPRKB levels.

We then sought to determine if the TPRKB-PRPK interaction was necessary for stabilization of TPRKB protein levels. To address this, we created two TPRKB mutants that we hypothesized may disrupt the interaction between PRPK and TPRKB based on computational modeling. The first was TPRKB p.N59F, which was postulated to disrupt a critical hydrogen bond. The second mutant was TPRKB p.S170R, which was predicted to be a similar mutation to the yeast TPRKB p.I176R, previously shown to disrupt a hydrophobic interaction between TPRKB and PRPK. While TPRKB p.N59F maintained interaction capabilities with PRPK, TPRKB p.S170R did not appear to interact with TPRKB in HEK293T cells even after normalization of TPRKB protein pulldown (**Figure 3.2E**). Interestingly, we noted that the TPRKB p.S170R mutant was expressed at far lower levels than either the wild type or p.N59F mutant. Additionally, while TPRKB p.S170R was still degraded by TP53 we did not see a rescue in TPRKB expression upon PRPK co-expression.

Taken together, our data demonstrates that TP53-dependent degradation of TPRKB can be inhibited through stabilization by PRPK or through proteasomal pathway inhibition. Furthermore, while TP53 degradation of TPRKB happens independently of direct protein interaction the TPRKB-PRPK interaction appears necessary for TPRKB stabilization.

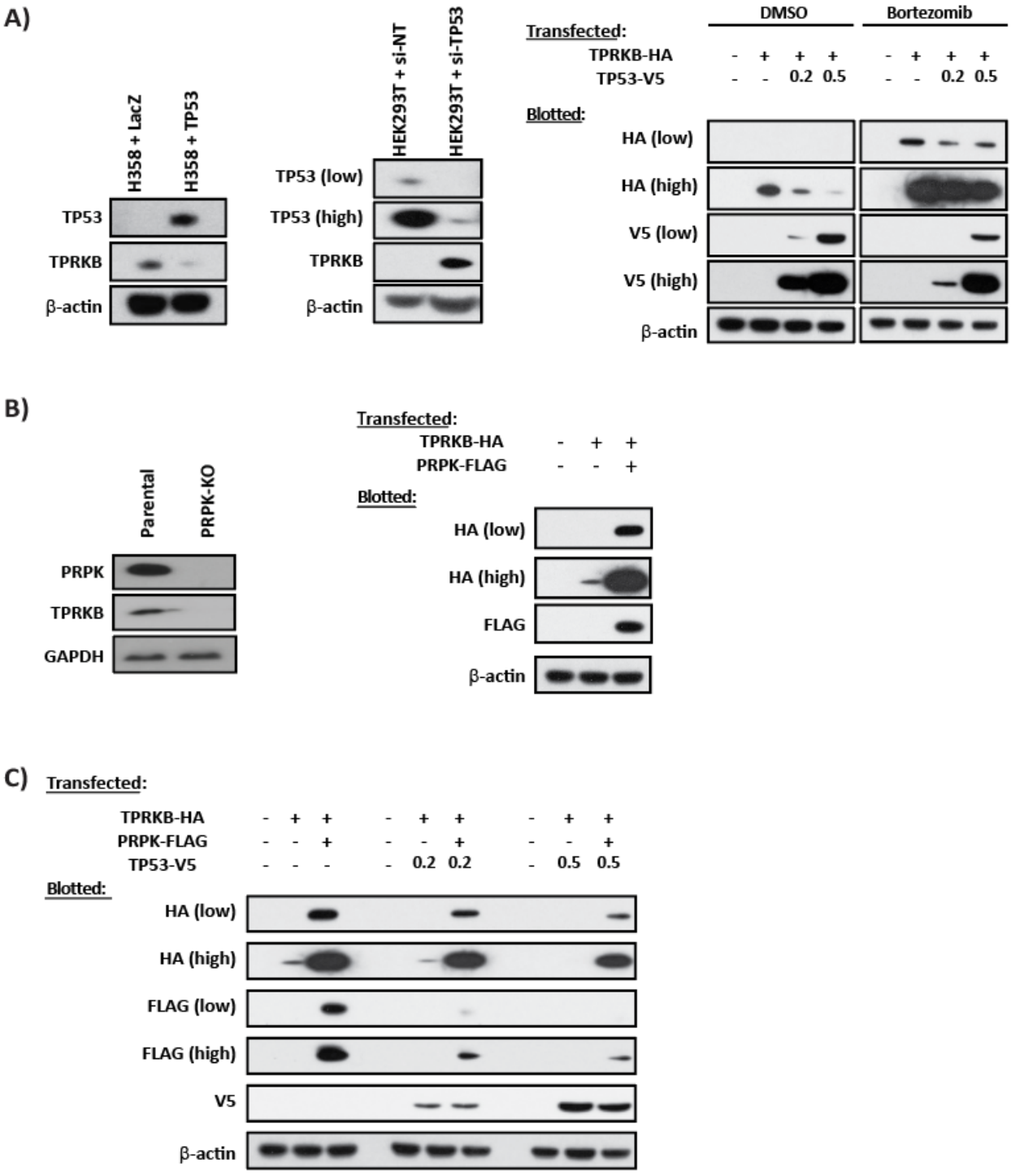
A)
H358 + LacZ
H358 + TP53
TP53
TPRKB
β-actin
HEK293T + si-NT
HEK293T + si-TP53
TP53 (low)
TP53 (high)
TPRKB
β-actin
Transfected:
DMSO
Bortezomib
TPRKB-HA - + + + - + + +
TP53-V5 - - 0.2 0.5 - - 0.2 0.5
Blotted:
HA (low)
HA (high)
V5 (low)
V5 (high)
β-actin
B)
Parental
PRPK-KO
PRPK
TPRKB
GAPDH
Transfected:
TPRKB-HA - + +
PRPK-FLAG - - +
Blotted:
HA (low)
HA (high)
FLAG
β-actin
C)
Transfected:
TPRKB-HA - + + - + + - + +
PRPK-FLAG - - + - - + - - +
TP53-V5 - - - - 0.2 0.2 - 0.5 0.5
Blotted:
HA (low)
HA (high)
FLAG (low)
FLAG (high)
V5
β-actin

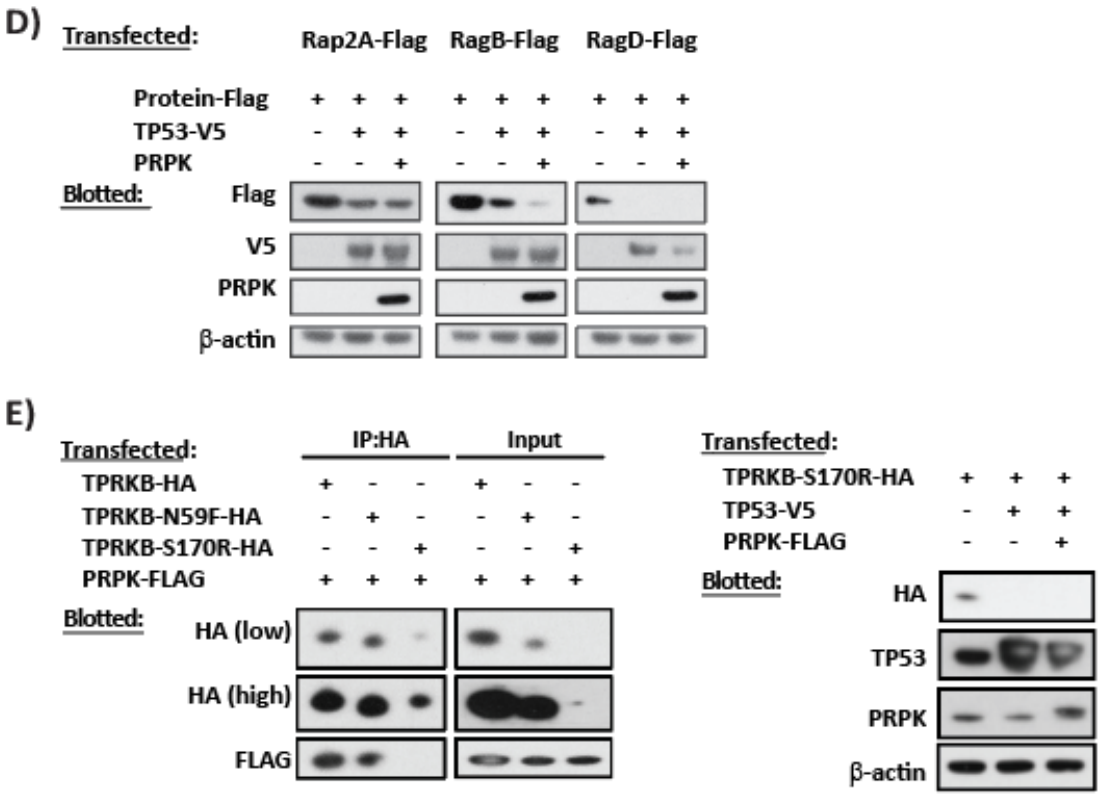

Figure 3.2: TP53 and PRPK dynamically regulate TPRKB protein levels

A) TPRKB protein levels were assessed by Western blot in H358 cells with stable overexpression of TP53 and HEK293T cells with transient depletion of TP53 through siRNA knockdown. Lower panel utilizes HEK293T cells with transient overexpression of TPRKB and increasing levels of TP53 in the presence of DMSO or proteasome inhibitor bortezomib. **B)** HEK293T cells with PRPK CRISPR knockout or co-expression of TPRKB with PRPK were blotted to assess impact on TPRKB protein levels. **C)** HEK293T cells were subjected to transient transfections of TPRKB, PRPK, and/or increasing concentration of TP53 to assess determinants of protein stability. **D)** Co-expression of random proteins Rap2A, RagB, and RagD with TP53 or PRPK were assessed for TPRKB-specific effects of regulation in HEK293T. **E)** The first panel shows co-IP experiments with wild-type TPRKB and mutants (N59F and S170R). Association with PRPK was assessed by Western. Next panel shows co-expression of TPRKB p.S170R with TP53 and PRPK.

TPRKB interacts with TRMT6 in TP53 wild-type and null cells

In order to identify novel protein interactors for TPRKB across a range of cell lines, we conducted IP:MS experiments in HEK293T, H358, U2OS expressing *LacZ* control (U2OS+*LacZ*), and U2OS overexpressing *MDM2* (U2OS+*MDM2*) cells transiently transfected with either puro-control vectors or FLAG-TPRKB. Using a fold-change of control (FC_A) cut-off of 2.0, we identified 242, 618, 279, and 501 potential interactions in HEK293T, H358, U2OS+LacZ, and U2OS+MDM2, respectively. Of those, only 9 potential interacting partners were found in all four cell lines (**Figure 3.3A&B;** a full list of interactors for each cell line above the 2.0 cut-off can be found in the appendices). As expected, the strongest of the common interactions identified were between TPRKB and the 4 other members of the EKC/KEOPS complex – TP53RK, OSGEP, LAGE3, and C14orf142, consistent with its known conserved function. The remaining interactions were with members of another tRNA modifying complex TRMT6 (tRNA Methyltransferase 6) and TRMT61A TRMT61A (tRNA Methyltransferase 61A), and with NME3 (NME/NM23 nucleoside diphosphate kinase 3), PIGT (Phosphatidylinositol Glycan Anchor Biosynthesis Class T), and VPS2A (Vacuolar Protein Sorting-Associated Protein 2-1).

TRMT6 and the catalytic subunit of its complex TRMT61A were previously proposed as potential TPRKB interactors by Wan et al, in 2017, but this was never validated[101]. Using two additional protein association methods, we show by co-immunoprecipitation (**Figure 3.3C**) and recombinant protein pulldown (**Figure 3.3D**) that TPRKB does associate with TRMT6 in human lysate. We attempted to validate TRMT61A in cell lines that identified this member as a strong interactor (HEK293T with FC-A= 4.02 and FC-B=1.49; H358 with FC-A=9.01 and FC-B=1.61).

However, due to the limitations of commercially available antibodies, we were unable to validate whether TPRKB also associates with TRMT61A in these cells.

We also looked at common interactors in TPRKB sensitive cell lines (H358 and U2OS+*MDM2*) versus common interactors in TPRKB non-sensitive cell lines (HEK293T and U2OS+*LacZ)* to see if we could determine potential mediators of sensitivity. Again, using a fold-change cut-off of compared to control of 2.0, we found 9 common interactors in TPRKB non-sensitive cell lines and 27 common interactors in TPRKB sensitive cell lines. Of note, these genes represent those interactions wild a fold-change greater than 2 in both cell lines of interest, while alternate cell lines had no detected interactions or interactions with a fold-change of less than 2. For example, ALG1 was detected in non-sensitive cell lines at a fold-change greater than 2, while H358 showed no interaction and U2OS+*MDM2* only had a fold-change of 1.02. Thus, we cannot rule out the possibility that these interactions may occur at greater or lesser frequency in some contexts, and the strength and extent of interactions should be determined for each individual cell line.

A)

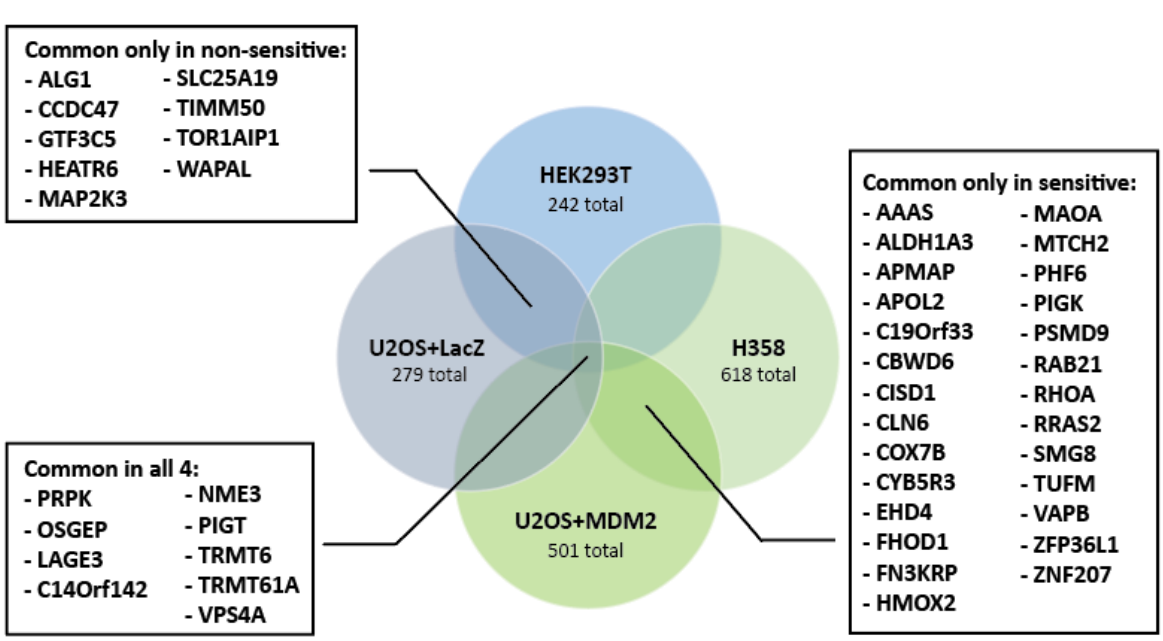

B)

HEK293T IP:FLAG-TPRKB - MS

Gene	FC_A	FC-B
TPRKB	714.74	116.82
OSGEP	78.5	10.34
C14orf142	34.64	4.93
TP53RK	24.96	4.66
LAGE3	24.82	2.55
TRMT6	6.17	1.07
TRMT61A	4.02	1.49
PIGT	2.24	1.38
VPS4A	2.13	1.41
NME3	2.13	0.9

H358 IP:FLAG-TPRKB - MS

Gene	FC_A	FC-B
TPRKB	492.64	38.49
OSGEP	55.07	5.12
TP53RK	51.07	4.82
LAGE3	26.03	2.91
C14orf142	13.02	1.92
TRMT6	12.01	1.84
TRMT61A	9.01	1.61
PIGT	4	1.23
VPS4A	4	1.23
NME3	2	1.08

U2OS+LacZ IP:FLAG-TPRKB - MS

Gene	FC_A	FC-B
TPRKB	146.27	280
OSGEP	48.68	44.75
TP53RK	24.84	22.87
C14orf142	8.95	8.29
LAGE3	7.95	7.38
TRMT6	5.97	5.56
VPS4A	9.94	9.2
TRMT61A	3.98	3.73
NME3	3.98	3.73
PIGT	2.99	2.82

U2OS+MDM2 IP:FLAG-TPRKB - MS

Gene	FC_A	FC_B
OSGEP	56.77	51.81
TPRKB	55.56	135.61
TP53RK	27.85	25.46
C14orf142	15.46	14.17
LAGE3	11.33	10.41
TRMT6	5.13	4.76
VPS4A	5.66	7.98
PIGT	2.57	3.65
TRMT61A	2.03	1.94
NME3	2.03	1.94

C)

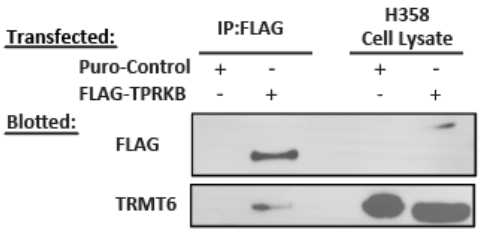

D)

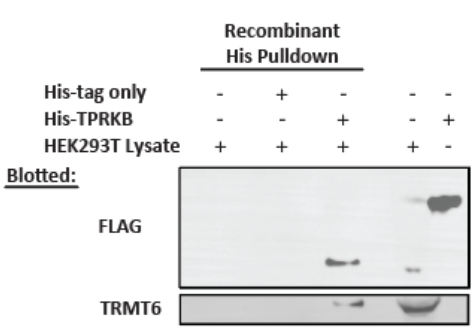

Figure 3.3: Identification and validation of TPRKB interaction with TRMT6

Co-IP experiments were carried out in HEK293T, H358, U2OS+*LacZ*, and U2OS+*MDM2* cells overexpressing TPRKB-FLAG, and mass spectrometry was performed to assess protein interactions. A) The Venn Diagram shows each cell line used, how many total hits were analyzed for commonality based on a fold change over control cut-off of 2.0. Blue circles represent non-responsive cell lines while green indicate responsive cell lines. Those interactions common between sensitive, non-sensitive, and all groups are highlighted in boxes outside of the Diagram. B) Mass spectrometry results highlighting common interactors between all four cell lines with FC_A cut-off of 2.0. Samples were analyzed with assistance from CRAPome (crapome.org) with FC_A indicating the standard fold change estimating background by averaging spectral counts across controls while FC_B indicates stringent fold change estimating the background by combining the top 3 values for each prey using geometric mean calculations. Interactions between TRMT6 and TPRKB were confirmed by **B)** co-IP in H358 cells and **C)** using recombinant TPRKB-His incubated with HEK293T protein lysate.

Although TPRKB depletion alters certain tRNA modifications, m1A remains largely unaffected

To date, the only known function for TRMT6 is its role within the TRMT6/TRMT61A complex providing the m1A58 modification on tRNAs. Since TPRKB is thought to act as an allosteric regulator of the EKC/KEOPS complex, enhancing its ability to provide the t6A37 modification, we hypothesized that perhaps TPRKB may modulate activities of multiple tRNA complexes. In order to assess this possibility, we performed tRNA modification profiling of HEK293T and H358 cells with *TPRKB* knockout and H358 cells with *TPRKB* knockdown with two independent *TPRKB* shRNAs. While no tRNA modifications tested were increased with *TPRKB* knockdown, we did find several that were decreased. TPRKB depletion led to reductions in t6A, ms2t6A. m3C, and m3U modifications in *TPRKB* knockdown cells, but m1A was not significantly altered (**Figure 3.4A**). Interestingly, *TPRKB* knockout cells, which needed to be propagated with knockdown for 1-2 months prior to RNA isolation, had a different tRNA modification signature than their *TPRKB* knockdown counterparts, which only needed 10-14 days propagation with knockdown before RNA isolation, suggesting adaptive molecular changes may occur with longer TPRKB depletion.

Further, we performed transient siRNA knockdown of *TRMT6* and *TRMT61A* in HEK293T and H358 cells. We found *TRMT6* or *TRMT61A* knockdown does not influence cell proliferation regardless of TP53 status (**Figure 3.4B)**. Since the TRMT6-TPRKB interaction

does not appear to critically affect m1A levels and TRMT6 loss does not recapitulate TPRKB phenotypes, the functional consequences of the TRMT6-TPRKB interaction remain unclear.

A)

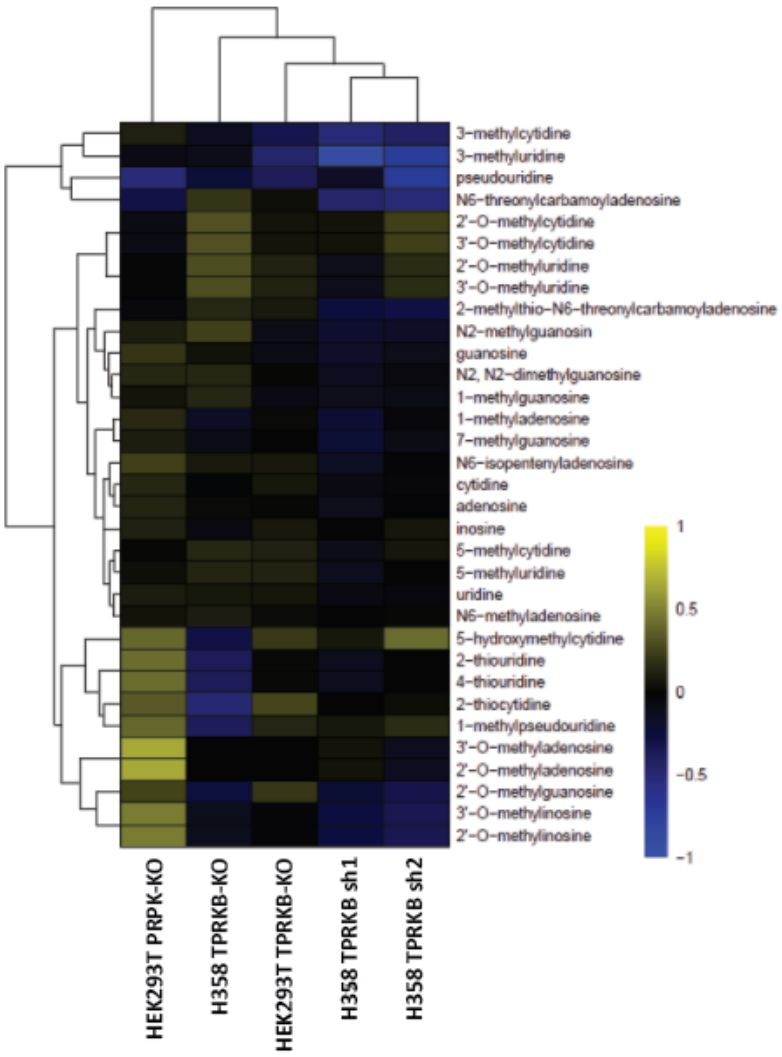
3-methylcytidine
3-methyluridine
pseudouridine
N6-threonylcarbamoyladenosine
2'-O-methylcytidine
3'-O-methylcytidine
2'-O-methyluridine
3'-O-methyluridine
2-methylthio-N6-threonylcarbamoyladenosine
N2-methylguanosin
guanosine
N2, N2-dimethylguanosine
1-methylguanosine
1-methyladenosine
7-methylguanosine
N6-isopentenyladenosine
cytidine
adenosine
inosine
5-methylcytidine
5-methyluridine
uridine
N6-methyladenosine
5-hydroxymethylcytidine
2-thiouridine
4-thiouridine
2-thiocytidine
1-methylpseudouridine
3'-O-methyladenosine
2'-O-methyladenosine
2'-O-methylguanosine
3'-O-methylinosine
2'-O-methylinosine
1
0.5
0
-0.5
-1
HEK293T PRPK-KO
H358 TPRKB-KO
HEK293T TPRKB-KO
H358 TPRKB sh1
H358 TPRKB sh2

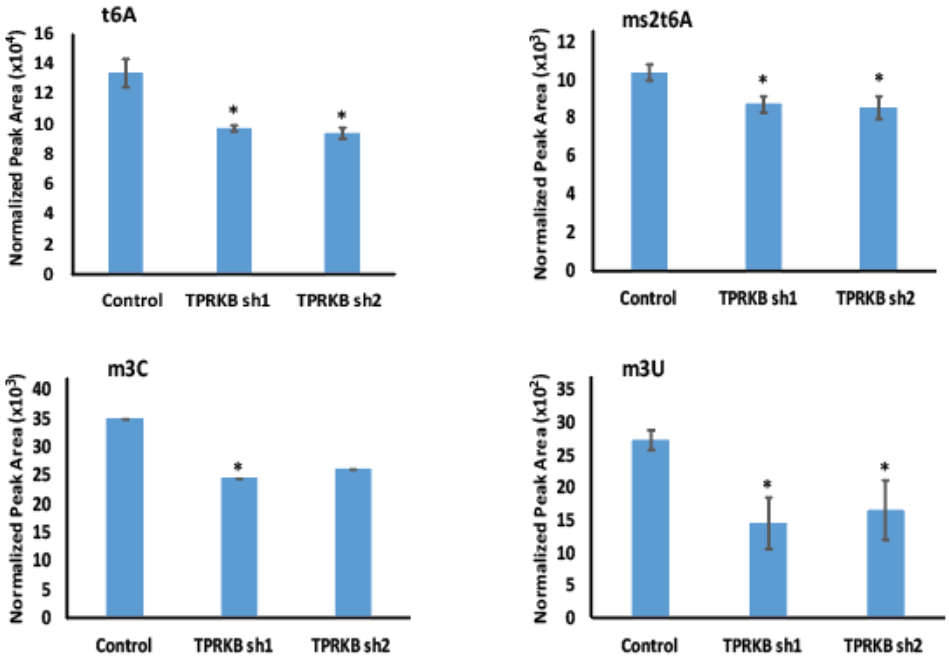
t6A
Normalized Peak Area (x10⁴)
Control
TPRKB sh1
TPRKB sh2
ms2t6A
Normalized Peak Area (x10³)
m3C
Normalized Peak Area (x10³)
m3U
Normalized Peak Area (x10²)

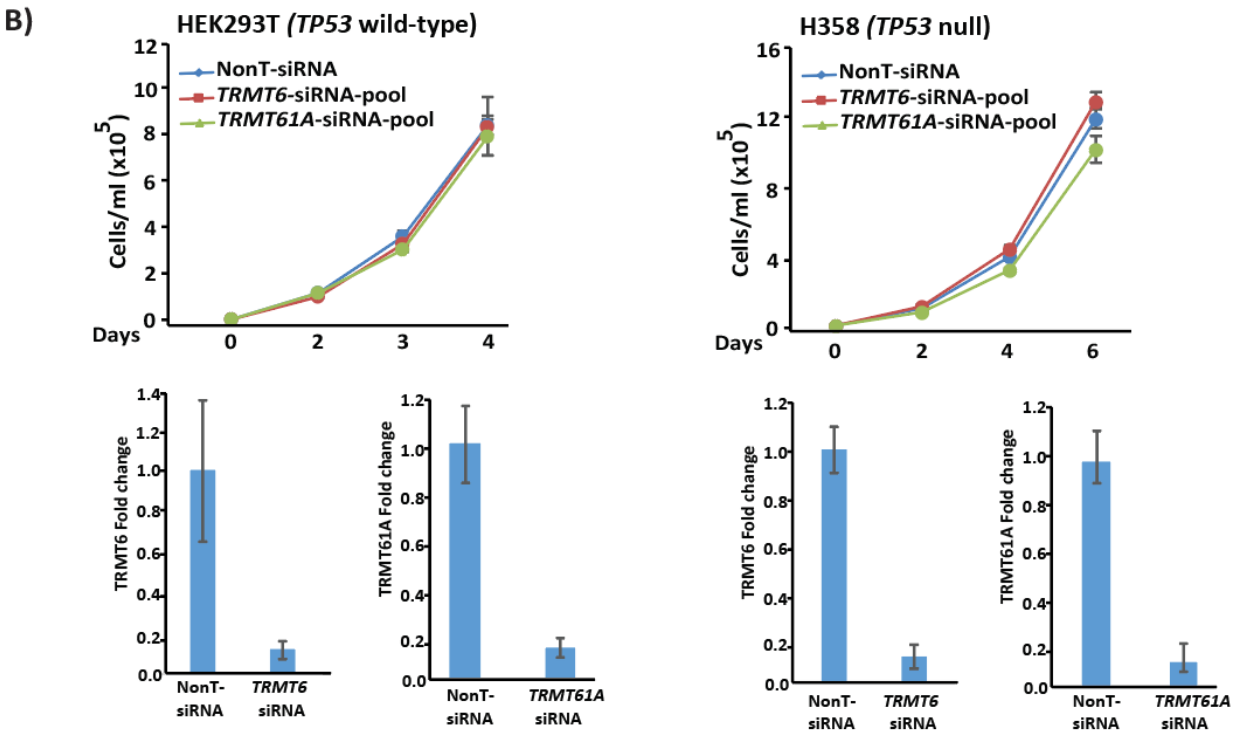

Figure 3.4: Although the abundance of several tRNA modifications are altered upon TPRKB knockdown, m1A was not and knockdown of members of the m1A-modifying complex *TRMT6/TRMT61A* does not significantly impact proliferation

A) LC-MS was used on tRNAs from HEK293T and H358 cells with *TPRKB* knockout and in H358 cells with *TPRKB* knockdown to assess the relative abundance of modifications compared to control cells. Results from all modifications tested are presented in heatmap compared to control while individual quantification of specific tRNA modifications that were found to be significant in H358 TPRKB shRNA knockdown cells are represented in bar graphs. **B)** Pooled siRNA knockdown of *TRMT6* or *TRMT61A* was carried out in HEK293T cells or H358 cells. Knockdown was confirmed by accompanying qPCR panels. All experiments utilized triplicate samples, with the average and standard error plotted. * indicate p-values < 0.05

TPRKB-deficient cells show alterations in translation and RNA polymerases

Since we witnessed alterations in multiple tRNA modifications, including t6A, ms2t6A, m3U, and m3C, we were curious if overall protein translation was affected in cells lacking TPRKB. Using TPRKB knockout cells generated through a CRISPR-Cas9 approach discussed in Chapter 1, we show TP53 wild-type HEK293T have enhanced translation compared to parental controls while TP53-null H358 cells had significantly reduced translation (**Figure 3.5A**). These alterations in translation are positively correlated with the proliferative changes we witness in TPRKB depleted cells. Consequently, the alterations in protein translation could either be the reason for or result of proliferative changes.

One aspect that contributes to overall translation rate is abundance of tRNAs and rRNAs, which can further be affected by their modification status. To determine if abundance of either tRNAs or rRNAs are key factors for TPRKB response, we utilized RNA Polymerase I inhibitor CX-5461 to block rRNA synthesis or an RNA Polymerase III inhibitor to block tRNA and some rRNA synthesis in HEK293T or H358 parental and TPRKB knockout cells. We would expect that if tRNAs or rRNAs were downregulated by TPRKB loss, that these inhibitors would be more effective at reducing proliferation in TPRKB-KO than parental cells. Interestingly, TPRKB knockout in H358 cells leads to less sensitivity to RNA polymerase inhibitors, while only inhibition of RNA polymerase III leads to enhanced sensitivity in HEK293T TPRKB-KO cells (**Figure 3.5B)**.

Furthermore, to assess gene expression alterations from TPRKB knockdown, we conducted an Affymetrix Human Gene ST 2.1 microarray in a panel of TP53-deficient cell lines (**Figure 3.5C**). Using a fold-change cut-off compared to non-targeting control of >1.5 or <-1.5 in at least 8 of the 10 samples, we found few consistent significant alterations in TPRKB depleted

cells, both demonstrating limited alterations in the mRNA pool and supporting that the phenotypes we witness are in fact due to TPRKB depletion and not some off target effect. One gene that caught our attention from the microarray analysis was a member of the RNA Polymerase III complex, *POLR3GL*. We found in our microarray and validated by qPCR, that *POLR3GL* was generally downregulated in cells with TPRKB loss (**Figure 3.5C**). Since our microarray only utilized TP53-deficient cells, we were curious if this trend would hold in TP53 wild-type cells. We chose a panel a cell lines that were commonly used throughout these studies to determine how *POLR3GL* expression was altered in various backgrounds. Although *POLR3GL* expression was generally downregulated across cell lines, independently of TP53 status, our TPRKB knockout cells showed increased expression (**Figure 3.5D**). We hypothesize that, like tRNA modifications, this could be indicative of an adaptive response to long-term loss of TPRKB.

A)

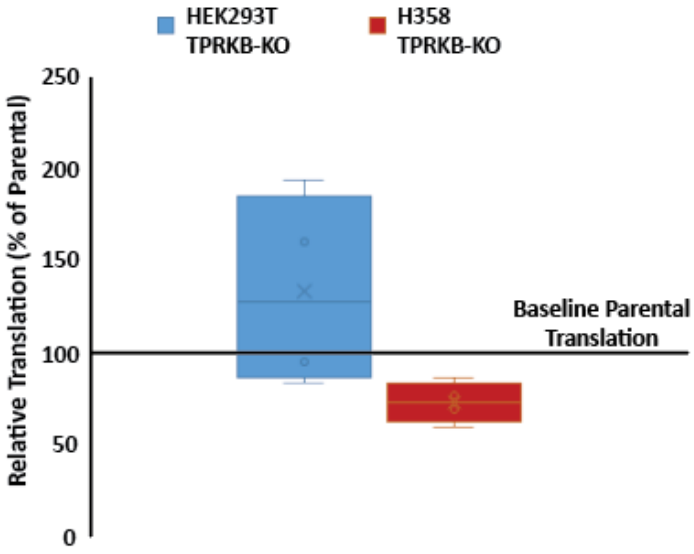
HEK293T
TPRKB-KO
H358
TPRKB-KO
Relative Translation (% of Parental)
250
200
150
100
50
0
Baseline Parental
Translation

B)

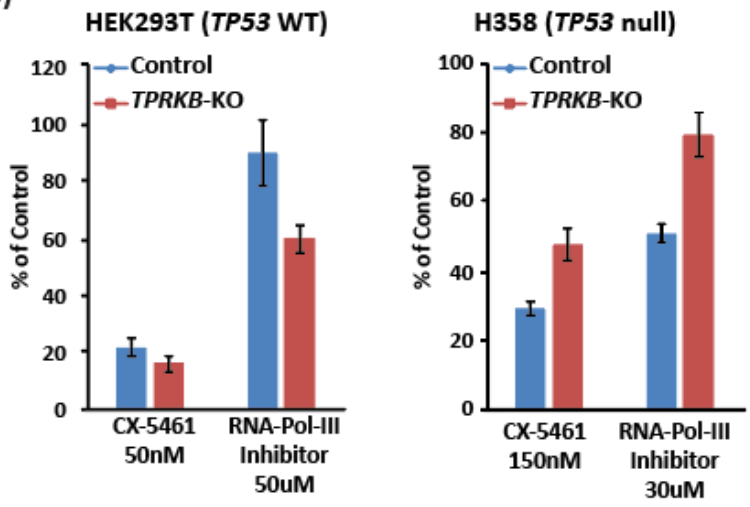
HEK293T (TP53 WT)
Control
TPRKB-KO
% of Control
120
100
80
60
40
20
0
CX-5461
50nM
RNA-Pol-III
Inhibitor
50uM
H358 (TP53 null)
Control
TPRKB-KO
% of Control
100
80
60
40
20
0
CX-5461
150nM
RNA-Pol-III
Inhibitor
30uM

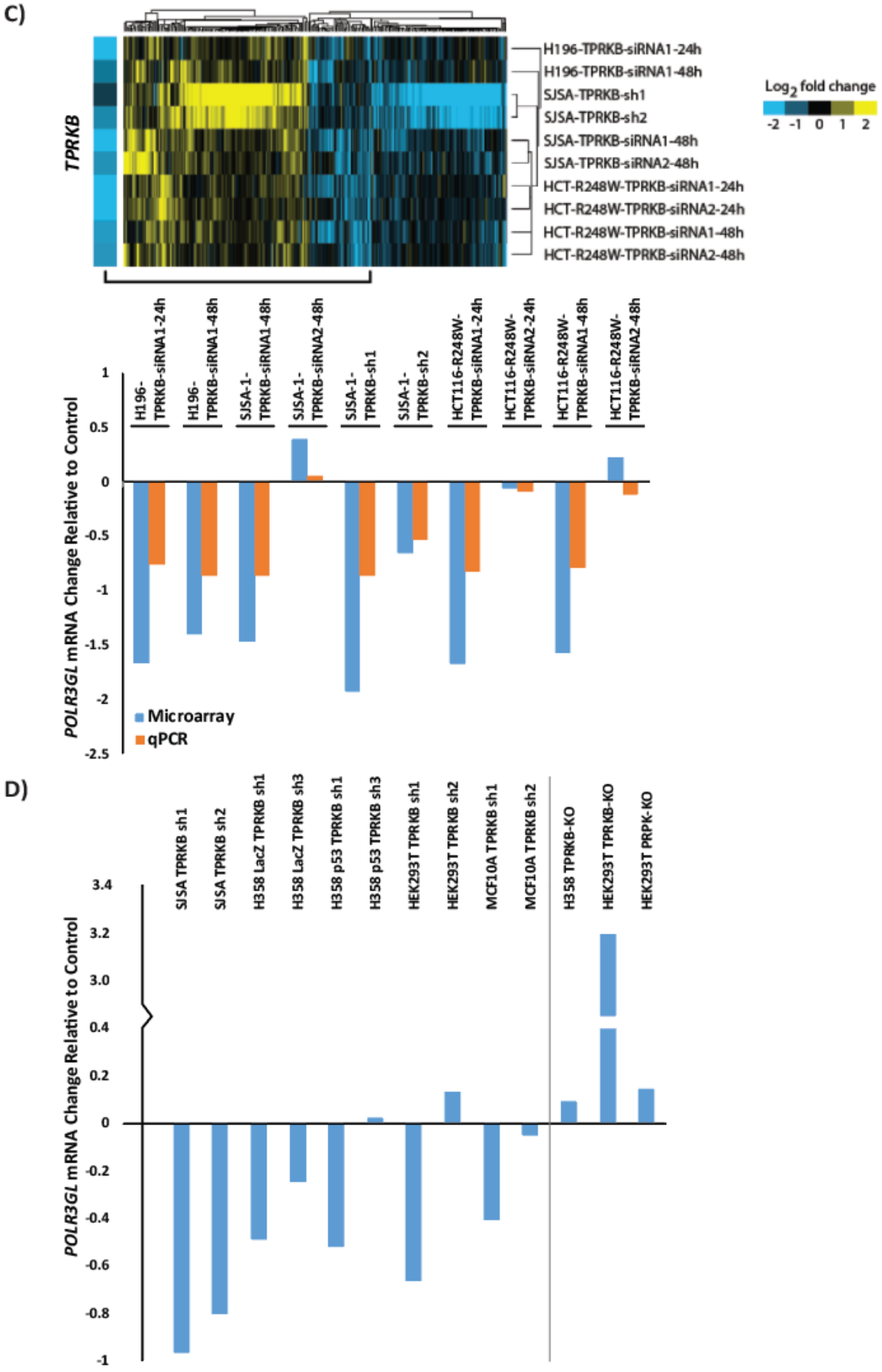
C)
TPRKB
H196-TPRKB-siRNA1-24h
H196-TPRKB-siRNA1-48h
SJSA-TPRKB-sh1
SJSA-TPRKB-sh2
SJSA-TPRKB-siRNA1-48h
SJSA-TPRKB-siRNA2-48h
HCT-R248W-TPRKB-siRNA1-24h
HCT-R248W-TPRKB-siRNA2-24h
HCT-R248W-TPRKB-siRNA1-48h
HCT-R248W-TPRKB-siRNA2-48h
Log2 fold change
-2 -1 0 1 2
POLR3GL mRNA Change Relative to Control
Microarray
qPCR
D)
POLR3GL mRNA Change Relative to Control
SJSA TPRKB sh1
SJSA TPRKB sh2
H358 LacZ TPRKB sh1
H358 LacZ TPRKB sh3
H358 p53 TPRKB sh1
H358 p53 TPRKB sh3
HEK293T TPRKB sh1
HEK293T TPRKB sh2
MCF10A TPRKB sh1
MCF10A TPRKB sh2
H358 TPRKB-KO
HEK293T TPRKB-KO
HEK293T PRPK-KO

Figure 3.5: TPRKB depletion leads to several alterations with respect to protein translation

A) HEK293T and H358 parental and TPRKB-KO cells were assessed for overall protein translation through OPP flow-based assay. Each box plot represents the percent change compared to parental of four independent experiments with standard error. Parental translation is indicated on the graph and was set at 100%. **B)** HEK293T and H358 parental and TPRKB-KO cells were treated with either RNA polymerase I inhibitor CX-5461 or RNA polymerase III inhibitor, and proliferative differences were assessed through Incucyte cell confluency measurements. **C)** A panel of cell lines with TPRKB transient or stable knockdown were used for Affymetrix Human Gene ST 2.1 microarray. Overall results are presented in the heatmap as log2 fold-change versus non-target control with the blue pop-out column on the left confirming TPRKB reductions across these cell lines. Several genes were chosen for qPCR validation, and the results of validation alongside microarray results for *POLR3GL* are shown relative to control cells. **D)** qPCR quantification of *POLR3GL* from a panel of cell lines frequently used throughout our studies are represented relative to control cells.

Discussion

To elucidate the mechanism of TPRKB dependency in TP53-deficient cells we investigated translational and protein-level events across several cell lines characterized in Chapter 2. Expanding on a previous report showing no interaction between exogenous TP53 and TPRKB[98], we confirmed these findings and demonstrated for the first time that endogenous TPRKB and TP53 do not interact. However, we find TP53 induces TPRKB degradation in a concentration-dependent manner that can be alleviated either through PRPK expression or proteosomal inhibition, providing a potential mechanism for TPRKB dependency only in the presence of TP53 alterations. Importantly, PRPK is unable to rescue expression of non-interacting mutant TPRKB p.S170R, indicating that direct protein interaction is required for maintained TPRKB stability in this context.

Aside from its function within the EKC/KEOPS complex, little is known about TPRKB alone. To identify other interactors of TPRKB outside the canonical complex, we conducted co-IP followed by mass spectrometry analysis across four cell lines. The identification of only 9 common interactors (4 of which were with the other members of the EKC/KEOPS complex) suggests two key aspects for TPRKB protein functionality. The first is that TPRKB has few conserved functional interactions across cell lines, such as that with the ubiquitous t6A-modifying EKC/KEOPS complex. The second is that TPRKB may have cell-line and context-

specific interactions. This is further supported by the observation that between isogenic cell lines U2OS+*LacZ* and U2OS+*MDM2* there are 152 common interactions between the 279 and 501 potential interactions identified (fold-change cut-off of 2.0).

Identification of TRMT6 and TRMT61A as other interactors common in all cell lines was an interesting find for several reasons. First, a previous report by Wan et al. also used AP:MS to identify TRMT6 and TRMT61A as potential interactors for both TPRKB and PRPK, but not other EKC/KEOPS complex members[101]; however, no formal validation was completed. Second, TRMT6/TRMT61A are members of a separate tRNA-modifying complex that is known to distribute the m1A58 mark on various tRNAs, including the initiator tRNA ($tRNA_iMet$)[194, 195]. $tRNA_iMet$ requires this mark for proper stabilization, and elevated $tRNA_iMet$ and TRMT6/TRMT61A expression has been associated with altered tRNA abundances[196], enhanced proliferation[196, 197], and anchorage-independent growth[198].

Within the EKC/KEOPS complex, TPRKB acts as an allosteric regulator able to enhance t6A-modifying activities[103]. We questioned whether TPRKB would similarly be able to modify activities of TRMT6/TRMT61A and if this contributed to TP53-dependent phenotypes. As tRNA modifications directly impact tRNA structure, stability, and functionality, alterations in tRNA modifications may impact the pool of tRNA within a cell further influencing protein translation and cell state. With TP53's emerging roles in translational regulation, we postulated that this might be a crucial factor determining vulnerability to TPRKB depletion.

Although Macari et al. claim that TRMT6 and TRMT61A are essential genes in mammalian cells, the authors only tested a single non-human cell line- rat C6 glioma cells[198]. Our analysis of two human cell lines found that upon depletion of *TRMT6* or *TRMT61A* there was no significant change in proliferation, indicating these genes are not necessarily required

among all mammalian cells and likely display cell line dependent phenotypes, like TPRKB. Additionally, tRNA modification analysis of TPRKB depleted cells showed no significant change in m1A levels. Together, these results suggest that TPRKB likely does not alter the m1A activity of the TRMT6/TRMT61A complex and that the TPRKB-TRMT6 interaction is not crucial for TP53-dependent effects of TPRKB. The nature of the TPRKB-TRMT6 interaction is still unknown as there are no known functions for these proteins outside of their role within their respective tRNA-modifying complexes. Furthermore, it is possible that those interactions occurring in TP53-altered and TPRKB-sensitive cells are more relevant to the phenotypes we witness, and future efforts should aim at further characterizing these interactions in particular.

Even so, we do witness other alterations within TPRKB-depleted cells suggesting translational regulation. *TP53*-null cells had reduced translation while *TP53* wild-type cells had increased translation. Although we cannot claim causality, these changes correlate with overall differences in proliferation (Chapter 2) and made us question what other changes may be happening at the tRNA level. We suspected that TPRKB-depleted cells would have altered tRNA modifications, which would impact overall tRNA stability and functionality and ultimately proliferative capacity. Consequently, we hypothesized these cells would be more reliant on RNA Polymerase III-mediated tRNA production to sustain tRNA pools. To our surprise, *TP53* wild-type HEK293T cells showed heightened sensitivity to RNA Polymerase III inhibition, while *TP53*-null H358 cells showed enhanced survival. Furthermore, expression of the RNA Polymerase III member *POLR3GL* was generally downregulated upon *TPRKB* knockdown regardless of TP53 status, suggesting an overall impaired tRNA system. However, we discovered that cells with sustained *TPRKB* knockout had different tRNA modification profiles than knockdown cells and had normalized (or even enhanced) *POLR3GL* expression. Thus, *TPRKB*

knockout cells appear to have adapted molecularly, and we propose that future investigations utilize transient or short-term knockdowns to better assess tRNA-related changes. Nonetheless, TPRKB-depleted cells show various translation level alterations that require further characterization.

Taken together, this study proposes TPRKB depletion has larger effects on protein translation in humans. We characterized novel regulation of TPRKB by indirect influences of TP53 and direct interaction with PRPK. Further, we identified and validated TPRKB-TRMT6 interaction in various cell lines. Although the functional consequence of this interaction is not tied to known functions, we provided evidence that several translational and protein-level changes occur in TPRKB-depleted cells, such as reductions in overall translation, certain tRNA modifications, and *POLR3GL* expression. We believe that further analysis of this landscape is pivotal to uncovering novel roles for TPRKB in human cells and potentially parsing the mechanism of TPRKB sensitivity in TP53-deficient cancers.

Materials and Methods

Cell Culture, Reagents, and Proliferation

HEK293T, H358, SJSA-1 MCF10A, and H196 were acquired from ATCC. HCT116 TP53+/R248W was acquired from Horizon-HD. U2OS was gifted by Elizabeth Lawlor's lab. H358,H196, and HCT116 TP53+/R248W were grown in RPMI + 10% FBS. SJSA-1 and HEK293T were grown in DMEM + 10% FBS. U2OS were grown in McCoy's 5a Modified Medium + 10% FBS. MCF10A were grown in MEBM with the addition of MEGM bullet kit. Upon receipt, cells were tested for *Mycoplasma* contamination using a commercially available kit and protocol (Sigma, LookOut Mycoplama PCR Detection Kit, MP0035). Negative cell lines

were propagated and frozen until needed. Cell lines were typically used for experiments within 2-3 months post-thawing.

Cell growth was monitored through either cell counting with Beckman Coulter's Z-series Cell Counter or through Essen Biosciences' Incucyte Live Cell Analysis. For Coulter counting, HEK293T cells were plated at $0.75x10^4$ cells/well and H358 were plated at $1.5x10^4$ cells/well in 24-well plates. HEK293T cells were trypsinized and counted on days 2, 3, and 4 after plating cells, and H358 cells were counted on days 2, 4 and 6 after plating and due to growth rate. For Incucyte experiments, HEK293T were plated at $0.75x10^3$ cells/well and H358 were plated at $1.5x10^3$ cells/well in 96-well plates. Readings were taken every 4 hours and were terminated once a cell line reached confluency. All experiments utilized triplicate samples, with the average and standard error plotted. All results were representative of at least three independent experiments.

For RNA polymerase inhibitor proliferative response studies, RNA polymerase I inhibitor II CX-5461 (Millipore Sigma, 5.09265.0001) and RNA polymerase III inhibitor (Millipore Sigma, 557403) were reconstituted in DMSO. 24 hours after plating, HEK293T cells were treated with 50nM CX-5461, 50uM RNA polymerase III inhibitor, or DMSO vehicle control. H358 were treated with 150nM CX-5461, 30uM RNA polymerase III inhibitor, or DMSO vehicle control. Growth was monitored via Incucyte as described above.

DNA constructs, lentivirus production, and cell transfection

Mammalian expression plasmids were generated or obtained from Addgene. shRNA constructs were created using System Biosciences or purchased from Open Biosystems (**Table 3.1**). The pLenti6 DNA vector for *LacZ* (V368–20) was obtained from Life Technologies. *TP53*-

V5 (22945- from Bernard Futscher's lab), *RALB*-HA (50989-from Anna Sablina's lab), *Rap2A*-HA (19311- from David Sabatini's lab), *RagB*-HA (19313- from David Sabatini's lab), and *RagD*-HA (19316- from David Sabatini's lab) were obtained from Addgene. *MDM2* was created by the University of Michigan Vector Core. Lentiviral DNA vectors for *PRPK*-FLAG, *TPRKB*-HA, and *TPRKB*-Flag were created using cDNA generated from MCF10A cells, adding a tag through PCR, and cloned into a pLenti6 background with the pLenti6/V5 Directional TOPO Cloning Kit per the manufacturer's instructions (ThermoFisher). Briefly, PCR was used to add our tag of interest (primer information can be found in **Table 3.2**) and create blunt end products. This was followed by TOPO cloning, gel purification, and transformation of STBL3 competent cells. 10-15 colonies were selected, and DNA was isolated with the use of PureLink Quick Plasmid Miniprep Kit per the manufacturer's instructions (Invitrogen). DNA was then submitted for Sanger sequencing DNA Sequencing Core (University of Michigan Medical School) to verify the end products. All lentiviruses were synthesized either from the UMICH Vector Core (University of Michigan) or System Biosciences.

For transient siRNA transfections, cells were plated in 6-well plates at 60-70% confluency. The day after plating, cells were transfected with 9ul of 20uM siRNA at a 1:1 ratio with Lipofectamine RNAiMAX, per manufacturer's protocol (Invitrogen, 13778). Cells were collected for qPCR analysis and plated for proliferation studies 48-72 hours post-transfection, depending on confluency.

To generate lentivirus, we started by using the aforementioned vectors to transform STBL3 competent cells. Colonies were selected, DNA was isolated with the use of PureLink Quick Plasmid Miniprep Kit per the manufacturer's instructions (Invitrogen), and DNA was submitted for Sanger sequencing DNA Sequencing Core (University of Michigan Medical

School) to verify the end products. DNA was then used for lentiviral production by either the UMICH Vector Core (University of Michigan) or System Biosciences. Active lentiviruses were infected to 50-60% confluent cells in either 6-well plate or 100-mm dish using polybrene (Millipore). 24 hours after infection, selection media was added. For exogenous expression plasmids, 5ug/ml blasticidin containing medium was used (Invivogen). For knockdown clones, 1ug/ml puromycin containing medium was used. For clones that had over-expression of protein and knockdown of gene; media containing both 2.5ug blasticidin and 0.5ug puromycin were used. Subsequent to selection, cells were tested for over-expression and/or knockdown either by qPCR and/or Western analysis.

Table 3.1: siRNA and shRNA sequences

Gene	shRNA sequences	Source	ID	Vector
TPRKB-sh1	GCGGGAGACUUGAGAAGAA	**Custom made-System Biosciences**		pLL-EF1a-GFP-T2A-Puro
TPRKB-sh2	TAAATAACAGAAGGGTTAC	Dharmacon	V2LHS_97346	pGIPZ
TPRKB-sh3	TTCAGTAGATAGAGTTCTT	Dharmacon	V3LHS_328180	pGIPZ
TPRKB-sh4	UUUCCCGAAUGCAGGGUAA	**Custom made-System Biosciences**		pLL-EF1a-GFP-T2A-Puro
Gene	**siRNA sequences**	**Source**	**ID**	
TP53	GAAAUUUGCGUGUGGAGUA	Dharmacon	LU-003329-00-0002	
TPRKB	pooled	Dharmacon	L-031944-02-0010	
TRMT6	pooled	Dharmacon	L-017324-02-0005	
TRMT61A	pooled	Dharmacon	L-015870-01-0005	

Table 3.2: Primer and gRNA sequences

Gene	Strand	Sequence	Application
HMBS	Forward	ATACAAGAGACCATGCAGGC	qPCR
HMBS	Reverse	AGTGATGCCTACCAACTGTG	qPCR
TRMT6	Forward	CTGCTGCTGTCTTTGCTGGATT	qPCR
TRMT6	Reverse	AGCATTCCAACAGAGGCTCTTTGTA	qPCR
TRMT61A	Forward	CACCGCACGCAGATCCTCTACT	qPCR
TRMT61A	Reverse	CCACTGCCGGTGCCAGACT	qPCR
POLR3GL	Forward	CACTGAAGCAAGAGCTACGAG	qPCR
POLR3GL	Reverse	GATATTTGTCTGAATAACGCTCCAC	qPCR
TPRKB-HA	Forward	CACCATGCAGTTAACACATCAGCTG	Cloning
TPRKB-HA	Reverse	TCAAGCGTAATCTGGAACATCGTATGGG TATAAAACATCTTTTGTTGACATTCT	Cloning
PRPK-FLAG	Forward	CACCATGGCGGCGGCCAGAGC	Cloning
PRPK-FLAG	Reverse	CTACTTGTCGTCATCGTCTTTGTAGTCC CCAACCATGGACCTCTTTC	Cloning
PRPK	Forward	GGGAGGCGTAACCACTTACA	Cloning
PRPK	Reverse	CACCCTGCTTCACCAGCTC	Cloning
TPRPK	Forward	CCTGGGGATGACAACAGAAC	Cloning
TPRPK	Reverse	CCTTCCATGGCCTTTCTTCT	Cloning
TPRKB-N59F-HA	Forward	GTAGAGGTGAACTGCTTTGAATGCTGCC ACAAGTATCTG	Cloning
TPRKB-N59F-HA	Reverse	TCAGATACTTGTGGCAGCATTCAAAGCT GTTCACCTCTAC	Cloning
TPRKB-S170R-HA	Forward	CGTATGGGTATAAAACATCTTTTGTTCT CATTCTACAAATGATAGCATCCAATA	Cloning
TPRKB-S170R-HA	Reverse	TATTGGATGCTATCATTTGTAGAATGAGAA CAAAAGATGTTTTATACCCATACG	Cloning
TPRKB-FLAG		ACTGCATTTCACAGATAAGCAGG	CRISPR gRNA
TPRKB	Forward	AATCTTTTGGTCTTTTCATTTTGTGTGCA GTAGAATCgTGCT TATCTGTGAA ATG*GACTACAAAGACGATGACGACAA* C AGTTAACACATCAGCTcGACCTATTTCC CGAATGCAGGGTAACCCTTCT	CRISPR gRNA
TPRKB	Reverse	AGAAGGGTTACCCTGCATTCGGGAAAT AGGTCgAGCTGATGTGTTAACTGCTTGT CGTCATCGTCTTTGTAGTCCATTTCACA GATAAGCAcGATTCTACTGCACACAAAA TGAAAAGACCAAAAGATT	CRISPR gRNA

Genomic editing using CRISPR-Cas9

The CRISPR plasmid for knockout of *TPRKB* and *PRPK* was purchased from Sigma with gRNA sequences shown in **Table 3.2**. The gRNA sequence was cloned into CRISPR-Cas9 and gRNA expression vector plentiCRIPSV2 (Gift from Feng Zhang, Addgene plasmid #52961). The cells were transfected using 500ng of Cas9+sgRNA vector in lipofectamine 3000 (Invitrogen) following manufacturer's protocol, and then were seeded into single cells following puromycin selection for 48 hours. Genomic DNA was extracted from the clonal lines using QuickExtract™ DNA Extraction Solution (Epicenter QE09050). Loci targeted by gRNAs were amplified using the primers listed in **Table 3.2**, and then sequenced by the DNA Sequencing Core (University of Michigan Medical School) using the forward primers.

Western Blot Analysis

Cell lysates were collected in NuPAGE LDS Sample Buffer and Reducing Agent (Life Technologies) at a 1x final concentration, sonicated, and denatured at 95ºC for 5-15 minutes. NuPAGE 4-12% Bis-Tris gels (Life Technologies) were run in 1x NuPAGE MES SDS running buffer at 120V for 1.5-2 hours, followed by semi-dry transfer in 1x NuPAGE transfer buffer containing 20% methanol at 25V for 1 hour onto Immobilon-P PVDF membranes (Millipore). Membranes were blocked in either 5% Milk or 5% Bovine Serum Albumin (based on primary antibody manufacturer's instructions) for 1 hour before probing with primary antibodies. A list of all antibodies used in this study can be found in **Table 3.3**. Washes were completed with 1x TBS + 0.1% Tween-20. Signals were detected using Immobilon Western Chemiluminescent HRP Substrate (Millipore). B-actin was used as a loading control unless otherwise specified.

Table 3.3: Antibody information

Name	Company	Catalogue #	Medium	Dilution (1:x)	Host
DYKDDDDK (Flag)	Cell Signaling	14793S	Milk	1000	Rabbit
DYKDDDDK (Flag)	Biolegend	902401	Milk	1000	Rabbit
V5	Abcam	206572	BSA	1000	Rabbit
HA	Cell Signaling	2367	Milk	1000	Mouse
HA	Biolegend	902301	Milk	1000	Rabbit
HA	Abcam	ab9110	(IP only)		Rabbit
TPRKB	Origene	TA800166	BSA	250	Mouse
PRPK	Origene	TA808226	Milk	1000	Mouse
p53 (DO-1): sc-126	Santa Cruz	sc-126	Milk	1000	Mouse
GAPDH	Cell Signaling	2118	Milk	5000	Rabbit
OSGEP	Abcam	ab119067	BSA	1000	Mouse
TRMT6	Bethyl	A303-007A	Milk	2000	Rabbit
β-actin (13E5) HRP-conjugate	Cell Signaling	5125	Milk	5000	
Mouse secondary-HRP conjugate	Cell Signaling	7076	Milk/BSA	5000	
Rabbit secondary-HRP conjugate	Cell Signaling	7074	Milk/BSA	5000	

Transient DNA Transfections for Protein Stability

For protein stability studies, HEK293T cells were plated in a 6-well plate for 24 hours. FuGENE HD transfection reagent was then used to perform transfections per manufacturer's protocol (Promega). In addition to plasmids of interest, pCDH-CMV-MCS-EF1a-copGFP (SBI Biosciences) construct was supplemented to normalize for total DNA transfection amounts between samples. Cell lysates were collected 48-72 hours later in NENT buffer: 100mM NaCl, 20mM Tris-HCl (ph = 8.0), 0.5 mM EDTA, and 0.5% (v/v) NP40 plus 1x Halt Protease and Phosphatase Inhibitor Cocktail (Thermo Scientific, 1861284). For analysis of protein degradation mechanism, cells were plated as described, but after 24 hours of transfection cells

were treated with either DMSO or 500 nM bortezomib. After an additional 16-18 hours, cells were collected in NENT buffer for Western analysis.

Co-immunoprecipitation and Mass Spectrometry

For endogenous Co-IP experiments, cells were collected in NENT buffer, briefly sonicated, and spun down. ANTI-FLAG M2 Magnetic Beads (Sigma-Aldrich) were used to perform co-IP per the manufacturer's instructions. Lysates were incubated with the beads overnight at 4^{o}C, and eluted directly into 20 uL of 2x NuPAGE sample buffer (without reducing reagent). Samples were then used for Western blot analysis.

For exogenous Co-IP experiments, cells were transfected as described above. After 48-72 hours, cells were collected in NENT buffer, briefly sonicated, and spun down. Antibodies (**Table 3.3**) were used in conjunction with the Immunoprecipitation Kit-Dynabeads Protein G (Invitrogen) per the manufacturer's instructions. After elution and denaturation, samples were used for Western blot analysis

For Co-IP experiments used in the mass spectrometry analysis, cells were transfected as described above, scaled for 150mm plates. After 48-72 hours, cells were collected in Triton-X buffer: 50mM Tris-HCl, 150mM NaCl, 1mM EDTA, and 1% (v/v) Triton-X plus 1x Halt Protease and Phosphatase Inhibitor Cocktail (Thermo Scientific, 1861284). Cells were briefly sonicated at 3x10 seconds, and lysates were cleared by centrifugation at >12,000xg for 15-20 minutes. Protein was quantified through Pierce 660nm Assay (Thermo Scientific,1861426). 2-5ug of protein were used with ANTI-FLAG M2 Magnetic Beads (Sigma-Aldrich) to perform co-IP. Briefly, 25ul of beads (50ul of packed gel volume) were washed 3x with lysis buffer and 2x with TBS. Lysates were incubated with the beads overnight at 4^{o}C, and beads were washed 2x

with lysis buffer and 2x with TBS. Beads were submitted to the University of Michigan Proteomics Resource Facility for mass spectrometry analysis, performed as follows. The beads were resuspended in 50 µl of 0.1M ammonium bicarbonate buffer (pH~8). Cysteines were reduced by adding 50 µl of 10 mM DTT and incubating at 45° C for 30 min. Samples were cooled to room temperature and alkylation of cysteines was achieved by incubating with 65 mM 2-Chloroacetamide, under darkness, for 30 min at room temperature. An overnight digestion with 1 ug sequencing grade, modified trypsin was carried out at 37° C with constant shaking in a Thermomixer. Digestion was stopped by acidification and peptides were desalted using SepPak C18 cartridges using manufacturer's protocol (Waters). Samples were completely dried using vacufuge. Resulting peptides were dissolved in 8 µl of 0.1% formic acid/2% acetonitrile solution and 2 µls of the peptide solution were resolved on a nano-capillary reverse phase column (Acclaim PepMap C18, 2 micron, 50 cm, ThermoScientific) using a 0.1% formic acid/2% acetonitrile (Buffer A) and 0.1% formic acid/95% acetonitrile (Buffer B) gradient at 300 nl/min over a period of 180 min (2-22% buffer B in 110 min, 22-40% in 25 min, 40-90% in 5 min followed by holding at 90% buffer B for 5 min and requilibration with Buffer A for 35 min). Eluent was directly introduced into Orbitrap Fusion tribrid mass spectrometer (Thermo Scientific, San Jose CA) using an EasySpray source. MS1 scans were acquired at 120K resolution (AGC target=$1x10^6$; max IT=50 ms). Data-dependent collision induced dissociation MS/MS spectra were acquired using Top speed method (3 seconds) following each MS1 scan (NCE ~32%; AGC target $1x10^5$; max IT 45 ms).

Proteins were identified by searching the MS/MS data against *Homo sapeiens* (Swissprot, v2016-11-30) using Proteome Discoverer (v2.1, Thermo Scientific). Search parameters included MS1 mass tolerance of 10 ppm and fragment tolerance of 0.2 Da; two missed cleavages were

allowed; carbamidimethylation of cysteine was considered fixed modification and oxidation of methionine, deamidation of aspergine and glutamine were considered as potential modifications. False discovery rate (FDR) was determined using Percolator and proteins/peptides with a FDR of ≤1% were retained for further analysis. To increase coverage and reduce additional background, we submitted results to the Contaminant Repository for Affinity Purification (the CRAPome) to score protein-protein interactions (www.crapome.org). Hits with a fold change compared to control of 2.0 or higher were reported in our analysis.

Recombinant protein pull-down

Recombinant TPRKB-His protein was acquired from Abcam (ab128435) and interactions were assayed with the Pierce Pull-down PolyHis Protein:Protein Interaction Kit, per manufacturer's instructions (Thermo Scientific, 21277). Briefly, resin was equilibrated with wash solution before binding 10ug of TPRKB-His or control 6x His tag peptide (Abcam, ab14943) for 1 hour at 4C. After washing, HEK293T cell lysate was added to the resin and incubated for 3 hours at 4C. After washing, proteins were eluted in 60ul of elution buffer for 10 minutes at room temperature. Protein interactions were visualized by Western blot protocol described above.

tRNA modification profiling

For TPRKB knockout and parental cells, cells were plated in triplicate in 6-well plates and propogated separately for one week prior to collection. For TPRKB knockdown cells, cells were plated in 6-well plates, infected with virus and polybrene as described above, and split into triplicates in 6 well plates. Cells underwent selection for 7-10 days prior to collection. Total

RNA was extracted with Qiagen miRNeasy Kit (Qiagen, 1038703), and NanoDrop 2000 spectrophotometer (Thermo Fisher) was used to quantify and ensure quality of isolated RNA. Samples were submitted to Arraystar Inc. for tRNA modification analysis.

To briefly describe Arraystar protocol, nanodrop was used to confirm quality control. Total RNA was run by Urea-PAGE electrophoresis. 60-90 nucleotide band of tRNA was excised and purified by ethanol precipitation and quantified with Qubit RNA HS Assay Kit (ThermoFisher, Q32855). Subsequently, tRNA was hydrolyzed to single nucleosides and dephosphorylated by enzyme mix. Pretreated nucleosides solution was deproteinized using Satorius 10,000-Da MWCO spin filter. Analysis of nucleoside mixtures was performed on Agilent 6460 QQQ mass spectrometer with an Agilent 1260 HPLC system. Multi reaction monitoring (MRM) mode was performed. LC-MS data was acquired using Agilent Qualitative Analysis software. MRM peaks of each modified nucleoside were extracted and normalized to quantity of tRNA purified.

OPP Protein Translation Assay

Protein translation was assayed through the use of an O-Propargyl-puromycin (OPP)-based Protein synthesis assay kit, per manufacturer's instructions for flow cytometry analysis (Cayman Chemical, 601100). Briefly, $1x10^6$ cells/sample were plated one day prior to experimentation. Cells were incubated with 0.5ml of OPP working solution for 1 hour at 37C. Samples were collected, washed, and fixed before staining with 5 FAM-Azide solution at room temperature for 30 minutes in the dark. After washing cells were submitted to the University of Michigan Flow Cytometry Core for FITC detection at 483nm/525nm. The presented data represents the results from four independent experiments.

Microarray

Gene expression changes upon TPRKB loss were assessed by expression profiling of cell lines using Human Gene ST 2.1 arrays. RNA was collected from 1) H196 cells treated with non-targeting (NT) siRNA or siRNA against TPRKB (siRNA1) for 24 and 48 hours ; 2) SJSA cells treated with non-targeting (NT) siRNA or siRNA against TPRKB (siRNA1 or siRNA2) for 48 hours; 3) SJSA cells infected with non-targeting shRNA or shRNA against TPRKB (shRNA1 or shRNA2); and 4) HCT-TP53-R248W cells treated with non-targeting (NT) siRNA or siRNA against TPRKB (siRNA1 or siRNA2) for 24 and 48 hours. Expression profiling on Affymetrix Human Gene ST 2.1 array were performed according to the manufacturer's instructions at the University of Michigan Comprehensive Cancer Center DNA Sequencing Core. Log_2 expression values were determined by robust multi-array using the oligo package of Bioconductor in R. The log2 ratio for each gene in the TPRKB siRNA or shRNA sample vs. the appropriate non-targeting shRNA or shRNA control sample was then determined. To identify genes differentially expressed consistently upon *TPRKB* knockdown, we filtered to include genes with an average > 1.5 fold (log2 ratio > 0.583) or <-1.5 fold expression across the 10 TPRKB knockdown experiments and at least 8 of 10 knockdown experiments showing concordant increased or decreased expression (e.g 8 of 10 experiments with log2 ratio greater than zero and an average log2 ratio greater than 0.583). Centroid linkage unsupervised hierarchical clustering of genes and composite arrays were performed using Cluster 3.0, and heatmaps were visualized using Java Treeview.

RNA extraction and qPCR analyses

Cells were pelleted, lysed, and RNA was extracted as per manufacturer's instructions (Purelink RNA Mini Kit, Life Technologies). Total RNA was quantified by NanoDrop 2000 spectrophotometer (Thermo Fisher). cDNA was prepared using High Capacity cDNA Reverse Transcription Kit, per manufacturer's instruction (Applied Biosciences). SYBR green-based qPCR was performed in triplicate using various primers, as listed in **Table 3.2**. HMBS was used as a normalization control for all experiments unless otherwise specified.

Notes

Portions of this work have been adapted from the following manuscript:

> Moloy T. Goswami*, Kelly R VanDenBerg*, Sumin Han, Lei Lucy Wang, Bhavneet Singh, Travis Weiss, Myles Barlow, Steven Kamberov, Kari Wilder-Romans, Daniel R. Rhodes, Felix Y. Feng, Scott A. Tomlins. *Identification of TP53RK Binding Protein (TPRKB) dependency in TP53-deficient cancers.* Mol Cancer Res, 2019. In Press.
>
> * Co-first authors

<u>Contributors to data in this chapter: Kelly R VanDenBerg (Kennaley), Moloy T. Goswami Sumin Han, Lei Lucy Wang, Scott A. Tomlins</u>

SH performed endogenous FLAG-tagging of TPRKB in HEK293T cells through CRISPR. SH and KRV performed CRISPR TPRKB knockout. KRV, SH, and LLW performed Western blot analysis. KRV performed Co-IP, recombinant protein pulldown, proliferation, and qPCR experiments. We would like to thank Alexey Nesvizhskii, Ph.D., and Venkatesha Basrur, Ph.D.,

from the University of Michigan Proteomics Resource Facility for conducting the Mass Spectrometry experiments and analysis. Samples for LC-MS based tRNA modification analysis were created and collected by KRV and LLW, and the analysis was completed by ArrayStar Inc. Protein translation studies were completed by KRV and LLW. Microarray samples were generated by MTG and run by the University of Michigan DNA Sequencing Core.

Chapter 4 Discussion, Conclusions, and Future Directions

Herein, we identified and validated TPRKB dependency across a range of TP53-deficient cells, but not in *TP53* wild-type and benign cells (**Figure 4.1A**). Using various isogenic cell lines, we confirmed that TP53 loss, TP53 dominant-negative mutant co-expression, or MDM2 overexpression is sufficient to induce sensitivity to TPRKB depletion. Furthermore, this vulnerability appears to pertain largely to TPRKB alone, instead of the entire EKC/KEOPS complex, representing the possibility for novel TPRKB functionality in humans. We further demonstrate that TP53 and PRPK, another member of the EKC/KEOPS complex, can dynamically regulate TPRKB protein levels; whereby TP53 indirectly reduces TPRKB partially through the proteasome and PRPK stabilizes TPRKB through direct binding capabilities (**Figure 4.1B**).

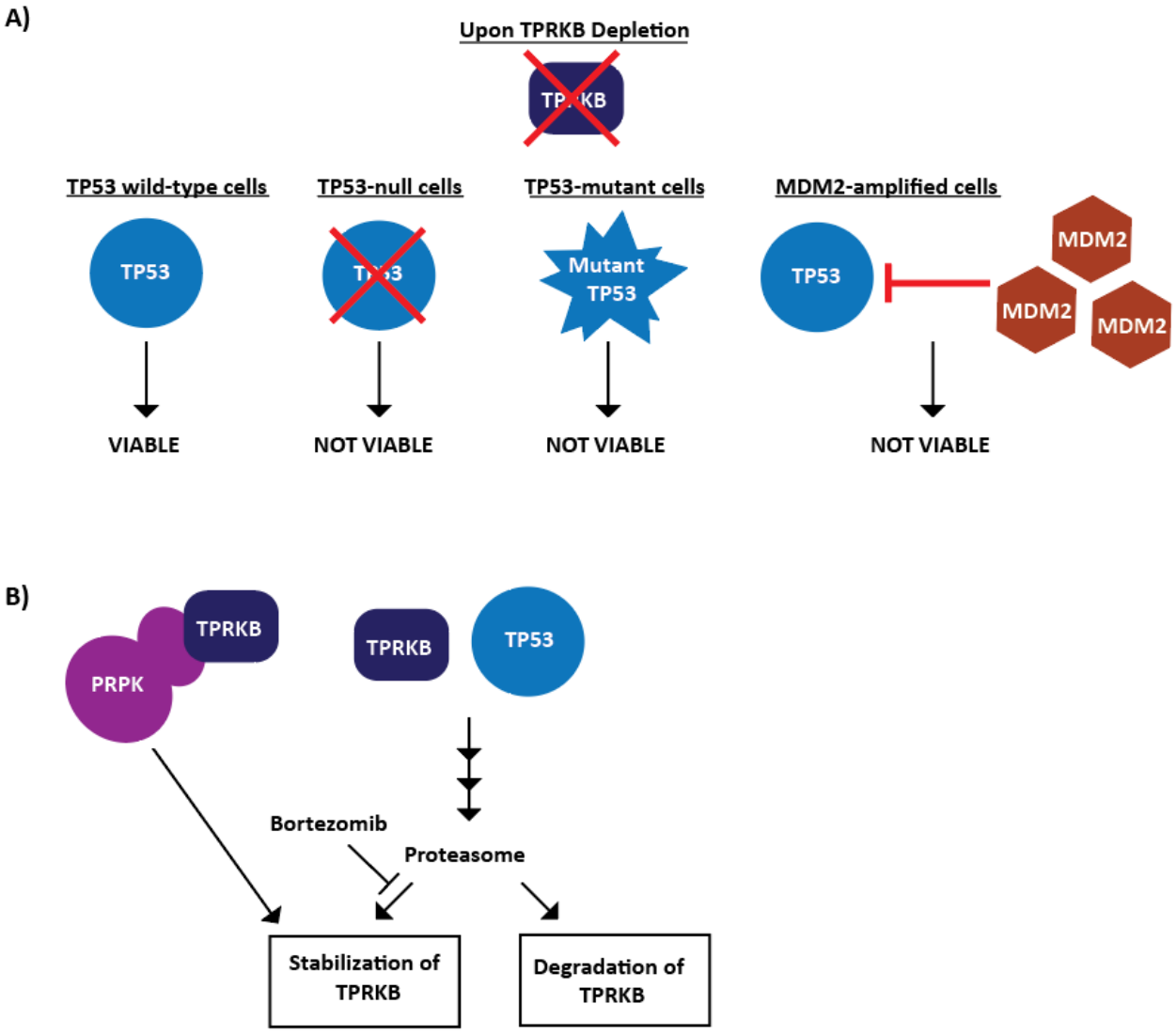

Figure 4.1: Model of TPRKB sensitivity in cancer

A) TP53-deficient cells are uniquely susceptible to TPRKB loss. **B)** TPRKB is dynamically regulated at the protein level. TP53 is able to indirectly mediate TPRKB degradation through the proteasome, while PRPK directly stabilizes TPRKB protein levels.

To identify novel TPRKB-interactors and potential mediators of susceptibility, we performed co-immunoprecipitation experiments followed by mass spectrometry analysis in TPRKB sensitive and insensitive cell lines. Interestingly, only five proteins outside the EKC/KEOPS complex were identified as interactors in all four cell lines, highlighting cell- and context- dependent interactomes for TPRKB. The common TRMT6/TRMT61A interactors are members of an m1A tRNA-modifying complex; however, TPRKB depletion had no effect on m1A levels and knockdown of *TRMT6/TRMT61A* did not affect cellular proliferation as *TPRKB* knockdown does. Thus, it does not appear that TRMT6 is the functional moderator of TPRKB sensitivity, and further studies aimed at characterizing the consequence of the TPRKB-TRMT6 interaction are necessary. Further, it is possible that only those TPRKB interactions that occur in TP53-altered or MDM2-overexpressing cells are functionally relevant. Towards that, our identification of specific interactions in TPRKB-sensitive H358 and U2OS+*MDM2* cells gives probable protein interaction candidates whose function can be queried in the context of TP53-deficient cancers.

The ultimate goal of this work is to provide evidence that will eventually assist in the development of therapeutic strategies to target TPRKB for the treatment of patients with TP53-deficient cancers. These approaches include therapeutics that could act through direct TPRKB protein binding inhibition, inhibition of the TPRKB-PRPK interaction (thus destabilizing TPRKB), inhibition of TPRKB's interaction with a potential mediator of response, or manipulating upstream or downstream pathways. Consequently, characterization of the mechanisms surrounding TPRKB vulnerability are of utmost importance, and pivotal next steps in this investigation should be aimed at further characterizing TPRKB in human cells to identify the mechanism by which TP53-deficient cells are susceptible to TPRKB loss.

Of importance, effectively modulating phenotypes was a persistent challenge within this study. Cells with *TPRKB* knockdown typically maintained phenotypes for approximately 1 month before adaptation or cell death occurred, and although our *TPRKB* knockout cells maintained phenotypes, there appeared to be molecular differences indicative of adaptive responses (as seen by tRNA analysis and *POLR3GL* expression). As such, we propose that an effective inducible knockdown system, particularly in cells that are highly sensitive to TPRKB loss, would be a valuable tool for studying mechanisms of vulnerability moving forward.

With that in mind, several approaches could be utilized to parse out mechanism of action. First, would be direct pathway manipulation, as we attempted with the treatment of DNA-damaging agents in Chapter 2. If the TP53-TPRKB relationship follows the pattern of a typical synthetic lethal relationship, whereby TPRKB has some functional redundancy with TP53, then targeting the common process with certain stressors should result in enhanced sensitivity, as indicated by previous studies[23]. For example, if TPRKB acted through the DNA damage response or cell cycle pathways, we would expect that TPRKB *knockdown* plus the addition of DNA-damaging agents, like etoposide or cisplatin, would enhance sensitivity. However, our studies found that TPRKB-depleted cells did not show substantial differential responses to either cisplatin or etoposide. These findings indicate that TPRKB sensitivity is not directly related to DNA damage response, despite previous studies associating the entire EKC/KEOPS complex in this process[108, 199]. Thus, it could be interesting to expand these studies to manipulation of other networks related to TP53 activity, such as metabolic processes or the anti-apoptotic BCL2/BCL2L1 pathway, to determine if they facilitate response.

To narrow down additional potential pathways, there are two approaches of interest. First, validation of hits from our IP:MS analysis in Chapter 3 could be used to identify particular

pathways. Manipulation through genomic (knockdowns/overexpression) or pharmacologic (activators/inhibitors) intervention could then determine if interactions are functionally important for phenotypes of interest, as was done with our TRMT6 and DNA-damaging agent investigations. For example, several potential interactors identified in our IP:MS analysis are associated with the mitochondria, and given TP53's role in metabolic processes, we propose this as a promising avenue for future investigation. Alternatively, crucial pathways could be determined through a CRISPR knockout screen among cells with inducible *TPRKB* knockdown to determine which other genes are potentially necessary to maintain viability in TP53 wild-type cells or reverse sensitivity in TP53-deficient cells. In this way, we could nominate mediators of TPRKB sensitivity for further analysis.

Additionally, we found that numerous translational alterations are present in TPRKB-depleted cells, including TP53-dependent reductions in overall protein translation, altered response to RNA Polymerase inhibitors, downregulation of the RNA Polymerase III gene *POLR3GL*, and reductions in specific tRNA modifications. Taken together, our data and others'[101, 108] indicate that TPRKB may have larger effects on protein translation than simply t6A modifications of tRNA, raising numerous fundamental questions. Are changes in tRNA modifications consistent across cell lines or does TP53 status contribute to the abundance of certain modifications? Do changes in tRNA modifications lead to alterations in overall tRNA pools in these cells? Can these changes be correlated to a cell's proliferative status, specific gene expression requirements, and overall proteome?

This investigation into TPRKB's larger role in protein translation could be particularly interesting in the context of TP53. Emerging evidence implicates TP53's involvement with various aspects of translation beyond its well-characterized ability to mediate the transcription of

specific genes in response to stress. TP53 can be activated by ribosomal protein-mediated inhibition of MDM2[165, 166]; TP53 can influence transcription of tRNAs and rRNAs through inhibiting RNA polymerase I and III[172, 173]; and TP53 can mediate the translation of mRNAs by binding directly to mRNA transcripts[175]. If TPRKB is in fact altering protein translation in diverse manners, as our data suggests, translational dysfunction may be the source of TPRKB-dependency in TP53-deficient cells. Thus, while additional experiments analyzing abundance of specific tRNA modifications and composition of overall tRNA pools could be helpful for determining TPRKB's role in this context, ribosomal profiling of translating proteins and complete proteomic analysis in a range of characterized cell lines may more directly determine how TPRKB depletion functionally affects TP53 wild-type versus deficient cells. In turn, this may further support identification of the mechanism by which certain cells display vulnerability to TPRKB loss.

A fundamental component of our study is that TPRKB sensitivity can be linked to numerous *TP53* alterations, from deletions to missense mutants and MDM2-mediated negative regulation. The expansion of our phenotype to *MDM2*-amplified cells is critical, as it creates the possibility for additional determinants of sensitivity not yet explored and raises the question of whether the mechanism of action between types of TP53 deficiency are the same. For example, in the Broad Institute's Project Achilles screen, HeyA8 is a *TP53* wild-type cell line that responds strongly to TPRKB loss. Interestingly, through querying the Cancer Cell Line Encyclopedia (https://portals.broadinstitute.org/ccle), we find that HeyA8 contains missense and frameshift mutations in TP53 Binding-Protein 1 (*TP53BP1*). This protein plays multiple roles in the DNA damage response and has been shown to interact with TP53 during transcriptional regulation[200-202]. Consequently, exploring the necessity of TPRKB in cells with this and

other alterations in pivotal TP53-pathway members may reveal additional facets of TPRKB sensitivity.

Lastly, as the majority of our study utilized cell lines to validate relationships and explore phenotypes, investigating TPRKB in the context of a more complex organismal system is desirable. During our work, we attempted to create a universal *TPRKB* knockout mouse model to study these TP53-dependent phenotypes *in vivo*. However, *TPRKB* knockout in *TP53* (also known as *Trp53* in mice) wild-type C57BL/6 resulted in early embryonic lethality, consistent with previous findings in zebrafish[108], suggesting that TPRKB plays an important role in development. Thus, to study the role of TPRKB *in vivo* it will be necessary to create a conditional knockout mouse in which *TPRKB* could be deleted after the mouse has reached maturity and/or in specific organs of interest. Of particular importance, *TP53*-null and -mutant mice are known to form tumors between 3-6 months of age[203]. Thus crossing these conditional *TPRKB* knockout mice with mice of varying *TP53* statuses would provide valuable models to explore not only how mice respond to *TPRKB* depletion in adulthood but also how *TPRKB* knockout affects tumor formation, providing significant validation of TPRKB dependency in more complex TP53-deficient contexts.

Taken together, we propose that TPRKB depletion offers a promising strategy for targeting a range of *TP53*-altered and -deficient cancers, and future investigations should be aimed at elucidating the mechanism and limitations for this sensitivity in order to optimize therapeutic targeting strategies.

Appendix

Tables of mass spectrometry-identified interactors for TPRKB in cell lines:

Table A.1: Potential TPRKB interactors identified through IP:MS in HEK293T cells

	HEK293T	
GENE	FC_A	FC_B
TPRKB	714.74	116.82
OSGEP	78.5	10.34
C14orf142	34.64	4.93
TP53RK	24.96	4.66
LAGE3	24.82	2.55
TRMT6	6.17	1.07
ABCF3	5.16	1.67
AIFM1	4.79	0.63
NELFCD	4.78	1.61
TRMT61A	4.02	1.49
ARFGAP1	3.72	1.27
TOMM70A	3.41	1.56
INTS2	3.35	1.47
HLA-A	3.27	1.04
VPS52	3.27	1.36
SLC39A1	3.27	1.37
ZZEF1	3.27	1.36
HRNR	3.27	1
RPL36	3.27	1.04
NUBP2	3.27	1.37
APOO	3.27	1.36
SNAP47	3.27	1.36
MAGED1	3.23	1.46
ATP13A1	3.22	0.72
TBC1D4	3.15	0.93
TMEM165	3.07	1.06

HMOX1	3.03	1.41
SACM1L	2.97	1.71
GOSR1	2.94	1.46
CERS2	2.92	1.46
RPL29	2.89	0.27
ZBTB1	2.89	1.29
EPB41L3	2.89	0.64
POLE	2.89	1.31
DICER1	2.89	1.31
TBL3	2.89	1
PML	2.89	1.31
MARCKSL1	2.89	0.16
VMP1	2.89	1.31
SNX2	2.89	0.7
THOC1	2.89	1.31
JUP	2.87	1.04
SLC25A20	2.85	1.45
WAPAL	2.83	1.45
TELO2	2.82	1.82
FANCD2	2.78	0.89
AASS	2.78	1.36
PPP2R5D	2.78	1.36
NUDT16L1	2.78	1.35
NNT	2.77	1.6
DSG2	2.76	0.85
ALG6	2.75	1.36
OSBPL11	2.75	1.36
TP53BP1	2.75	1.36
BTAF1	2.72	1.58
CPT1A	2.71	1.48
GALNT1	2.71	1.41
MED23	2.71	1.4
FAM162A	2.7	1.53
CAND2	2.7	0.79
RAF1	2.69	1.41
STX7	2.67	0.3
SHPK	2.67	1.35
ORC3	2.67	0.54
HSPBP1	2.64	0.73

VPS18	2.64	1.45
MAP7D3	2.63	1.49
PFKM	2.62	0.6
TUBGCP2	2.61	1.48
RAB2B	2.6	1.39
TCEB1	2.57	0.42
AKAP8L	2.57	1.44
HLA-C	2.54	1.52
PHF3	2.52	1.48
ESYT2	2.52	1.59
ERLIN2	2.51	0.31
CHMP6	2.51	1.25
YTHDF2	2.51	0.95
ARFGEF2	2.51	1.25
BICD2	2.51	1.25
SSSCA1	2.51	0.63
EMC10	2.51	1.24
FYCO1	2.51	0.84
DNM1L	2.51	0.27
TMX4	2.51	1.24
B2M	2.51	1.25
TMUB1	2.51	1.25
OSTC	2.51	1.25
CHCHD4	2.51	1.24
PPP4R1	2.51	1.25
AMPD2	2.51	1.25
HNRNPUL2	2.51	1.25
SPNS1	2.51	1.24
RPA2	2.51	0.34
DNAJC1	2.51	1.25
SLC25A19	2.51	1.24
BABAM1	2.51	0.34
TRAPPC12	2.51	1.24
USP38	2.51	1.22
ANAPC5	2.51	1.22
MYO1B	2.49	0.14
LRCH2	2.49	1.3
TMEM97	2.49	1.3
CDK5RAP3	2.49	1.3

GALNT7	2.49	1.3
NISCH	2.49	1.3
NUP214	2.48	1.35
TK1	2.48	1.35
MYO1D	2.48	0.13
HLA-A	2.48	1.05
TOR1AIP1	2.47	1.35
HLA-B	2.45	1.05
TFB2M	2.45	1.35
POLD1	2.44	1.34
PIGS	2.44	1.35
CPD	2.41	1.51
MARCKS	2.4	0.2
MPG	2.4	1.34
TMOD3	2.4	0.38
BASP1	2.39	0.09
USP10	2.39	1.29
CLCC1	2.39	1.29
SPCS1	2.39	1.29
TXLNA	2.38	0.62
OXA1L	2.38	1.34
CLINT1	2.37	0.94
HSD17B11	2.35	1.5
ARMC6	2.32	1.64
CCDC47	2.3	1.76
KDM1A	2.26	1.39
HYOU1	2.26	0.22
CUL2	2.25	0.43
RAB2A	2.25	0.66
HLA-B	2.25	1.17
PEX3	2.24	1.29
PIGT	2.24	1.38
RHOT2	2.24	1.42
CHTF18	2.23	1.37
NDC1	2.23	1.37
PFKL	2.22	0.21
CALR	2.22	0.12
SCO2	2.22	0.59
HEATR6	2.22	1.29

PRAF2	2.21	1.29
TNRC6B	2.2	1.24
VPS51	2.2	1.24
BRCC3	2.2	1.23
MAP2K3	2.2	1.23
PIK3R4	2.2	1.24
COX7A2L	2.2	1.24
FAM115A	2.2	1.11
TRAPPC8	2.2	1.24
WNK1	2.2	0.7
CIR1	2.19	0.91
CNOT11	2.18	1.24
SNX1	2.18	0.81
MAP2K2	2.18	0.96
HK1	2.17	0.6
SLC35B2	2.17	1.29
KRT5	2.15	0.44
MGST3	2.15	1.45
CLPTM1	2.15	1.47
NCDN	2.14	1.41
VPS33A	2.14	1.4
NME3	2.13	0.9
FNDC3A	2.13	1.18
SLC25A15	2.13	1.18
ATP6V1F	2.13	0.35
TAF12	2.13	1.18
BUB1	2.13	0.67
VTI1B	2.13	1.18
WDR43	2.13	1.18
GOLT1B	2.13	1.18
MLH1	2.13	1.18
TFRC	2.13	0.47
TAF6	2.13	1.18
UTP6	2.13	1.18
VPS4A	2.13	1.41
LRBA	2.13	0.95
CBWD2	2.13	1.18
POLR1D	2.13	1.18
DCAF8	2.13	1.18

SPC24	2.13	0.92
SKA1	2.13	1.17
RPTOR	2.13	1.18
TRABD	2.13	1.18
IDH2	2.13	0.45
POLA1	2.13	0.92
PTPN13	2.13	1.18
CBWD1	2.13	1.18
SLC35F6	2.13	1.18
LSM2	2.13	0.39
ZGPAT	2.13	1.18
RPL18	2.13	0.21
ALG3	2.13	1.18
GBA	2.13	1.18
DARS2	2.13	0.58
CNN2	2.13	1.18
PRKAG1	2.13	1.18
	2.13	1.18
RB1	2.13	1.18
NDUFB8	2.13	1.18
TRAPPC2L	2.13	1.18
FAM83D	2.13	1.18
EXOC3	2.13	0.7
CDC16	2.13	1.18
ECSIT	2.13	1.18
KIAA1147	2.13	1.18
HAUS5	2.13	1.18
PARL	2.13	1.18
LRPAP1	2.13	0.59
TCF25	2.13	1.17
LNPEP	2.13	0.88
KIF23	2.13	0.7
TTC7B	2.13	0.67
TRAM1	2.13	1.18
OTUB1	2.13	0.35
ANAPC2	2.13	1.18
UNC45A	2.12	1.66
RAD21	2.12	1.44
LRRC40	2.12	0.95

UFL1	2.12	1.47
MAGT1	2.12	1.23
NDUFA11	2.12	1.23
RPAP1	2.11	1.34
MRPS21	2.11	1.34
TIMM50	2.11	0.4
BAG2	2.09	0.65
SORT1	2.08	1.37
TM9SF2	2.07	1.43
SCD	2.06	1.33
AP2A2	2.06	1
FADS2	2.06	1.33
XPO7	2.05	1.3
GTF3C5	2.05	1.36
TBCD	2.05	1.36
ATP6V0D1	2.02	0.8
ILK	2.02	1.28
ADPGK	2.01	1.24
ERCC6L	2.01	1.34
LPCAT1	2.01	1.39
MGST2	2.01	1.24
ATP11C	2.01	1.24
ARHGAP17	2.01	1.24
ALG1	2.01	1.24
NUP153	2	1.45
SDHA	2	1.09
ABCB7	2	1.43

Table A.2: Potential TPRKB interactors identified through IP:MS in H358 cells

H358		
GENE	**FC_A**	**FC_B**
TPRKB	492.64	38.49
OSGEP	55.07	5.12
TP53RK	51.07	4.82
LAGE3	26.03	2.91
C14orf142	13.02	1.92
TRMT6	12.01	1.84

TRMT61A	9.01	1.61
TMEM43	8.01	1.53
ROCK2	7.01	1.07
MTMR14	6.01	1.38
MGST3	6.01	1.38
CCAR1	5.01	1.31
PACSIN2	5.01	1.31
PPIG	5.01	1.31
JAK1	5.01	0.17
SNRNP40	5.01	0.43
MTCH2	5.01	1.31
NUFIP2	5.01	0.25
MCM4	4.67	0.21
SART3	4.51	1.57
TAP1	4.51	1.57
PSMC4	4	0.23
BZW2	4	1.23
B3GAT3	4	1.23
CSTF3	4	1.23
NDUFA12	4	1.23
STIM1	4	1.23
ERGIC1	4	1.5
ADNP	4	1.23
DHRS7	4	1.23
TLE3	4	1.23
COX5B	4	1.03
PIGT	4	1.23
ADD1	4	0.31
PPM1B	4	0.01
NUP88	4	1.23
VPS4A	4	1.23
EMC2	4	1.23
TM9SF3	4	1.5
NUP98	4	1.23
ABHD12	4	1.75
CCDC50	4	1.23
TAF2	4	1.23
MLLT4	4	0.26
RABL6	4	1.23

PDS5A	4	1.23
SEL1L	4	1.23
PLGRKT	4	1.23
RNF213	3.67	1.68
SRPR	3.67	0.69
SLC25A24	3.67	1.68
SLC39A4	3.5	1.42
CD2AP	3.5	1.42
PSMA1	3.34	0.73
ATL3	3.34	1.61
IDH2	3	1.35
SUCLG2	3	1.15
PTK7	3	1.15
SUN1	3	1.15
PC	3	1.15
POLR2B	3	1.15
PUM1	3	1.15
EIF2B2	3	1.15
YTHDF2	3	0.45
PPM1A	3	0.02
OSBPL10	3	1.15
NRBP1	3	1.15
WDR61	3	0.35
APOL2	3	1.15
RPL36A	3	0.08
RBMX2	3	1.15
CDC42BPG	3	1.15
PRSS8	3	1.15
KIAA1407	3	1.15
PSMC1	3	0.58
AP3B1	3	1.1
IKBKAP	3	0.63
VPS51	3	1.15
ACIN1	3	0.15
ICAM1	3	1.15
FLOT2	3	0.7
FAM49B	3	1.15
GPX1	3	1.15
SMPD4	3	1.15

STK39	3	1.15
IPO7	3	0.92
SH3BP1	3	1.15
EFTUD2	3	0.18
ALDH1B1	3	1.15
VPS16	3	1.15
SYT16	3	1.15
ARL2	3	1.15
SKP1	3	0.09
GATAD2B	3	0.78
COPS2	3	1.53
COPRS	3	0.13
MDK	3	1.15
NCSTN	3	1.15
XPO5	3	1.53
SBF1	3	1.15
NCEH1	3	1.15
IDH3G	3	1.15
PSMD6	3	0.36
TBCD	3	1.15
IFFO2	3	1.15
LSR	3	1.35
NNT	3	1.35
CRKL	3	1.15
CDIPT	3	0.93
SNIP1	3	1.35
NDUFS3	3	0.91
TTC1	3	1.15
CAPN5	3	1.15
EMC7	3	1.15
ADAM15	3	1.15
FAM120A	3	1.15
NUP85	3	1.15
BZW1	3	1.71
SDC4	3	1.15
SIN3A	3	1.15
DDX42	3	0.56
CYB5A	3	1.15
OSBPL3	3	1.15

RAB27B	3	1.15
CDS2	3	1.15
COIL	3	1.15
CNIH4	3	1.15
PDS5B	3	1.15
PIGK	3	1.15
EIF2S2	3	0.36
UQCRFS1	3	1.15
PAF1	3	1.15
RIN1	3	1.15
SF3B4	3	0.23
MSH2	3	1.35
PDHA1	3	0.16
UTRN	3	1.15
ACADM	3	0.93
ATP1B3	3	1.15
RHOT1	3	1.15
RBM26	3	1.15
CDK9	3	1.15
PSMB5	3	0.31
SERF2	3	0.23
NOMO2	2.75	1.1
MAP4	2.75	1.16
ESYT2	2.75	1.64
NOMO1	2.75	1.1
VAPB	2.67	0.89
ARHGEF1	2.67	1.46
EMC1	2.67	1.19
TNFAIP2	2.67	2.29
STOML2	2.67	0.88
HNRNPUL2	2.67	0.44
SF3A1	2.67	0.34
CYB5R3	2.67	0.86
43352	2.6	0.22
SRP68	2.6	1.22
ALDH18A1	2.5	0.33
CKAP5	2.5	0.5
DYSF	2.5	1.27
SUN2	2.5	0.14

PDXDC1	2.5	1.27
RRBP1	2.5	0.63
MAL2	2.5	1.27
PLEKHA5	2.5	1.27
GART	2.5	0.81
SDHB	2.5	1.27
CRIP1	2.5	0.76
DERL1	2.5	1.27
P4HA1	2.5	1.57
MRPS12	2.5	1.27
UFL1	2.5	1.27
MAVS	2.5	1.27
RAB12	2.5	1.27
MAOA	2.5	1.27
NSDHL	2.5	1.27
SERPINB5	2.5	1.27
ACTL6A	2.5	1.27
U2SURP	2.5	0.07
TMEM165	2.5	1.27
NCLN	2.5	1.57
CYFIP2	2.5	1.27
DDX46	2.43	0.09
PSMC2	2.4	0.16
FIP1L1	2.4	0.46
EIF4A3	2.4	0.37
MOGS	2.34	1.43
CBR1	2.34	0.01
STAT3	2.34	1.39
SEC61A1	2.34	1.39
USP9X	2.34	0.53
EIF3M	2.34	0.34
TAF4	2.34	0.48
VDAC2	2.34	1.25
NUP155	2.34	1.39
XPOT	2.34	1.77
CWC25	2.34	0.58
DDX41	2.34	0.17
HMGN2	2.34	0.37
NCKAP1	2.34	1.39

RAB7A	2.34	1.07
AP3D1	2.34	1.2
NELFB	2.34	1.11
APMAP	2.29	1.31
PSMD1	2.25	0.48
	2.25	1.5
AFG3L2	2.25	1.5
NIPSNAP1	2.25	1.49
OAS1	2.25	1.5
ACADVL	2.25	1.49
PSMB8	2.25	1.5
RHOA	2.25	1.2
HERC5	2.2	1.38
ATP2B1	2.2	1.6
RIOK1	2.17	0.04
NSF	2.15	1.26
ITGAV	2.15	1.8
DNAJA1	2.15	0.41
UGGT1	2.13	1.89
PSMD12	2	0.17
GPN1	2	1.08
SH3GLB1	2	1.08
CYR61	2	0.52
MOB1B	2	1.08
CDK5	2	1.08
BRE	2	1.08
SPTA1	2	1.08
OTUD4	2	0.11
RBM12	2	1.08
UNC93B1	2	1.08
NDUFS6	2	1.08
SEMA3A	2	1.08
SMNDC1	2	0.52
SCAF8	2	1.08
TRIM33	2	0.89
CNOT1	2	1.53
NME3	2	1.08
CDC42EP4	2	1.08
TNPO2	2	1.31

TUFM	2	0.66
APOO	2	1.08
RAB39A	2	1.2
MANF	2	0.26
ADRM1	2	1.08
DOCK9	2	1.08
CLN6	2	1.08
HMOX2	2	1.2
GOSR1	2	1.08
WDR82	2	1.08
MRE11A	2	0.15
ZFP36L1	2	1.08
PGLS	2	1.08
PSAT1	2	0.85
FHOD1	2	1.08
RFC2	2	0.71
FAM114A1	2	1.08
TFG	2	0.5
RALY	2	0.25
MAN1B1	2	1.08
TBL2	2	0.66
C19orf47	2	1.08
VASN	2	1.08
PRKAA1	2	1.08
TBC1D15	2	1.08
LSM10	2	1.08
EPB41L1	2	1.08
RSRC2	2	0.06
PTGES	2	1.08
AIM1L	2	1.08
TOMM7	2	1.08
ATP13A1	2	0.42
UFSP2	2	1.08
MCCC2	2	1.08
HCFC1	2	0.89
ITM2B	2	1.08
SUPT5H	2	0.87
PTPN11	2	1.08
PTPLB	2	1.08

MRPL17	2	1.08
ARHGEF18	2	1.08
PHKB	2	1.08
FAM32A	2	0.58
RFT1	2	1.08
CBWD6	2	1.08
CUL5	2	1.08
NDUFC2	2	1.08
TIMP1	2	1.08
RAB34	2	1.08
C11orf57	2	1.08
GOLGA7	2	1.08
PHLDA1	2	1.08
IPO4	2	1.53
SPP1	2	1.08
ASNA1	2	1.2
PFKFB3	2	0.56
CIR1	2	0.68
PPP2R5C	2	1.08
RAB43	2	1.2
GTF3C3	2	1.08
CISD1	2	1.08
NDUFB11	2	1.08
LANCL2	2	1.08
DCTN1	2	0.28
NHP2L1	2	1.08
RIF1	2	1.08
ATPIF1	2	0.35
IGHG1	2	1.08
CPT2	2	1.08
SOWAHB	2	1.08
TP53BP1	2	1.2
OVGP1	2	1.08
COG6	2	1.08
GLMN	2	1.08
NPTN	2	1.08
RAB21	2	1.08
PRPF40A	2	1.43
SNRPC	2	0.11

GORASP2	2	1.08
A2M	2	1.08
C20orf27	2	1.08
KLC1	2	1.43
FRG1	2	0.15
MME	2	1.31
ZC3H15	2	0.41
CASP8	2	1.08
SLC1A5	2	0.21
RTN1	2	1.08
RAB11FIP1	2	1.08
PVRL4	2	1.08
UBE2K	2	1.08
SF3B5	2	0.12
AAAS	2	1.08
ANP32E	2	0.16
PFKFB2	2	1.08
TRIM16	2	1.08
PDE7A	2	1.08
SMC4	2	0.74
BUD13	2	1.08
BCS1L	2	1.08
IFITM3	2	1.31
PPP1R10	2	0.89
NUCKS1	2	0.42
YIPF3	2	1.08
EPS15	2	1.08
GRB2	2	1.08
ACSM3	2	1.08
RP2	2	0.87
TLE1	2	1.08
AKAP10	2	1.08
FAM98B	2	0.64
AKAP8L	2	1.08
RAD21	2	1.2
MCCC1	2	1.08
ERGIC2	2	1.08
COMT	2	1.08
MAGED2	2	0.81

ILK	2	1.08
IMPAD1	2	1.08
RRAS2	2	0.64
IQGAP2	2	0.97
PSMD9	2	1.08
HMGN1	2	0.82
RBM17	2	0.05
SNX2	2	1.08
DLG1	2	0.8
CHCHD6	2	1.08
MTPN	2	0.85
RAP2C	2	1.2
RAE1	2	1.2
FNDC3A	2	1.08
SCCPDH	2	0.85
AP1G1	2	1.2
SYMPK	2	1.08
PI4KA	2	0.58
DAK	2	1.08
C19orf33	2	0.51
CDK1	2	0.32
ADH5	2	1.08
RPL37A	2	0.22
PRKAR2B	2	1.08
EDC3	2	1.08
CBWD2	2	1.08
CTHRC1	2	1.08
EMC3	2	1.2
ZCCHC17	2	1.08
RRAGD	2	1.08
STARD13	2	1.08
FAU	2	0.16
GLG1	2	1.08
PIGS	2	0.98
TRMT10C	2	1.2
EPCAM	2	1.31
EMC8	2	1.08
NDUFB9	2	1.08
SLC4A7	2	1.08

TM9SF4	2	1.08
DPF2	2	1.08
BRCC3	2	1.08
SRSF11	2	0.34
SMARCC2	2	0.29
ATP6AP1	2	1.08
SEC24D	2	1.08
TIMMDC1	2	1.08
NUP210L	2	1.08
HK1	2	1.08
TRIP6	2	1.08
LSM12	2	1.08
MGST1	2	1.08
UQCRC2	2	1.31
B4GALT1	2	1.08
RMDN3	2	1.2
KIAA0368	2	1.53
PGD	2	0.63
UBE2V1	2	0.63
ALG6	2	1.08
TFIP11	2	0.59
MTX3	2	1.08
POLR2L	2	1.08
NOP56	2	0.17
APOE	2	1.08
PPP1R12C	2	1.08
PRKD2	2	1.2
EIF3G	2	0.19
ADPGK	2	1.08
AIMP2	2	0.27
CDA	2	1.08
MTA1	2	0.44
MAGED1	2	1.08
SCAMP3	2	1.05
CHCHD3	2	0.49
PITPNB	2	1.08
PSMD14	2	0.4
NDUFA4	2	1.08
PHF6	2	0.79

COX7B	2	1.08
UQCC2	2	1.08
C16orf58	2	1.08
VMA21	2	1.08
COMMD2	2	1.08
SLC12A9	2	1.08
ULBP2	2	1.08
DCAKD	2	1.08
PPA2	2	1.08
CPSF2	2	1.08
ORMDL2	2	1.08
SMARCC1	2	0.36
MOB4	2	0.7
GHITM	2	1.08
ECE1	2	1.2
XIAP	2	1.08
SLC30A7	2	1.08
CD9	2	1.08
UBA2	2	0.43
ALDH1A3	2	1.2
SERPING1	2	1.08
MRPL1	2	1.08
CASP6	2	1.08
PHKA2	2	1.08
PPP6C	2	1.08
MST1R	2	1.08
DLAT	2	0.17
PPIL3	2	1.08
MIF	2	1.08
TLE4	2	1.08
CERS6	2	1.08
PLIN3	2	2.08
NAA15	2	1.08
TLDC1	2	0.87
CDK5RAP3	2	1.08
UBE4A	2	1.08
PLD3	2	1.08
TMEM245	2	1.08
DPY19L1	2	1.08

SNX5	2	1.08
COG4	2	1.08
BTF3L4	2	1.08
PSMB7	2	0.74
CD2BP2	2	1.08
SLC9A3R2	2	1.08
MTX1	2	1.08
PSMD8	2	0.7
VAC14	2	1.08
AIP	2	1.08
CLDN4	2	1.08
MTMR1	2	1.08
EHD4	2	1.31
SDHD	2	1.08
SCAF4	2	1.08
SF3A3	2	0.21
SFSWAP	2	0.64
FAM47E-STBD1	2	1.08
TMEM9	2	1.08
SPCS1	2	1.2
BAX	2	1.08
BCL2L1	2	1.08
AHCYL1	2	1.08
COPS5	2	1.2
UBAC2	2	1.08
CCNL1	2	1.08
PVRL2	2	1.08
RABL3	2	1.08
PTPN1	2	1.2
C12orf23	2	1.08
SRP54	2	0.85
CDCP1	2	1.2
NOV	2	1.08
UCHL5	2	1.08
KLHL38	2	1.08
ABHD16A	2	1.08
SLC38A2	2	1.08
TRAPPC8	2	1.08
ADAM10	2	1.08

RBMS2	2	1.08
SMG8	2	1.08
PROCR	2	1.2
SYNPO	2	1.08
RAB6A	2	1.63
NDUFV1	2	1.2
G3BP2	2	0.4
CD274	2	1.08
FAM210A	2	1.08
AKAP13	2	1.2
LSM1	2	1.08
FEN1	2	0.21
FAM96B	2	1.08
ALG2	2	1.08
GSR	2	1.08
PDIA5	2	1.08
PALLD	2	1.08
DNAJA4	2	1.08
GNPDA1	2	1.08
FAM134C	2	1.08
SPINT1	2	1.08
GPAA1	2	1.08
ABI1	2	1.08
PTPN12	2	1.08
TRAPPC5	2	1.08
WDFY1	2	1.08
FKBP4	2	0.31
DPYSL2	2	1.2
SPCS3	2	1.31
ZNF207	2	1.08
COX6A1	2	1.08
TNPO3	2	1.08
YEATS2	2	1.08
RAB4A	2	1.2
DOCK6	2	0.55
NSRP1	2	0.15
DENND4A	2	1.08
TMEM65	2	1.08
EIF4E	2	0.61

NUP188	2	1.08
CD151	2	1.08
FAM213A	2	1.08
WDR83	2	1.2
C8orf4	2	1.08
CWF19L2	2	1.08
HSD17B4	2	0.43
LYPD3	2	1.08
NDUFAF3	2	1.08
SLK	2	1.08
HMGB1	2	0.07
PSMB9	2	1.08
NFKB1	2	0.56
DMXL1	2	1.08
GSN	2	0.17
HPRT1	2	1.2
GOLT1B	2	1.08
SRSF2	2	0.17
CEPT1	2	1.08
NAPA	2	1.08
PIGU	2	1.08
ACAT1	2	0.44
MFF	2	1.08
C17orf97	2	1.08
SGPL1	2	1.2
BIRC2	2	1.08
NFXL1	2	1.08
MAP3K7	2	1.2
SYAP1	2	1.08
BCAR1	2	1.08
FMNL2	2	0.63
TOR1A	2	1.08
CDK2	2	0.79
SMARCA4	2	0.86
FN3KRP	2	1.2
ARMC10	2	1.08
TNS1	2	1.08
SMCHD1	2	0.36
DAP3	2	0.47

SMARCB1	2	1.08
C8orf59	2	0.79
H3F3A;H3F3B	2	0.1
PHACTR4	2	1.08
ARHGDIA	2	0.61
MTFR1	2	1.08
GIGYF2	2	0.95
CCNT1	2	1.08
THNSL2	2	1.08
LMNB2	2	0.2
TMEM87A	2	1.08
AGRN	2	1.08
CSTF1	2	1.08
RNF20	2	1.08
DOCK5	2	1.08
HP	2	1.08
FRYL	2	0.55
NAA10	2	1.08
GBF1	2	1.08
NDUFB3	2	1.08
GSPT1	2	0.95
RNF40	2	1.08
SDF2	2	1.08
ITGA2	2	1.08
SQRDL	2	1.43
NOLC1	2	0.43
LAMTOR1	2	1.08
TMEM14C	2	1.08

Table A.3: Potential TPRKB interactors identified through IP:MS in U2OS+*LacZ* cells

U2OS+*LacZ*

GENE	FC_A	FC_B
TPRKB	146.27	280
OSGEP	48.68	44.75
TP53RK	24.84	22.87
AIP	15.9	14.67
PPM1F	14.91	13.76
SLC25A22	12.92	3.82

VPS4A	9.94	9.2
MAP2K3	9.94	3.36
SRM	9.94	9.2
C2orf47	9.94	9.2
ACAT1	9.94	9.2
RAF1	8.95	3.01
GALK1	8.95	4.88
HSD17B11	8.95	8.29
DIS3	8.95	8.29
C14orf142	8.95	8.29
AIFM1	8.45	9.37
LAGE3	7.95	7.38
HSD17B12	7.95	5.5
ARAF	7.95	2.37
NPTN	6.96	6.47
VPS4B	6.96	6.47
PBDC1	6.96	6.47
SPANXB1;SPANXB2	6.96	6.47
ABCE1	6.96	4.82
NUBP2	6.96	6.47
PARK7	6.46	9.14
SEC11A	5.97	5.56
TRMT6	5.97	5.56
TMEM126A	5.97	5.56
PSMD10	5.97	5.56
TARDBP	5.97	4.14
RHOT1	5.97	4.14
CACYBP	5.97	2.7
STOML2	5.97	5.56
RHOF	5.97	5.56
SUCLG1	5.97	5.56
FKBP10	5.97	5.56
SDF4	5.97	5.56
MOGS	5.96	8.44
UBXN1	5.47	7.75
SLC16A1	5.47	3.74
UMPS	5.47	7.75
DDX39B	4.97	1.27
HSDL2	4.97	4.65

CTBP1	4.97	3.42
TMX3	4.97	4.65
AFAP1	4.97	4.65
PLAA	4.97	4.65
DERL1	4.97	3.42
NSUN2	4.97	3.46
CCZ1B	4.97	4.65
DYNLRB1	4.97	4.65
AAR2	4.97	2.74
NEDD4L	4.97	7.05
FAM210A	4.97	3.46
ITPRIP	4.97	4.65
TFB2M	4.97	1.7
ACADM	4.97	1.49
SPARC	4.97	4.65
CHP1	4.97	4.65
ALDH1B1	4.64	7.97
RHOT2	4.64	4.85
NTPCR	4.47	6.35
NCLN	4.47	6.35
GMPS	4.22	8.13
SUCLG2	3.98	3.73
RPP30	3.98	4.48
FASTKD5	3.98	3.73
NME3	3.98	3.73
NUDT1	3.98	3.73
OXSR1	3.98	3.73
CTBP2	3.98	3.73
ARL4C	3.98	3.73
SLC25A25	3.98	3.73
TIMM23	3.98	3.73
EIF2S3	3.98	3.73
TRMT61A	3.98	3.73
ACSL4	3.98	3.73
ACTR2	3.98	2.3
COMT	3.98	5.65
MEF2D	3.98	3.73
TTC27	3.98	2.78
RAB13	3.98	3.73

RAE1	3.98	3.73
BSG	3.98	6.84
METTL13	3.98	3.73
CPSF3	3.98	1.81
PPM1G	3.98	6.84
ARPC2	3.98	1.24
NARS	3.98	3.73
AUP1	3.98	3.73
C6orf120	3.98	3.73
SLC25A11	3.98	1.36
AASDHPPT	3.98	3.73
CHCHD4	3.98	3.73
SPECC1	3.98	3.73
GORASP1	3.98	3.73
ALDH5A1	3.98	3.73
MGAT2	3.98	3.73
PBK	3.98	2.75
RIN1	3.98	3.73
PELO	3.98	4.44
MAT1A	3.98	2.2
HMOX1	3.98	3.73
SARS	3.98	3.73
SLFN5	3.98	3.73
ALG1	3.98	2.2
ILVBL	3.98	3.73
DNAJA2	3.58	2.45
HAT1	3.48	4.95
PDLIM2	3.48	4.95
EEF1A1	3.45	4.16
FAF2	3.31	3.98
SLC1A5	3.31	4.71
AGK	3.31	3.06
CCDC47	3.31	5.71
DDX39A	3.23	1.67
PWWP2A	2.99	2.82
ZC2HC1A	2.99	2.82
UBA6	2.99	2.82
NEK7	2.99	2.08
NDUFS6	2.99	2.82

NUBP1	2.99	2.82
NEU1	2.99	2.08
ALDH7A1	2.99	2.82
ITPA	2.99	2.82
AGPAT9	2.99	2.82
MSRA	2.99	2.82
SLC25A15	2.99	1.18
SFXN4	2.99	2.82
CTDP1	2.99	2.82
NRBP1	2.99	2.82
MTCH1	2.99	1.36
CEP55	2.99	2.82
IGF2BP2	2.99	0.09
HDGF	2.99	2.82
GPD1L	2.99	2.82
CHORDC1	2.99	2.82
RDH11	2.99	2.82
GTF3C5	2.99	1.16
TOMM22	2.99	2.82
MAPRE1	2.99	2.82
NHP2L1	2.99	2.1
MAP1S	2.99	2.82
RNF126	2.99	2.82
GORASP2	2.99	2.82
HEATR6	2.99	2.82
IPO11	2.99	2.82
USMG5	2.99	2.82
GRN	2.99	0.15
CEPT1	2.99	2.82
RRM2B	2.99	2.08
MLH1	2.99	2.82
ILF2	2.99	0.29
L2HGDH	2.99	2.82
FUBP3	2.99	2.82
RBM15	2.99	0.29
PIGT	2.99	2.82
GEMIN4	2.99	0.25
TOR1AIP1	2.99	2.82
DCP1B	2.99	2.82

UBE2V1	2.99	2.82
USP5	2.99	2.82
SLC30A1	2.99	2.82
SMS	2.99	2.82
NDUFS2	2.99	1.66
RFTN1	2.99	2.82
IDH3A	2.99	2.82
PPP3CA	2.99	2.82
PRPF4B	2.99	2.1
RAB32	2.99	2.1
CRIP2	2.99	2.82
SAE1	2.99	2.82
GGT7	2.99	2.82
NDUFS7	2.99	2.08
PISD	2.99	2.82
TIMM21	2.99	2.82
FAS	2.99	2.82
CLPTM1L	2.99	2.82
NIPSNAP1	2.99	2.82
STEAP3	2.99	2.82
SLC25A32	2.99	2.82
IARS2	2.99	2.82
NEMF	2.99	2.82
UBE3A	2.99	2.82
CAPN5	2.99	2.82
NDUFA5	2.99	2.82
NUP54	2.99	2.82
THTPA	2.99	2.82
VPS35	2.99	2.82
CLEC2B	2.99	2.82
SLC25A19	2.99	2.82
PRAME	2.99	2.82
RIC8A	2.99	2.82
GNL3L	2.99	1.37
SH3BGRL2	2.99	2.82
TAP1	2.99	2.08
ELAVL1	2.99	0.37
PGRMC1	2.99	2.82
SPTLC1	2.99	1.18

C19orf70	2.99	2.82
TELO2	2.99	2.08
GBF1	2.99	2.82
TRADD	2.99	2.82
ZC3H11A	2.99	0.63
UACA	2.99	2.82
PARP14	2.99	2.82
CNBP	2.98	0.15
IRAK1	2.98	4.26
FAM105B	2.98	4.26
FAM98B	2.98	3.34
RPS29	2.98	4.26
ATL3	2.98	4.26
DNAJB11	2.98	3.34
SFXN1	2.98	1.8
VAT1	2.98	4.26
ILF3	2.98	0.14
POLD3	2.98	4.26
PTPN1	2.98	4.26
TOMM40	2.98	4.26
RPL15	2.98	0.5
MTHFD2	2.73	3.84
YES1	2.65	4.58
HK2	2.65	4.58
KIAA0368	2.65	4.58
MAGEA1	2.65	3.17
SSR4	2.65	2.78
DDX19B	2.65	4.58
EEF1A2	2.54	3.61
SSFA2	2.54	6.11
PCBP1	2.52	2.85
TUBA4A	2.5	1.63
LARS	2.49	3.56
RFC4	2.49	1.97
NDUFA10	2.49	3.56
SLC25A12	2.49	0.99
TOR1AIP2	2.49	3.56
SQSTM1	2.49	3.56
SLC1A4	2.49	3.56

YARS	2.49	3.56
FAM91A1	2.49	3.56
CDKAL1	2.49	3.56
LARP4	2.49	0.5
NDUFA4	2.49	3.56
EIF2B3	2.49	3.56
TPRN	2.49	3.56
EHD1	2.49	3.56
GCLM	2.49	3.56
MAD2L1	2.49	3.56
DDX6	2.49	2.32
AIF1L	2.49	3.56
LZTS2	2.49	3.56
PEAK1	2.49	3.56
IPO4	2.48	5.44
PCNA	2.48	1.5
TUBB6	2.46	2.49
HNRNPM	2.41	0.37
AFG3L2	2.39	2.05
EPRS	2.34	6.2
PCBP2	2.32	1.98
WAPAL	2.32	4.01
GSPT2	2.32	4.01
GLB1	2.32	4.01
STAT1	2.32	4.01
KHSRP	2.32	4.01
TRIP13	2.32	1
PTPN12	2.32	4.01
KPNA2	2.32	1.75
NOMO1	2.32	4.01
MMS19	2.24	4.32
PCBP3	2.24	1.64
ARPC1B	2.24	2.48
GSN	2.24	4.32
TIMM50	2.19	3.92
GIGYF2	2.19	4.55
NPM1	2.13	2.06
TUBB	2.09	2.19
CAPZA2	2.08	3.85

Table A.4: Potential TPRKB interactors identified through IP:MS in U2OS+*MDM2* cells

U2OS+*MDM2*		
GENE	FC_A	FC_B
OSGEP	56.77	51.81
TPRKB	55.56	135.61
TP53RK	27.85	25.46
C14orf142	15.46	14.17
SLC25A22	14.43	4.22
AIP	13.39	12.29
MYO1D	12.36	0.89
LAGE3	11.33	10.41
MYO6	10.31	6.1
SFXN1	10.29	1.82
AGK	9.26	3.55
RHOT2	9.26	4.17
DIS3	9.26	8.53
ACAT1	9.26	8.53
NTPCR	8.23	7.59
NOP58	8.23	2.19
RFC5	7.2	2.75
IRAK1	7.2	6.65
TMX3	7.2	6.65
SAE1	7.2	6.65
NUBP2	7.2	6.65
PRAME	7.2	6.65
RIC8A	7.2	6.65
MTCH2	7.2	1.75
NAMPT	6.16	5.7
NPTN	6.16	5.7
VPS4B	6.16	5.7
COMT	6.16	5.7
RHOF	6.16	5.7
DAPK3	6.16	5.7
UMPS	5.66	7.98
BSG	5.66	7.98
VPS4A	5.66	7.98
PARK7	5.15	7.26
DDX19B	5.15	7.26
RPL7	5.13	0.3

FBXO21	5.13	1.97
TRMT6	5.13	4.76
BRAT1	5.13	3.55
RAF1	5.13	1.73
RAB32	5.13	3.55
ARPC4	5.13	1.53
HRNR	5.13	0.64
SRM	5.13	4.76
MTHFD2	4.63	4.22
UBXN1	4.11	5.82
CPSF3	4.11	1.85
FASTKD5	4.1	3.82
HNRNPD	4.1	0.24
AGPAT9	4.1	3.82
GMPPB	4.1	3.82
SEC11A	4.1	3.82
FASTKD2	4.1	1.23
FAM91A1	4.1	3.82
KRT31	4.1	0.11
VWA5A	4.1	3.82
RRAS2	4.1	3.82
PBDC1	4.1	3.82
TMEM126A	4.1	3.82
METTL13	4.1	3.82
HNRNPDL	4.1	0.39
RHOT1	4.1	2.85
AURKB	4.1	0.55
IDH3A	4.1	3.82
APMAP	4.1	3.82
CCZ1B	4.1	3.82
ATIC	4.1	3.82
SLC25A32	4.1	3.82
MMGT1	4.1	3.82
RPL18	4.1	0.3
DYNLRB1	4.1	3.82
AP2A2	4.1	1.86
MICALL2	4.1	3.82
TPRN	4.1	3.82
THTPA	4.1	3.82

ALDH5A1	4.1	3.82
TFB2M	4.1	1.39
ARHGEF17	4.1	3.82
KRT34	4.1	0.22
PGM3	4.1	3.82
CNTN2	4.1	3.82
MAML2	4.1	3.82
ZC3H11A	4.1	0.85
AIFM1	3.86	6.24
PPP1R18	3.78	8.24
TNKS1BP1	3.78	6.48
STOML2	3.78	6.48
SIPA1L3	3.71	7.67
RFC4	3.6	2.81
EHD4	3.6	4
FAM105B	3.6	5.1
TWF2	3.6	5.1
NDUFA4	3.6	5.1
POLD3	3.6	5.1
PELO	3.6	4
AP2A1	3.6	1.76
RHOA	3.6	5.1
IPO4	3.5	7.25
EIF2S1	3.43	5.89
MOGS	3.09	5.3
SLC1A5	3.09	4.37
MATR3	3.09	0.14
GSN	3.09	5.3
RPL4	3.09	0.26
RAB34	3.08	4.38
ARHGAP11A	3.08	4.38
PSMD9	3.08	4.38
ARPC2	3.08	0.96
SLC25A11	3.08	1.86
TMOD2	3.08	4.38
LARP4	3.08	0.61
ARAF	3.08	1.67
MARS	3.08	2.1
IL18	3.08	4.38

ALDH7A1	3.07	2.88
ITPA	3.07	2.88
NUDT1	3.07	2.88
S100A6	3.07	2.88
OXSR1	3.07	2.88
SUGT1	3.07	2.88
SLC25A15	3.07	1.2
NEK7	3.07	2.12
C11orf83	3.07	2.88
RARS2	3.07	2.12
MRFAP1	3.07	2.88
RHBDD2	3.07	2.88
COTL1	3.07	2.88
DKC1	3.07	2.15
PCBP4	3.07	1.69
TBRG4	3.07	2.88
ARPC1A	3.07	2.88
UCK2	3.07	2.88
PLAUR	3.07	2.88
USMG5	3.07	2.88
SLC27A4	3.07	2.12
GPX8	3.07	2.88
MLH1	3.07	2.88
L2HGDH	3.07	2.88
HLA-B	3.07	2.88
TTC27	3.07	2.15
BCCIP	3.07	2.88
ABCF2	3.07	2.12
XAGE1A;XAGE1B;XAGE1C;XAGE1D;XAGE1E	3.07	2.88
ATAD1	3.07	2.88
ATP6AP2	3.07	2.88
SMS	3.07	2.88
HBD	3.07	2.88
TGOLN2	3.07	2.88
SARS	3.07	2.88
AP2S1	3.07	2.88
EP300	3.07	2.88
CHCHD4	3.07	2.88
ARHGEF40	3.07	1.4

TOM1	3.07	2.88
ATP2C1	3.07	2.88
FAS	3.07	2.88
SAAL1	3.07	2.88
SPANXD	3.07	2.88
CAPN5	3.07	2.88
CLN6	3.07	2.88
ASNS	3.07	2.88
METAP1	3.07	2.88
CLEC2B	3.07	2.88
PPAT	3.07	2.88
LRRC14	3.07	2.88
MGAT2	3.07	2.88
TUBG1	3.07	1.2
ITPRIP	3.07	2.88
MAOA	3.07	2.88
SENP1	3.07	2.88
SH3BGRL2	3.07	2.88
TAP2	3.07	2.12
SPARC	3.07	2.88
ACADM	3.07	0.92
ELAVL1	3.07	0.37
CLU	3.07	2.88
IARS2	3.07	2.88
TELO2	3.07	2.12
TRADD	3.07	2.88
KIAA1671	2.91	7.24
TUBB6	2.84	2.65
MYO18A	2.84	7.17
DPM1	2.83	2.6
KRT5	2.75	0.15
FAF2	2.74	3.29
MISP	2.74	4.72
NSUN2	2.74	3.89
RHOC	2.74	4.72
HSD17B11	2.74	4.72
FARSA	2.68	4.81
DDX39A	2.68	1.65
SIPA1	2.63	6.54

CORO1B	2.58	5.63
RPL3	2.57	0.27
TRIM27	2.57	3.65
FHOD1	2.57	3.65
PFKL	2.57	3.65
ITPR1	2.57	3.65
GJC1	2.57	3.65
VAT1	2.57	3.65
AP2M1	2.57	1.25
TRMT112	2.57	3.65
UNC45A	2.57	1.4
RAB13	2.57	3.65
PIGT	2.57	3.65
IGF2BP2	2.57	0.15
KHSRP	2.57	4.95
HK2	2.57	3.65
GALK1	2.57	2.38
SHC1	2.57	3.65
AAR2	2.57	2.38
BAG2	2.57	4.95
FANCI	2.57	2.87
CLPTM1	2.57	3.65
C2orf47	2.57	3.65
NACA	2.57	2.87
SPANXB1;SPANXB2	2.57	3.65
SDF4	2.57	3.65
PCBP1	2.53	2.55
NUP93	2.5	1.98
PCNA	2.5	1.35
EEF1A1	2.5	3.71
ACTR2	2.47	2.1
DST	2.46	6.66
TWF1	2.45	5.15
TUFM	2.41	1.42
ITPR3	2.41	5.78
RPL6	2.4	0.23
AP1M1	2.4	4.13
KRT77	2.4	0.16
DNAJB11	2.4	2.22

SPTLC1	2.4	2.21
ACTC1	2.39	2.65
KRT6B	2.37	0.22
AHSA1	2.36	5.36
ACTBL2	2.3	2.93
TRIP13	2.27	1.46
TUBB1	2.26	1.85
RPLP0	2.23	1.06
KRT16	2.23	0.11
MFGE8	2.23	4.88
PPM1G	2.23	4.88
AFAP1L1	2.18	5.23
SSFA2	2.18	5.23
TUBB4B	2.17	2.17
KRT6A	2.16	0.21
PHGDH	2.15	4.11
TUBAL3	2.15	1.58
KRT9	2.12	0.21
ZNF185	2.11	5.78
LIMA1	2.1	5.72
TUBB	2.09	2.25
TUBB4A	2.07	2.27
CFL2	2.06	4.2
PCBP3	2.06	1.49
SFXN3	2.06	1.63
SLC25A4	2.06	1.67
RPL10	2.06	0.73
ATP5C1	2.06	1.49
NEDD4L	2.06	3.97
CAPZB	2.06	1.91
NCLN	2.06	4.28
KRT2	2.06	0.1
PEAK1	2.06	3.97
RPLP2	2.05	1.21
CTBP2	2.05	2.93
VAPB	2.05	2.93
FN3KRP	2.05	2.3
HAT1	2.05	3.55
CTBP1	2.05	2.9

TOMM22	2.05	2.93
HSD17B12	2.05	2.93
CHERP	2.05	0.14
GLB1	2.05	2.93
DNAJA3	2.05	2.3
EEF1A2	2.05	3.17
KIAA1462	2.05	2.93
TARDBP	2.05	2.93
ATL3	2.05	2.93
CRMP1	2.05	2.93
DERL1	2.05	2.3
RPL13	2.05	0.33
APOOL	2.05	1.91
DNAJC7	2.05	1.91
SUCLG1	2.05	3.55
SLIRP	2.05	2.93
ARPC1B	2.05	1.88
TAF15	2.05	1.9
EHD1	2.05	2.93
KRT4	2.05	0.27
PPM1F	2.05	3.55
RPL10A	2.05	0.79
PXN	2.05	2.93
PGK1	2.05	2.93
SUCLG2	2.03	1.94
SPC25	2.03	1.94
RING1	2.03	1.94
MT-ND3	2.03	1.94
RER1	2.03	1.94
POLR1B	2.03	1.94
TKT	2.03	0.94
MLLT11	2.03	1.94
DHRS7B	2.03	1.94
EIF2D	2.03	1.94
CHTOP	2.03	0.27
NME3	2.03	1.94
EIF2A	2.03	1.94
USP28	2.03	1.94
RMND1	2.03	1.94

SCD5	2.03	1.94
HMOX2	2.03	1.94
HDDC2	2.03	1.94
ZFP36L1	2.03	0.71
PBK	2.03	1.43
LEPROT	2.03	1.94
INPP5K	2.03	1.94
ARFGEF1	2.03	1.94
DNAJB5	2.03	1.45
SOD1	2.03	1.94
HUS1	2.03	1.94
CPSF3L	2.03	1.14
BOP1	2.03	0.43
CTDP1	2.03	1.94
NME7	2.03	1.94
SLC25A16	2.03	1.43
ZNF615	2.03	1.94
ARL4C	2.03	1.94
CDC45	2.03	1.43
CBWD6	2.03	1.94
HMGB3	2.03	1.94
GUF1	2.03	1.94
SLC25A25	2.03	1.94
C5orf15	2.03	1.94
ATP6V1G1	2.03	1.94
MYLK	2.03	1.94
SLC7A11	2.03	1.94
SCRN1	2.03	1.94
TRMT61A	2.03	1.94
GDI1	2.03	0.71
KDSR	2.03	1.94
AAMP	2.03	1.94
NDUFV3	2.03	1.94
NUDT5	2.03	1.94
DAAM1	2.03	1.94
COX20	2.03	1.94
ATRAID	2.03	1.94
TPX2	2.03	1.94
TCERG1	2.03	1.94

MCU	2.03	1.94
CLP1	2.03	0.69
PDHX	2.03	1.94
NDUFA3	2.03	1.94
PDCD2L	2.03	1.94
SOWAHC	2.03	1.45
HIGD1A	2.03	1.94
PKP2	2.03	0.95
CC2D1A	2.03	1.94
RRM2B	2.03	1.43
PET100	2.03	1.94
ABCF3	2.03	1.94
C17orf85	2.03	0.51
CORO1C	2.03	4.25
MYO5B	2.03	1.94
GNG5	2.03	1.94
TOMM34	2.03	1.94
LYPLA2	2.03	1.94
CIRH1A	2.03	1.94
THUMPD3	2.03	1.94
RAB21	2.03	1.94
ANTXR1	2.03	1.94
SLC15A1	2.03	1.94
EARS2	2.03	1.94
APOL2	2.03	1.94
SLC20A1	2.03	1.94
C19orf33	2.03	1.94
PGBD4	2.03	1.94
NEK6	2.03	1.43
SERPINB8	2.03	1.94
UPF1	2.03	0.09
ARL8A	2.03	1.94
ALDH8A1	2.03	1.94
ETFB	2.03	1.94
FASTKD3	2.03	1.94
ZC3H14	2.03	0.17
UFD1L	2.03	1.94
DPP9	2.03	1.94
SLC30A1	2.03	1.94

SLC37A4	2.03	1.94
TROVE2	2.03	1.94
TM9SF2	2.03	1.94
FAM83D	2.03	1.94
RAB11B	2.03	1.94
FRMD4A	2.03	1.94
HMGN3	2.03	1.94
ZC3H4	2.03	1.94
PANK4	2.03	1.94
ZFPL1	2.03	1.94
MRPS18B	2.03	0.47
ATXN10	2.03	1.94
SPCS2	2.03	1.94
UBL5	2.03	1.94
OXA1L	2.03	1.94
TAX1BP1	2.03	1.94
KIFAP3	2.03	1.94
KRT24	2.03	0.07
TRABD	2.03	1.94
GPR98	2.03	1.94
ATG3	2.03	1.94
ETNK1	2.03	1.94
COQ5	2.03	1.94
PHF6	2.03	1.94
RAP1GDS1	2.03	1.94
ISCU	2.03	1.94
OSTC	2.03	1.94
GGT7	2.03	1.94
FAM186B	2.03	1.94
TTI1	2.03	1.94
SCFD1	2.03	1.94
IKBIP	2.03	0.56
GXYLT1	2.03	1.94
CLPTM1L	2.03	1.94
ALDH1A3	2.03	1.94
SV2A	2.03	1.94
CDYL	2.03	1.94
COX11	2.03	1.94
TMEM109	2.03	1.94

AAAS	2.03	1.94
DCAF8L2	2.03	1.43
HNRNPLL	2.03	0.33
UBE3A	2.03	1.94
NEDD8	2.03	1.94
FAR1	2.03	1.94
ARF6	2.03	1.94
CISD1	2.03	1.94
SLC22A18	2.03	1.94
UBE2N	2.03	1.94
OPA3	2.03	1.94
OLA1	2.03	1.94
CCDC96	2.03	1.94
NIP7	2.03	1.94
EIF2AK4	2.03	1.94
ACBD3	2.03	1.94
GTSF1	2.03	1.94
PRKAG1	2.03	1.43
UACA	2.03	1.94
GPRIN1	2.03	1.14
SMARCAD1	2.03	1.94
CD58	2.03	1.94
MTFP1	2.03	1.94
KISS1	2.03	1.94
BTAF1	2.03	1.94
QKI	2.03	0.35
STAM	2.03	1.94
SAR1A	2.03	1.94
APEH	2.03	1.94
PRKCI	2.03	1.94
ESYT2	2.03	0.94
SMG8	2.03	1.94
DNM2	2.03	1.94
CMPK1	2.03	1.94
RRP1	2.03	1.94
COX7B	2.03	1.94
TAF9	2.03	1.94
KRT71	2.03	0.19
DNLZ	2.03	1.94

VMP1	2.03	1.94
ZNF207	2.03	1.94
MGEA5	2.03	1.94
ARPC5L	2.03	1.94
GCLM	2.03	1.94
TOE1	2.03	1.94
NDUFA11	2.03	1.94
HOOK1	2.03	1.94
RBM4	2.03	1.94
SMDT1	2.03	1.94
ENTPD1	2.03	1.94
HMOX1	2.03	1.94
GLRX3	2.03	1.94
TAP1	2.03	1.43
SPTLC2	2.03	1.94
PTRH2	2.03	1.94
PPME1	2.03	1.94
CYB5R3	2.03	1.94
NDUFA8	2.03	1.94
SLC5A6	2.03	1.94
AGPAT6	2.03	1.94
EFTUD1	2.03	1.94
N4BP3	2.03	1.94
PIGK	2.03	1.94
TYMS	2.03	1.43
LRRC27	2.03	1.94
MYO19	2.03	1.43
MON2	2.03	1.94
ACTR1B	2.03	1.94
SSR3	2.03	1.14
C19orf43	2.03	1.94
ERBB2IP	2.03	1.94
SLC25A33	2.03	1.94
MYOZ2	2.03	1.94
COX16	2.03	1.94
HSPD1	2.02	3.02

Bibliography

1. DeLeo, A.B., et al., *Detection of a transformation-related antigen in chemically induced sarcomas and other transformed cells of the mouse.* Proc Natl Acad Sci U S A, 1979. **76**(5): p. 2420-4.
2. Kress, M., et al., *Simian virus 40-transformed cells express new species of proteins precipitable by anti-simian virus 40 tumor serum.* J Virol, 1979. **31**(2): p. 472-83.
3. Lane, D.P. and L.V. Crawford, *T antigen is bound to a host protein in SV40-transformed cells.* Nature, 1979. **278**(5701): p. 261-3.
4. Linzer, D.I. and A.J. Levine, *Characterization of a 54K dalton cellular SV40 tumor antigen present in SV40-transformed cells and uninfected embryonal carcinoma cells.* Cell, 1979. **17**(1): p. 43-52.
5. Melero, J.A., et al., *Identification of new polypeptide species (48-55K) immunoprecipitable by antiserum to purified large T antigen and present in SV40-infected and -transformed cells.* Virology, 1979. **93**(2): p. 466-80.
6. Smith, A.E., R. Smith, and E. Paucha, *Characterization of different tumor antigens present in cells transformed by simian virus 40.* Cell, 1979. **18**(2): p. 335-46.
7. Finlay, C.A., P.W. Hinds, and A.J. Levine, *The p53 proto-oncogene can act as a suppressor of transformation.* Cell, 1989. **57**(7): p. 1083-93.
8. Kruse, J.P. and W. Gu, *Modes of p53 regulation.* Cell, 2009. **137**(4): p. 609-22.
9. Yamamoto, S. and T. Iwakuma, *Regulators of Oncogenic Mutant TP53 Gain of Function.* Cancers (Basel), 2018. **11**(1).
10. Vogelstein, B., D. Lane, and A.J. Levine, *Surfing the p53 network.* Nature, 2000. **408**(6810): p. 307-10.
11. Bieging, K.T., S.S. Mello, and L.D. Attardi, *Unravelling mechanisms of p53-mediated tumour suppression.* Nat Rev Cancer, 2014. **14**(5): p. 359-70.
12. Kastenhuber, E.R. and S.W. Lowe, *Putting p53 in Context.* Cell, 2017. **170**(6): p. 1062-1078.
13. Zhou, R., et al., *Li-Fraumeni Syndrome Disease Model: A Platform to Develop Precision Cancer Therapy Targeting Oncogenic p53.* Trends Pharmacol Sci, 2017. **38**(10): p. 908-927.
14. Kandoth, C., et al., *Mutational landscape and significance across 12 major cancer types.* Nature, 2013. **502**(7471): p. 333-339.
15. Soussi, T. and K.G. Wiman, *TP53: an oncogene in disguise.* Cell Death Differ, 2015. **22**(8): p. 1239-49.
16. Terzian, T., et al., *The inherent instability of mutant p53 is alleviated by Mdm2 or p16INK4a loss.* Genes Dev, 2008. **22**(10): p. 1337-44.
17. Brosh, R. and V. Rotter, *When mutants gain new powers: news from the mutant p53 field.* Nat Rev Cancer, 2009. **9**(10): p. 701-13.
18. Sabapathy, K. and D.P. Lane, *Therapeutic targeting of p53: all mutants are equal, but some mutants are more equal than others.* Nat Rev Clin Oncol, 2018. **15**(1): p. 13-30.

19. Momand, J., et al., *The MDM2 gene amplification database.* Nucleic Acids Res, 1998. **26**(15): p. 3453-9.
20. Kato, S., et al., *Analysis of MDM2 Amplification: Next-Generation Sequencing of Patients With Diverse Malignancies.* JCO Precis Oncol, 2018. **2018**.
21. Oliner, J.D., A.Y. Saiki, and S. Caenepeel, *The Role of MDM2 Amplification and Overexpression in Tumorigenesis.* Cold Spring Harb Perspect Med, 2016. **6**(6).
22. Forbes, S.A., et al., *COSMIC: somatic cancer genetics at high-resolution.* Nucleic Acids Res, 2017. **45**(D1): p. D777-D783.
23. Gurpinar, E. and K.H. Vousden, *Hitting cancers' weak spots: vulnerabilities imposed by p53 mutation.* Trends Cell Biol, 2015. **25**(8): p. 486-95.
24. Hong, B., et al., *Targeting tumor suppressor p53 for cancer therapy: strategies, challenges and opportunities.* Curr Drug Targets, 2014. **15**(1): p. 80-9.
25. Parrales, A. and T. Iwakuma, *Targeting Oncogenic Mutant p53 for Cancer Therapy.* Front Oncol, 2015. **5**: p. 288.
26. Bykov, V.J.N., et al., *Targeting mutant p53 for efficient cancer therapy.* Nat Rev Cancer, 2018. **18**(2): p. 89-102.
27. Dotsch, V., et al., *p63 and p73, the ancestors of p53.* Cold Spring Harb Perspect Biol, 2010. **2**(9): p. a004887.
28. Roth, J.A., *Adenovirus p53 gene therapy.* Expert Opin Biol Ther, 2006. **6**(1): p. 55-61.
29. Shaikh, M.F., et al., *Emerging Role of MDM2 as Target for Anti-Cancer Therapy: A Review.* Ann Clin Lab Sci, 2016. **46**(6): p. 627-634.
30. Zhao, Y., et al., *Small-molecule inhibitors of the MDM2-p53 protein-protein interaction (MDM2 Inhibitors) in clinical trials for cancer treatment.* J Med Chem, 2015. **58**(3): p. 1038-52.
31. Zhang, B., B.T. Golding, and I.R. Hardcastle, *Small-molecule MDM2-p53 inhibitors: recent advances.* Future Med Chem, 2015. **7**(5): p. 631-45.
32. Tisato, V., et al., *MDM2/X inhibitors under clinical evaluation: perspectives for the management of hematological malignancies and pediatric cancer.* J Hematol Oncol, 2017. **10**(1): p. 133.
33. Jung, J., et al., *TP53 mutations emerge with HDM2 inhibitor SAR405838 treatment in de-differentiated liposarcoma.* Nat Commun, 2016. **7**: p. 12609.
34. Duffy, M.J., N.C. Synnott, and J. Crown, *Mutant p53 as a target for cancer treatment.* Eur J Cancer, 2017. **83**: p. 258-265.
35. Bykov, V.J., et al., *Restoration of the tumor suppressor function to mutant p53 by a low-molecular-weight compound.* Nat Med, 2002. **8**(3): p. 282-8.
36. Lambert, J.M., et al., *Mutant p53 reactivation by PRIMA-1MET induces multiple signaling pathways converging on apoptosis.* Oncogene, 2010. **29**(9): p. 1329-38.
37. Lambert, J.M., et al., *PRIMA-1 reactivates mutant p53 by covalent binding to the core domain.* Cancer Cell, 2009. **15**(5): p. 376-88.
38. Bykov, V.J., et al., *Reactivation of mutant p53 and induction of apoptosis in human tumor cells by maleimide analogs.* J Biol Chem, 2005. **280**(34): p. 30384-91.
39. Zache, N., et al., *Mutant p53 targeting by the low molecular weight compound STIMA-1.* Mol Oncol, 2008. **2**(1): p. 70-80.
40. Weinmann, L., et al., *A novel p53 rescue compound induces p53-dependent growth arrest and sensitises glioma cells to Apo2L/TRAIL-induced apoptosis.* Cell Death Differ, 2008. **15**(4): p. 718-29.

41. Demma, M., et al., *SCH529074, a small molecule activator of mutant p53, which binds p53 DNA binding domain (DBD), restores growth-suppressive function to mutant p53 and interrupts HDM2-mediated ubiquitination of wild type p53.* J Biol Chem, 2010. **285**(14): p. 10198-212.
42. Issaeva, N., et al., *Small molecule RITA binds to p53, blocks p53-HDM-2 interaction and activates p53 function in tumors.* Nat Med, 2004. **10**(12): p. 1321-8.
43. Zhao, C.Y., et al., *Rescue of the apoptotic-inducing function of mutant p53 by small molecule RITA.* Cell Cycle, 2010. **9**(9): p. 1847-55.
44. Nagata, Y., et al., *The stabilization mechanism of mutant-type p53 by impaired ubiquitination: the loss of wild-type p53 function and the hsp90 association.* Oncogene, 1999. **18**(44): p. 6037-49.
45. Peng, Y., et al., *Inhibition of MDM2 by hsp90 contributes to mutant p53 stabilization.* J Biol Chem, 2001. **276**(44): p. 40583-90.
46. Alexandrova, E.M., et al., *Improving survival by exploiting tumour dependence on stabilized mutant p53 for treatment.* Nature, 2015. **523**(7560): p. 352-6.
47. Trepel, J., et al., *Targeting the dynamic HSP90 complex in cancer.* Nat Rev Cancer, 2010. **10**(8): p. 537-49.
48. Lee, A.S., et al., *Reversible amyloid formation by the p53 tetramerization domain and a cancer-associated mutant.* J Mol Biol, 2003. **327**(3): p. 699-709.
49. Ishimaru, D., et al., *Fibrillar aggregates of the tumor suppressor p53 core domain.* Biochemistry, 2003. **42**(30): p. 9022-7.
50. Higashimoto, Y., et al., *Unfolding, aggregation, and amyloid formation by the tetramerization domain from mutant p53 associated with lung cancer.* Biochemistry, 2006. **45**(6): p. 1608-19.
51. Ano Bom, A.P., et al., *Mutant p53 aggregates into prion-like amyloid oligomers and fibrils: implications for cancer.* J Biol Chem, 2012. **287**(33): p. 28152-62.
52. Xu, J., et al., *Gain of function of mutant p53 by coaggregation with multiple tumor suppressors.* Nat Chem Biol, 2011. **7**(5): p. 285-95.
53. De Smet, F., et al., *Nuclear inclusion bodies of mutant and wild-type p53 in cancer: a hallmark of p53 inactivation and proteostasis remodelling by p53 aggregation.* J Pathol, 2017. **242**(1): p. 24-38.
54. Kanapathipillai, M., *Treating p53 Mutant Aggregation-Associated Cancer.* Cancers (Basel), 2018. **10**(6).
55. Chen, Z., et al., *Polyarginine and its analogues inhibit p53 mutant aggregation and cancer cell proliferation in vitro.* Biochem Biophys Res Commun, 2017. **489**(2): p. 130-134.
56. Chen, Z. and M. Kanapathipillai, *Inhibition of p53 Mutant Peptide Aggregation In Vitro by Cationic Osmolyte Acetylcholine Chloride.* Protein Pept Lett, 2017. **24**(4): p. 353-357.
57. Soragni, A., et al., *A Designed Inhibitor of p53 Aggregation Rescues p53 Tumor Suppression in Ovarian Carcinomas.* Cancer Cell, 2016. **29**(1): p. 90-103.
58. Bridges, C.B., *The origin of variations in sexual and sex-limited characters.* American Naturalist, 1922. **56**: p. 51-63.
59. Dobzhansky, T., *Genetics of natural populations; recombination and variability in populations of Drosophila pseudoobscura.* Genetics, 1946. **31**: p. 269-90.
60. Leung, A.W., et al., *Synthetic lethality in lung cancer and translation to clinical therapies.* Mol Cancer, 2016. **15**(1): p. 61.

61. Paddison, P.J., et al., *A resource for large-scale RNA-interference-based screens in mammals.* Nature, 2004. **428**(6981): p. 427-31.
62. Berns, K., et al., *A large-scale RNAi screen in human cells identifies new components of the p53 pathway.* Nature, 2004. **428**(6981): p. 431-7.
63. Aza-Blanc, P., et al., *Identification of modulators of TRAIL-induced apoptosis via RNAi-based phenotypic screening.* Mol Cell, 2003. **12**(3): p. 627-37.
64. Farmer, H., et al., *Targeting the DNA repair defect in BRCA mutant cells as a therapeutic strategy.* Nature, 2005. **434**(7035): p. 917-921.
65. Bryant, H.E., et al., *Specific killing of BRCA2-deficient tumours with inhibitors of poly(ADP-ribose) polymerase.* Nature, 2005. **434**(7035): p. 913-917.
66. Kim, G., et al., *FDA Approval Summary: Olaparib Monotherapy in Patients with Deleterious Germline BRCA-Mutated Advanced Ovarian Cancer Treated with Three or More Lines of Chemotherapy.* Clin Cancer Res, 2015. **21**(19): p. 4257-61.
67. Shen, J.P. and T. Ideker, *Synthetic Lethal Networks for Precision Oncology: Promises and Pitfalls.* J Mol Biol, 2018. **430**(18 Pt A): p. 2900-2912.
68. Nagel, R., E.A. Semenova, and A. Berns, *Drugging the addict: non-oncogene addiction as a target for cancer therapy.* EMBO Rep, 2016. **17**(11): p. 1516-1531.
69. Wang, Q., et al., *UCN-01: a potent abrogator of G2 checkpoint function in cancer cells with disrupted p53.* J Natl Cancer Inst, 1996. **88**(14): p. 956-65.
70. Nghiem, P., et al., *ATR inhibition selectively sensitizes G1 checkpoint-deficient cells to lethal premature chromatin condensation.* Proc Natl Acad Sci U S A, 2001. **98**(16): p. 9092-7.
71. Jiang, H., et al., *The combined status of ATM and p53 link tumor development with therapeutic response.* Genes Dev, 2009. **23**(16): p. 1895-909.
72. Ruzankina, Y., et al., *Tissue regenerative delays and synthetic lethality in adult mice after combined deletion of Atr and Trp53.* Nat Genet, 2009. **41**(10): p. 1144-9.
73. Ma, C.X., J.W. Janetka, and H. Piwnica-Worms, *Death by releasing the breaks: CHK1 inhibitors as cancer therapeutics.* Trends Mol Med, 2011. **17**(2): p. 88-96.
74. Matheson, C.J., D.S. Backos, and P. Reigan, *Targeting WEE1 Kinase in Cancer.* Trends Pharmacol Sci, 2016. **37**(10): p. 872-881.
75. Leijen, S., et al., *Phase II Study of WEE1 Inhibitor AZD1775 Plus Carboplatin in Patients With TP53-Mutated Ovarian Cancer Refractory or Resistant to First-Line Therapy Within 3 Months.* J Clin Oncol, 2016. **34**(36): p. 4354-4361.
76. Leijen, S., et al., *Phase I Study Evaluating WEE1 Inhibitor AZD1775 As Monotherapy and in Combination With Gemcitabine, Cisplatin, or Carboplatin in Patients With Advanced Solid Tumors.* J Clin Oncol, 2016. **34**(36): p. 4371-4380.
77. Wang, X. and R. Simon, *Identification of potential synthetic lethal genes to p53 using a computational biology approach.* BMC Med Genomics, 2013. **6**: p. 30.
78. Degenhardt, Y., et al., *Sensitivity of cancer cells to Plk1 inhibitor GSK461364A is associated with loss of p53 function and chromosome instability.* Mol Cancer Ther, 2010. **9**(7): p. 2079-89.
79. Smith, L., et al., *The responses of cancer cells to PLK1 inhibitors reveal a novel protective role for p53 in maintaining centrosome separation.* Sci Rep, 2017. **7**(1): p. 16115.
80. Sur, S., et al., *A panel of isogenic human cancer cells suggests a therapeutic approach for cancers with inactivated p53.* Proc Natl Acad Sci U S A, 2009. **106**(10): p. 3964-9.

81. Sanhaji, M., et al., *p53 is not directly relevant to the response of Polo-like kinase 1 inhibitors.* Cell Cycle, 2012. **11**(3): p. 543-53.
82. Louwen, F. and J. Yuan, *Battle of the eternal rivals: restoring functional p53 and inhibiting Polo-like kinase 1 as cancer therapy.* Oncotarget, 2013. **4**(7): p. 958-71.
83. Matoba, S., et al., *p53 regulates mitochondrial respiration.* Science, 2006. **312**(5780): p. 1650-3.
84. Wu, M., et al., *Multiparameter metabolic analysis reveals a close link between attenuated mitochondrial bioenergetic function and enhanced glycolysis dependency in human tumor cells.* Am J Physiol Cell Physiol, 2007. **292**(1): p. C125-36.
85. Emerling, B.M., et al., *Depletion of a putatively druggable class of phosphatidylinositol kinases inhibits growth of p53-null tumors.* Cell, 2013. **155**(4): p. 844-57.
86. Maddocks, O.D., et al., *Serine starvation induces stress and p53-dependent metabolic remodelling in cancer cells.* Nature, 2013. **493**(7433): p. 542-6.
87. Kumar, R., et al., *Mitochondrial uncoupling reveals a novel therapeutic opportunity for p53-defective cancers.* Nat Commun, 2018. **9**(1): p. 3931.
88. Liu, Y., et al., *TP53 loss creates therapeutic vulnerability in colorectal cancer.* Nature, 2015. **520**(7549): p. 697-701.
89. Fan, Y., et al., *FXR1 regulates transcription and is required for growth of human cancer cells with TP53/FXR2 homozygous deletion.* Elife, 2017. **6**.
90. Speetjens, F.M., et al., *Induction of p53-specific immunity by a p53 synthetic long peptide vaccine in patients treated for metastatic colorectal cancer.* Clin Cancer Res, 2009. **15**(3): p. 1086-95.
91. Leffers, N., et al., *Immunization with a P53 synthetic long peptide vaccine induces P53-specific immune responses in ovarian cancer patients, a phase II trial.* Int J Cancer, 2009. **125**(9): p. 2104-13.
92. Hardwick, N.R., et al., *p53-Reactive T Cells Are Associated with Clinical Benefit in Patients with Platinum-Resistant Epithelial Ovarian Cancer After Treatment with a p53 Vaccine and Gemcitabine Chemotherapy.* Clin Cancer Res, 2018. **24**(6): p. 1315-1325.
93. Chiappori, A.A., et al., *INGN-225: a dendritic cell-based p53 vaccine (Ad.p53-DC) in small cell lung cancer: observed association between immune response and enhanced chemotherapy effect.* Expert Opin Biol Ther, 2010. **10**(6): p. 983-91.
94. Nikitina, E.Y., et al., *An effective immunization and cancer treatment with activated dendritic cells transduced with full-length wild-type p53.* Gene Ther, 2002. **9**(5): p. 345-52.
95. Dijkgraaf, E.M., et al., *A phase 1/2 study combining gemcitabine, Pegintron and p53 SLP vaccine in patients with platinum-resistant ovarian cancer.* Oncotarget, 2015. **6**(31): p. 32228-43.
96. Antonia, S.J., et al., *Combination of p53 cancer vaccine with chemotherapy in patients with extensive stage small cell lung cancer.* Clin Cancer Res, 2006. **12**(3 Pt 1): p. 878-87.
97. Soliman, H., et al., *A phase-1/2 study of adenovirus-p53 transduced dendritic cell vaccine in combination with indoximod in metastatic solid tumors and invasive breast cancer.* Oncotarget, 2018. **9**(11): p. 10110-10117.
98. Miyoshi, A., et al., *Identification of CGI-121, a novel PRPK (p53-related protein kinase)-binding protein.* Biochem Biophys Res Commun, 2003. **303**(2): p. 399-405.
99. Downey, M., et al., *A genome-wide screen identifies the evolutionarily conserved KEOPS complex as a telomere regulator.* Cell, 2006. **124**(6): p. 1155-1168.

100. Kisseleva-Romanova, E., et al., *Yeast homolog of a cancer-testis antigen defines a new transcription complex.* Embo Journal, 2006. **25**(15): p. 3576-3585.
101. Wan, L.C., et al., *Proteomic analysis of the human KEOPS complex identifies C14ORF142 as a core subunit homologous to yeast Gon7.* Nucleic Acids Res, 2017. **45**(2): p. 805-817.
102. Srinivasan, M., et al., *The highly conserved KEOPS/EKC complex is essential for a universal tRNA modification, t6A.* EMBO J, 2011. **30**(5): p. 873-81.
103. Perrochia, L., et al., *Functional assignment of KEOPS/EKC complex subunits in the biosynthesis of the universal t6A tRNA modification.* Nucleic Acids Res, 2013. **41**(20): p. 9484-99.
104. Peng, J., et al., *Inhibition of telomere recombination by inactivation of KEOPS subunit Cgi121 promotes cell longevity.* PLoS Genet, 2015. **11**(3): p. e1005071.
105. Drew, K., et al., *Identifying direct contacts between protein complex subunits from their conditional dependence in proteomics datasets.* PLoS Comput Biol, 2017. **13**(10): p. e1005625.
106. Lauhon, C.T., *Mechanism of N6-threonylcarbamoyladenonsine (t(6)A) biosynthesis: isolation and characterization of the intermediate threonylcarbamoyl-AMP.* Biochemistry, 2012. **51**(44): p. 8950-63.
107. Wan, L.C., et al., *Structural and functional characterization of KEOPS dimerization by Pcc1 and its role in t6A biosynthesis.* Nucleic Acids Res, 2016. **44**(14): p. 6971-80.
108. Braun, D.A., et al., *Mutations in KEOPS-complex genes cause nephrotic syndrome with primary microcephaly.* Nat Genet, 2017. **49**(10): p. 1529-1538.
109. Wang, P.Z.T., et al., *Nephrological and urological complications of homozygous c.974G>A (p.Arg325Gln) OSGEP mutations.* Pediatr Nephrol, 2018. **33**(11): p. 2201-2204.
110. Lin, P.Y., et al., *Galloway-Mowat syndrome in Taiwan: OSGEP mutation and unique clinical phenotype.* Orphanet J Rare Dis, 2018. **13**(1): p. 226.
111. Hyun, H.S., et al., *A familial case of Galloway-Mowat syndrome due to a novel TP53RK mutation: a case report.* BMC Med Genet, 2018. **19**(1): p. 131.
112. Jobst-Schwan, T., et al., *Acute multi-sgRNA knockdown of KEOPS complex genes reproduces the microcephaly phenotype of the stable knockout zebrafish model.* PLoS One, 2018. **13**(1): p. e0191503.
113. Costessi, A., et al., *The human EKC/KEOPS complex is recruited to Cullin2 ubiquitin ligases by the human tumour antigen PRAME.* PLoS One, 2012. **7**(8): p. e42822.
114. Hermes, N., S. Kewitz, and M.S. Staege, *Preferentially Expressed Antigen in Melanoma (PRAME) and the PRAME Family of Leucine-Rich Repeat Proteins.* Curr Cancer Drug Targets, 2016. **16**(5): p. 400-14.
115. Hideshima, T., et al., *p53-related protein kinase confers poor prognosis and represents a novel therapeutic target in multiple myeloma.* Blood, 2017. **129**(10): p. 1308-1319.
116. Zykova, T.A., et al., *The T-LAK Cell-originated Protein Kinase Signal Pathway Promotes Colorectal Cancer Metastasis.* EBioMedicine, 2017. **18**: p. 73-82.
117. Abe, Y., et al., *Cloning and characterization of a p53-related protein kinase expressed in interleukin-2-activated cytotoxic T-cells, epithelial tumor cell lines, and the testes.* J Biol Chem, 2001. **276**(47): p. 44003-11.
118. Hanahan, D. and R.A. Weinberg, *Hallmarks of cancer: the next generation.* Cell, 2011. **144**(5): p. 646-74.

119. Schwanhausser, B., et al., *Global quantification of mammalian gene expression control.* Nature, 2011. **473**(7347): p. 337-42.
120. Vogel, C. and E.M. Marcotte, *Insights into the regulation of protein abundance from proteomic and transcriptomic analyses.* Nat Rev Genet, 2012. **13**(4): p. 227-32.
121. Derenzini, M., L. Montanaro, and D. Trere, *Ribosome biogenesis and cancer.* Acta Histochem, 2017. **119**(3): p. 190-197.
122. Marcel, V., F. Nguyen Van Long, and J.J. Diaz, *40 Years of Research Put p53 in Translation.* Cancers (Basel), 2018. **10**(5).
123. Hellen, C.U. and P. Sarnow, *Internal ribosome entry sites in eukaryotic mRNA molecules.* Genes Dev, 2001. **15**(13): p. 1593-612.
124. Lacerda, R., J. Menezes, and L. Romao, *More than just scanning: the importance of cap-independent mRNA translation initiation for cellular stress response and cancer.* Cellular and Molecular Life Sciences, 2017. **74**(9): p. 1659-1680.
125. Lopez-Lastra, M., A. Rivas, and M.I. Barria, *Protein synthesis in eukaryotes: the growing biological relevance of cap-independent translation initiation.* Biol Res, 2005. **38**(2-3): p. 121-46.
126. Richter, J.D. and J. Coller, *Pausing on Polyribosomes: Make Way for Elongation in Translational Control.* Cell, 2015. **163**(2): p. 292-300.
127. Chan, P.P. and T.M. Lowe, *GtRNAdb: a database of transfer RNA genes detected in genomic sequence.* Nucleic Acids Res, 2009. **37**(Database issue): p. D93-7.
128. Kutter, C., et al., *Pol III binding in six mammals shows conservation among amino acid isotypes despite divergence among tRNA genes.* Nat Genet, 2011. **43**(10): p. 948-55.
129. Holley, R.W., et al., *Structure of a Ribonucleic Acid.* Science, 1965. **147**(3664): p. 1462-5.
130. Lorenz, C., C.E. Lunse, and M. Morl, *tRNA Modifications: Impact on Structure and Thermal Adaptation.* Biomolecules, 2017. **7**(2).
131. Kim, S.H., et al., *Three-dimensional tertiary structure of yeast phenylalanine transfer RNA.* Science, 1974. **185**(4149): p. 435-40.
132. Gu, C., T.J. Begley, and P.C. Dedon, *tRNA modifications regulate translation during cellular stress.* FEBS Lett, 2014. **588**(23): p. 4287-96.
133. Boccaletto, P., et al., *MODOMICS: a database of RNA modification pathways. 2017 update.* Nucleic Acids Res, 2018. **46**(D1): p. D303-D307.
134. Pan, T., *Modifications and functional genomics of human transfer RNA.* Cell Res, 2018. **28**(4): p. 395-404.
135. Pereira, M., et al., *Impact of tRNA Modifications and tRNA-Modifying Enzymes on Proteostasis and Human Disease.* Int J Mol Sci, 2018. **19**(12).
136. Ranjan, N. and M.V. Rodnina, *tRNA wobble modifications and protein homeostasis.* Translation (Austin), 2016. **4**(1): p. e1143076.
137. Kirchner, S. and Z. Ignatova, *Emerging roles of tRNA in adaptive translation, signalling dynamics and disease.* Nat Rev Genet, 2015. **16**(2): p. 98-112.
138. Dittmar, K.A., J.M. Goodenbour, and T. Pan, *Tissue-specific differences in human transfer RNA expression.* PLoS Genet, 2006. **2**(12): p. e221.
139. Gingold, H., et al., *A dual program for translation regulation in cellular proliferation and differentiation.* Cell, 2014. **158**(6): p. 1281-1292.

140. Koh, C.S. and L.P. Sarin, *Transfer RNA modification and infection - Implications for pathogenicity and host responses.* Biochim Biophys Acta Gene Regul Mech, 2018. **1861**(4): p. 419-432.
141. Montanaro, L., D. Trere, and M. Derenzini, *Nucleolus, ribosomes, and cancer.* Am J Pathol, 2008. **173**(2): p. 301-10.
142. Barna, M., et al., *Suppression of Myc oncogenic activity by ribosomal protein haploinsufficiency.* Nature, 2008. **456**(7224): p. 971-5.
143. Truitt, M.L. and D. Ruggero, *New frontiers in translational control of the cancer genome.* Nat Rev Cancer, 2016. **16**(5): p. 288-304.
144. Zhou, Y., et al., *High levels of tRNA abundance and alteration of tRNA charging by bortezomib in multiple myeloma.* Biochem Biophys Res Commun, 2009. **385**(2): p. 160-4.
145. Pavon-Eternod, M., et al., *tRNA over-expression in breast cancer and functional consequences.* Nucleic Acids Res, 2009. **37**(21): p. 7268-80.
146. Rodriguez, V., et al., *Chromosome 8 BAC array comparative genomic hybridization and expression analysis identify amplification and overexpression of TRMT12 in breast cancer.* Genes Chromosomes Cancer, 2007. **46**(7): p. 694-707.
147. Kwon, N.H., et al., *Transfer-RNA-mediated enhancement of ribosomal proteins S6 kinases signaling for cell proliferation.* RNA Biol, 2018. **15**(4-5): p. 635-648.
148. Goodarzi, H., et al., *Modulated Expression of Specific tRNAs Drives Gene Expression and Cancer Progression.* Cell, 2016. **165**(6): p. 1416-1427.
149. Begley, U., et al., *A human tRNA methyltransferase 9-like protein prevents tumour growth by regulating LIN9 and HIF1-alpha.* EMBO Mol Med, 2013. **5**(3): p. 366-83.
150. Wang, S., et al., *Expression of KIAA1456 in lung cancer tissue and its effects on proliferation, migration and invasion of lung cancer cells.* Oncol Lett, 2018. **16**(3): p. 3791-3795.
151. Chen, Z., et al., *Transfer RNA demethylase ALKBH3 promotes cancer progression via induction of tRNA-derived small RNAs.* Nucleic Acids Res, 2019. **47**(5): p. 2533-2545.
152. Frohlich, K.M., et al., *Post-Transcriptional Modifications of RNA: Impact on RNA Function and Human Health*, in *Modified Nucleic Acids in Biology and Medicine*, S. Jurga, V.A. Erdmann, and J. Barciszewski, Editors. 2016, Springer International Publishing: Cham. p. 91-130.
153. El Yacoubi, B., et al., *A role for the universal Kae1/Qri7/YgjD (COG0533) family in tRNA modification.* EMBO J, 2011. **30**(5): p. 882-93.
154. Rojas-Benitez, D., et al., *The Levels of a Universally Conserved tRNA Modification Regulate Cell Growth.* J Biol Chem, 2015. **290**(30): p. 18699-707.
155. Daugeron, M.C., et al., *Gcn4 misregulation reveals a direct role for the evolutionary conserved EKC/KEOPS in the t6A modification of tRNAs.* Nucleic Acids Res, 2011. **39**(14): p. 6148-60.
156. Naor, A., et al., *A genetic investigation of the KEOPS complex in halophilic Archaea.* PLoS One, 2012. **7**(8): p. e43013.
157. Thiaville, P.C., et al., *Cross kingdom functional conservation of the core universally conserved threonylcarbamoyladenosine tRNA synthesis enzymes.* Eukaryot Cell, 2014. **13**(9): p. 1222-31.

158. Weissenbach, J. and H. Grosjean, *Effect of threonylcarbamoyl modification (t6A) in yeast tRNA Arg III on codon-anticodon and anticodon-anticodon interactions. A thermodynamic and kinetic evaluation.* Eur J Biochem, 1981. **116**(1): p. 207-13.
159. Thiaville, P.C., et al., *Global translational impacts of the loss of the tRNA modification t(6)A in yeast.* Microb Cell, 2016. **3**(1): p. 29-45.
160. El Yacoubi, B., M. Bailly, and V. de Crecy-Lagard, *Biosynthesis and function of posttranscriptional modifications of transfer RNAs.* Annu Rev Genet, 2012. **46**: p. 69-95.
161. Haussuehl, K., et al., *Eukaryotic GCP1 is a conserved mitochondrial protein required for progression of embryo development beyond the globular stage in Arabidopsis thaliana.* Biochem J, 2009. **423**(3): p. 333-41.
162. Suzuki, T. and T. Suzuki, *A complete landscape of post-transcriptional modifications in mammalian mitochondrial tRNAs.* Nucleic Acids Res, 2014. **42**(11): p. 7346-57.
163. Oberto, J., et al., *Qri7/OSGEPL, the mitochondrial version of the universal Kae1/YgjD protein, is essential for mitochondrial genome maintenance.* Nucleic Acids Res, 2009. **37**(16): p. 5343-52.
164. Loayza-Puch, F., et al., *p53 induces transcriptional and translational programs to suppress cell proliferation and growth.* Genome Biol, 2013. **14**(4): p. R32.
165. Donati, G., et al., *The balance between rRNA and ribosomal protein synthesis up- and downregulates the tumour suppressor p53 in mammalian cells.* Oncogene, 2011. **30**(29): p. 3274-88.
166. Deisenroth, C. and Y. Zhang, *Ribosome biogenesis surveillance: probing the ribosomal protein-Mdm2-p53 pathway.* Oncogene, 2010. **29**(30): p. 4253-60.
167. Dai, M.S. and H. Lu, *Inhibition of MDM2-mediated p53 ubiquitination and degradation by ribosomal protein L5.* J Biol Chem, 2004. **279**(43): p. 44475-82.
168. Dai, M.S., et al., *Ribosomal protein L23 activates p53 by inhibiting MDM2 function in response to ribosomal perturbation but not to translation inhibition.* Mol Cell Biol, 2004. **24**(17): p. 7654-68.
169. Jin, A., et al., *Inhibition of HDM2 and activation of p53 by ribosomal protein L23.* Mol Cell Biol, 2004. **24**(17): p. 7669-80.
170. Lohrum, M.A., et al., *Regulation of HDM2 activity by the ribosomal protein L11.* Cancer Cell, 2003. **3**(6): p. 577-87.
171. Zhang, Y., et al., *Ribosomal protein L11 negatively regulates oncoprotein MDM2 and mediates a p53-dependent ribosomal-stress checkpoint pathway.* Mol Cell Biol, 2003. **23**(23): p. 8902-12.
172. Zhai, W. and L. Comai, *Repression of RNA polymerase I transcription by the tumor suppressor p53.* Mol Cell Biol, 2000. **20**(16): p. 5930-8.
173. Felton-Edkins, Z.A., et al., *Direct regulation of RNA polymerase III transcription by RB, p53 and c-Myc.* Cell Cycle, 2003. **2**(3): p. 181-4.
174. Cairns, C.A. and R.J. White, *p53 is a general repressor of RNA polymerase III transcription.* EMBO J, 1998. **17**(11): p. 3112-23.
175. Riley, K.J. and L.J. Maher, 3rd, *p53 RNA interactions: new clues in an old mystery.* RNA, 2007. **13**(11): p. 1825-33.
176. Samad, A. and R.B. Carroll, *The tumor suppressor p53 is bound to RNA by a stable covalent linkage.* Mol Cell Biol, 1991. **11**(3): p. 1598-606.
177. Oberosler, P., et al., *p53-catalyzed annealing of complementary single-stranded nucleic acids.* EMBO J, 1993. **12**(6): p. 2389-96.

178. Galy, B., et al., *p53 directs conformational change and translation initiation blockade of human fibroblast growth factor 2 mRNA.* Oncogene, 2001. **20**(34): p. 4613-20.
179. Miller, S.J., et al., *p53 binds selectively to the 5' untranslated region of cdk4, an RNA element necessary and sufficient for transforming growth factor beta- and p53-mediated translational inhibition of cdk4.* Mol Cell Biol, 2000. **20**(22): p. 8420-31.
180. Tournillon, A.S., et al., *p53 binds the mdmx mRNA and controls its translation.* Oncogene, 2017. **36**(5): p. 723-730.
181. Mosner, J., et al., *Negative feedback regulation of wild-type p53 biosynthesis.* EMBO J, 1995. **14**(18): p. 4442-9.
182. Riley, K.J., et al., *Recognition of RNA by the p53 tumor suppressor protein in the yeast three-hybrid system.* RNA, 2006. **12**(4): p. 620-30.
183. Luo, J., N.L. Solimini, and S.J. Elledge, *Principles of cancer therapy: oncogene and non-oncogene addiction.* Cell, 2009. **136**(5): p. 823-37.
184. Cheung, H.W., et al., *Systematic investigation of genetic vulnerabilities across cancer cell lines reveals lineage-specific dependencies in ovarian cancer.* Proc Natl Acad Sci U S A, 2011. **108**(30): p. 12372-7.
185. Facchin, S., et al., *Functional homology between yeast piD261/Bud32 and human PRPK: both phosphorylate p53 and PRPK partially complements piD261/Bud32 deficiency.* FEBS Lett, 2003. **549**(1-3): p. 63-6.
186. Helming, K., et al., *ARID1B is a specific vulnerability in ARID1A-mutant cancers.* Cancer Research, 2014. **74**(19).
187. Bamford, S., et al., *The COSMIC (Catalogue of Somatic Mutations in Cancer) database and website.* Br J Cancer, 2004. **91**(2): p. 355-8.
188. Niknafs, Y.S., et al., *MiPanda: A Resource for Analyzing and Visualizing Next-Generation Sequencing Transcriptomics Data.* Neoplasia, 2018. **20**(11): p. 1144-1149.
189. Janumyan, Y.M., et al., *Bcl-xL/Bcl-2 coordinately regulates apoptosis, cell cycle arrest and cell cycle entry.* EMBO J, 2003. **22**(20): p. 5459-70.
190. Morandell, S., et al., *A reversible gene-targeting strategy identifies synthetic lethal interactions between MK2 and p53 in the DNA damage response in vivo.* Cell Rep, 2013. **5**(4): p. 868-77.
191. Harada, N., et al., *Identification of a checkpoint modulator with synthetic lethality to p53 mutants.* Anticancer Drugs, 2011. **22**(10): p. 986-94.
192. Baldwin, A., et al., *Kinase requirements in human cells: V. Synthetic lethal interactions between p53 and the protein kinases SGK2 and PAK3.* Proc Natl Acad Sci U S A, 2010. **107**(28): p. 12463-8.
193. Tomayko, M.M. and C.P. Reynolds, *Determination of subcutaneous tumor size in athymic (nude) mice.* Cancer Chemother Pharmacol, 1989. **24**(3): p. 148-54.
194. Anderson, J., L. Phan, and A.G. Hinnebusch, *The Gcd10p/Gcd14p complex is the essential two-subunit tRNA(1-methyladenosine) methyltransferase of Saccharomyces cerevisiae.* Proc Natl Acad Sci U S A, 2000. **97**(10): p. 5173-8.
195. Anderson, J., et al., *The essential Gcd10p-Gcd14p nuclear complex is required for 1-methyladenosine modification and maturation of initiator methionyl-tRNA.* Genes Dev, 1998. **12**(23): p. 3650-62.
196. Pavon-Eternod, M., et al., *Overexpression of initiator methionine tRNA leads to global reprogramming of tRNA expression and increased proliferation in human epithelial cells.* RNA, 2013. **19**(4): p. 461-6.

197. Shi, L., et al., *Expression and significance of m1A transmethylase, hTrm6p/hTrm61p and its related gene hTrm6/hTrm61 in bladder urothelial carcinoma.* Am J Cancer Res, 2015. **5**(7): p. 2169-79.
198. Macari, F., et al., *TRM6/61 connects PKCalpha with translational control through tRNAi(Met) stabilization: impact on tumorigenesis.* Oncogene, 2016. **35**(14): p. 1785-96.
199. He, M.H., et al., *KEOPS complex promotes homologous recombination via DNA resection.* Nucleic Acids Res, 2019.
200. Iwabuchi, K., et al., *Stimulation of p53-mediated transcriptional activation by the p53-binding proteins, 53BP1 and 53BP2.* J Biol Chem, 1998. **273**(40): p. 26061-8.
201. Iwabuchi, K., et al., *Two cellular proteins that bind to wild-type but not mutant p53.* Proc Natl Acad Sci U S A, 1994. **91**(13): p. 6098-102.
202. DiTullio, R.A., Jr., et al., *53BP1 functions in an ATM-dependent checkpoint pathway that is constitutively activated in human cancer.* Nat Cell Biol, 2002. **4**(12): p. 998-1002.
203. Donehower, L.A., et al., *Mice deficient for p53 are developmentally normal but susceptible to spontaneous tumours.* Nature, 1992. **356**(6366): p. 215-21.